2-8-2011

Research Towards the Development of an Optically Pumped Cesium Dimer Laser

Omar Qassim

Omar Karim Qassim
Candidate

Department of Electrical and Computer Engineering
Department

This thesis is approved, and it is acceptable in quality and form for publication on microfilm:

Approved by the Thesis Committee:

Prof. Wolfgang Rudolph , Chairperson

Prof. Luke F. Lester

Dr. David Hostutler

Accepted:

Dean, Graduate School

Date

Research Towards the Development of an Optically Pumped Cesium Dimer Laser

BY

OMAR KARIM QASSIM

B.S. Electrical Engineering, UNIVERSITY OF NEW MEXICO, 2006

THESIS

Submitted in Partial Fulfillment of the
Requirements for the Degree of

Master of Science
Electrical Engineering

The University of New Mexico
Albuquerque, New Mexico

December, 2010

DEDICATION

To my loving parents, Karim and Linda Qassim

ACKNOWLEDGMENTS

The research for this thesis was carried out at the Center of Excellence on Kirtland Air Force Base. First I would like to thank Allah (SWT) for giving me the guidance and ability to seek knowledge and pursue a master's degree in optoelectronics.

I would like to thank my advisor, Dr. Wolfgang Rudolph, for his direction in this project. His expertise and ability to teach concepts in the field made my journey pleasurable and enlightening and will remain with me as I continue my career.

I also thank my committee members, Prof. Luke Lester and Dr. David Hostutler, for their valuable recommendations pertaining to this study and assistance in my professional development.

I would like to thank Dr. David Hostutler and Wade Klennert, for all their guidance in the laboratory and their eagerness to see me succeed. Their efforts helped make this thesis work possible.

I would like to thank my office members for their support and assistance. I thank Nathan Zamaroski, Wade Klennert, Amanda Haymond, and Andrew Sandoval for their help in the laboratory and discussions about various topics.

I would like to thank Furqan Chiragh and Mohamad El-Emawy for their help during my graduate studies and thesis edits.

I would also like to thank my family: Dad, Mom, Mona, Dena, and Bilal. Without their loving care and compassion I would not be where I am today. Thank you everyone for helping me with whatever I needed help with.

RESEARCH TOWARDS THE DEVELOPMENT OF AN OPTICALLY PUMPED CESIUM DIMER LASER

BY

OMAR KARIM QASSIM

ABSTRACT OF THESIS

Submitted in Partial Fulfillment of the
Requirements for the Degree of

Master of Science
Electrical Engineering

The University of New Mexico
Albuquerque, New Mexico

December, 2010

Research towards the Development of an Optically Pumped Cesium Dimer Laser

by

Omar Karim Qassim

B.S., Electrical Engineering, University of New Mexico, 2006
M.S., Electrical Engineering, University of New Mexico, 2010

ABSTRACT

Metal vapor lasers are a promising candidate for high power laser systems and have been a recent area of interest. These types of lasers seem to combine all the strengths of both gas/chemical and solid state lasers without the weaknesses attributed to them. Metal vapor lasers have very efficient operation and there is a sub-section of metal vapor lasers that have captured the attention of the research community; they are the metal vapor lasers pumped with laser diodes (DPAL). The absorption spectra of most alkali vapor lasers are roughly $1/100^{th}$ of the width of the diode pump width and broadening is desired to achieve the best overlap of emission width and absorption width.

Mixing of a buffer gas to spectrally broaden the alkali vapor is usually done, but also causes issues such as accommodating high pressures as well as thermal issues. What I am doing that no one else has done is to try to make an alkali (Cs) laser using diatomic alkali molecules. Cesium (Cs_2) was chosen because of its many interesting and attractive characteristics. Cs_2 has a dimer configuration of vibrational and rotational structure. Cesium is the heaviest of all alkali metals, and has the densest vibrational and rotational levels compared to any other alkali metal. With the most rotational and vibrational

sublevels this leads to the most compact dimer emission. Research was completed to determine if Cs_2 could be a desirable gain medium for the future of Diode Pumped Alkali Lasers (DPAL). Some of the achievements completed were finding a suitable enclosure to achieve higher temperatures of over 200 C, finding a solution to stopping the cesium from reaching the enclosure windows and corroding the anti-reflection coatings, calculating Frank-Condon coefficients of the first 90 levels of the ground and excited vibrational states of Cs_2, and recording all of the Cs_2 emission spectra from 750 nm to 800 nm. Each of these achievements will be discussed in detail, and conclusions will be given at the end.

TABLE OF CONTENTS

LIST OF FIGURES ..... *XI*

CHAPTER 1 -INTRODUCTION *1*

1.1 High Power Laser Development 1

1.1.1 Gas and Chemical Lasers 1

1.1.2 Semiconductor Lasers 2

1.1.3 Diode Pumped Alkali Lasers 3

1.2 Goals 7

CHAPTER 2 -THEORY AND EXPERIMENTAL SETUP *9*

2.1 Nomenclature 10

2.1.1 Rotational Energy of Molecules 12

2.1.2 Vibrational Energy of Molecules 14

2.1.3 Selection rules and branching types 17

2.1.4 Franck-Condon Factors 19

2.2 How an Alkali Dimer Laser Works 23

2.3 Cesium Dimer Simulations 24

2.4 Laser Calculations 26

2.4.1 Number Density 26

2.4.2 Absorption Cross Section 27

2.4.3 Gain Length 28

2.5 Device Design 31

2.5.1 Glass Cell 31

2.5.2 Heat pipe 32

CHAPTER 3 -DATA AND MEASUREMENT 37

3.1 Measurements 37

3.2 Fluorescence Measurements 39

3.3 Pump Probe Measurements 46

3.4 Heat Pipe Measurements 51

CHAPTER 4 -ISSUES WITH CS_2 55

4.1 Heat pipe Issues 55

4.2 Multiple Cs_2 Absorption Band Overlaps 60

4.3 Cesium Dimer Concentration Measurements 61

4.4 Simulated Cs_2 emission spectra issues 63

4.5 Summary 64

CHAPTER 5 -INTERESTING PHENOEMON WITH CS MOLECULE 65

5.1 Experimental results 65

5.2 Four-wave mixing 68

5.3 Optical Parametric Oscillator 72

CHAPTER 6 -SUMMARY AND FUTURE WORK 74

6.1 Accomplishments 74

6.2 Conclusions 75

6.3 Future Work 76

LIST OF FIGURES

Figure 1.1 Diode laser spectral width versus atomic absorption spectral width.....5

Figure 2.1 Example of potential energy well.....11

Figure 2.2 (a) Graphical representation of a diatomic molecule with 2 rotational degrees of freedom, (b) Examples of allowed rotational energy levels.....13

Figure 2.3 (a) Spring model representation of a diatomic molecule, (b) Example of allowed vibrational energy levels 15

Figure 2.4 Zoom in image of vibrational and rotational energy levels on the ground state of Cs_2.....16

Figure 2.5 Examples of different branch level transitions.....18

Figure 2.6 Examples of dimer transitions [20] 20

Figure 2.7 3-D graph of Frank Condon Factors for the first 90 states of the ground X state and excited B state. 21

Figure 2.8 (a)Zoomed in 3-D graph of Frank Condon Factors pump probe graph (b) energy level representation of example potential pump probe measurement.....22

Figure 2.9 Example of an alkali dimer laser operation.....24

Figure 2.10 Plotted results of stimulated emission from calculations being pumped at 756.6 nm 25

Figure 2.11 Diagram of the Beer-Lambert Law 28

Figure 2.12 Plotted I/I_0 versus gain length of (a), cesium cell at 240 C and (b), cesium cell at 320 C. 30

Figure 2.13. Heat pipe used in experiments.....33

Figure 2.14 Picture of heat pipe used in experiments 35

Figure 2.15 Picture of (a) Nitrogen purged glove box and (b)fill station 37

Figure 3.1 Florescence measurement set up diagram 39

Figure 3.2 (a) side view with both laser beam entrance and observation hole. (b) cell wrapped in metal “oven”, evenly wrapped heater rope, and insulated with fiberglass rope. 40

Figure 3.3 Emission Spectra of Cs_2 pumping at 754nm 43

Figure 3.4 Overlap of simulated Cs_2 emission and experimental Cs_2 output emission 46

Figure 3.5 Visual for pump probe experiments 47

Figure 3.6 Diagram of pump probe experiments 48

Figure 3.7 Experimental setup for absorption experiments 53

Figure 3.8 Absorption results showing as the temperature goes up, the absorption increases 54

Figure 4.1 Locations of thermocouples on heat pipe measurement 56

Figure 4.2 Plot of different temperature measurements on the heat pipe 57

Figure 4.3 Graphs of Cs_2 emission output at (a) 220 C and (b) 260 C 59

Figure 4.4 Graphs of Cs_2 emission output at (a) 235 C and (b) 260 C 62

Figure 4.5 Overlap of simulated Cs_2 emission and experimental Cs_2 output emission showing very little similarities. 64

Figure 5.1 Set up for pump probe measurements for the cesium atom 66

Figure 5.2 Emission transitions of pumping Cs with a pulsed 742 nm pump laser. Relative emission wavelengths are noted in top right corner. 67

Figure 5.3 Arbitrary example of two photon absorption with a “virtual” state 69

Figure 5.4. Energy diagram of pumping Cs2 at 742 nm and emitting at 455 nm.....70

Figure 5.5 Experimental set up for spectral width measurements 71

Figure 5.6 Spectral width determined by integrating the curve fit of the intensity emission of 455 nm output transition at 320 C. 72

CHAPTER 1 - INTRODUCTION

Since the inception of the laser, the desire to create high power laser output while maintaining a small size has been of immense importance. Although there are many different types of lasers, there are only a few types that have been able to achieve exceptional power growth without incorporating a massive size. In the following paragraphs, discussion of high power laser development as well as an overview of metal vapor lasers is given.

1.1 High Power Laser Development

Current research endeavors involve the development of lasers with higher output powers and smaller sizes compared to the current laser leaders in high power output. High power lasers can be used to develop a variety of industries such as laser welding[1], laser nuclear fusion[2], and astronomical adaptive optics imaging[3] just to name a few. Traditionally, there were three main types of lasers that showed potential as a scalable high power laser: gas, chemical, and solid state lasers. Gas and chemical lasers are usually put into the same category when the military is comparing different types of high power lasers and will be combined in this thesis.

1.1.1 Gas and Chemical Lasers

Gas and chemical lasers have been researched for a variety of reasons. The biggest strength is their scalability of power. The gas/chemical lasers are scaled linearly, so by just increasing the amount of chemicals and the size, the output power increases.

Gas/chemical lasers also have high output powers, with some powers reaching in excess of several megawatts [4]. Gas/chemical lasers have good beam quality which can also be fine tuned with optics. These types of lasers are currently being researched by the Air Force Research Laboratory (AFRL) to increase the power in these systems. As the laser's output power is increased by scaling, so does its size. For any systems greater than 1kw, the laser starts taking up small rooms. An example would be the ATL (Airborne Tactical Laser) whose chemical laser fills an entire C130 transport airplane [5]. The chemicals that are used for these Chemical Oxygen Iodine Laser (COIL) lasers are also known to be extremely hazardous to humans and extreme caution must be taken when working with them. As these lasers continually grow larger in size to achieve megawatt powers, the logistics in making the chemical laser work gets more complicated. These are just a few of the numerous reasons why traditional gas/chemical laser development is not the future for high power laser systems.

1.1.2 Semiconductor Lasers

Semiconductor lasers also possess great strengths and are researched accordingly. One of their biggest strengths is their ease of electrical pumping. Electricity is relatively easy to acquire, and makes the laser easy to pump by just providing it with electrical energy. There is no mixing of gases or pressures that have to be monitored. Another great strength is their compact size, typically ranging from small blocks measuring 2x2x1 mm to meter long rods [6]. This makes handling the laser much easier than the room sized gas/chemical lasers. Once semiconductor lasers are manufactured, any adjustments needed to be made would have to be done on the next batch, since modifications cannot

be done after processing the lasers. The only parameter that is adjustable is the current applied to the P-N junction and a few nanometers of temperature tuning through heat handling. As the laser is cooled down, the laser wavelength blue shifts because the bandgap changes and gets smaller. This effect is undesirable as specific wavelengths are needed. If anything else needs to be changed, building another laser would be the only choice. Although all these strengths appear to place them at the forefront of research, there are weaknesses that keep semiconductor lasers from ever reaching high power outputs. Since semiconductor lasers are so miniature and compact, thermal management is a very big issue. Improper thermal management usually results in the destruction of the laser. Also, when a semiconductor laser is power scaled, the beam quality reduces and laser output broadens thus making the laser unusable. Increasing the current reduces the focusing power of the thermal lens, which leads to lensing, a detrimental lasing effect due to temperature gradients [7]. The highest recorded output power of a semiconductor laser to date had an average power of 100 W [8]. The semiconductor laser was demonstrated by Sony and produces a output peak power of 100 W and a repetition frequency of 1 Ghz.

1.1.3 Diode Pumped Alkali Lasers

Metal vapor lasers are a promising candidate for high power laser systems and have been a recent area of interest. These types of lasers seem to combine all the positives strengths of both gas/chemical and solid state lasers without taking the weaknesses attributed to them. These lasers have been able to output power levels of 17 watts with rubidium and 48 watts with cesium [9][10], and they are continually improving. Alkali lasers have also been shown to power scale efficiently [11], with

reports of 80% slope efficiency [12]. For the higher output powered lasers still in laboratories, their sizes are smaller than similar powered gas/chemical lasers and bigger than similar power sized solid state lasers. There is a sub-section of electronic hybrid lasers that have captured the attention of the research community; they are the metal vapor lasers pumped with laser diodes. This also includes interest in alkali dimer lasers. These new types of lasers are gaining interest because the dimer absorption spectrum is broad and the output wavelengths are of interest. They are electrically pumped, since it is a solid state diode laser that is pumping the alkali metal, and that diode laser is pumped electrically. These types of lasers will be referred to as Diode Pumped Alkali Lasers (DPAL).

These alkali lasers usually consist of a pump source, a gain medium, and reflecting mirrors to create a cavity. The pump source would be the diode laser that is pumping the alkali cell with the pump wavelength. The reflecting mirrors are to bounce the desired radiation a few times through the cell that holds the gain medium to increase power of output. The issue that needs to be overcome is the overlap between the pump's spectral width and the absorption spectral width. A typical spectral width of a diode laser is about 2 nm. The absorption spectral width of an atomic transition for an alkali metal is about .001 nm. As can be seen in Figure 1.1, the overlap is very small. Solving this issue is usually done in 2 ways: by spectrally broadening the absorption profile by adding a buffer gas to the gain medium, or by spectrally narrowing the broad band diode. Another way is to use a combination of both.

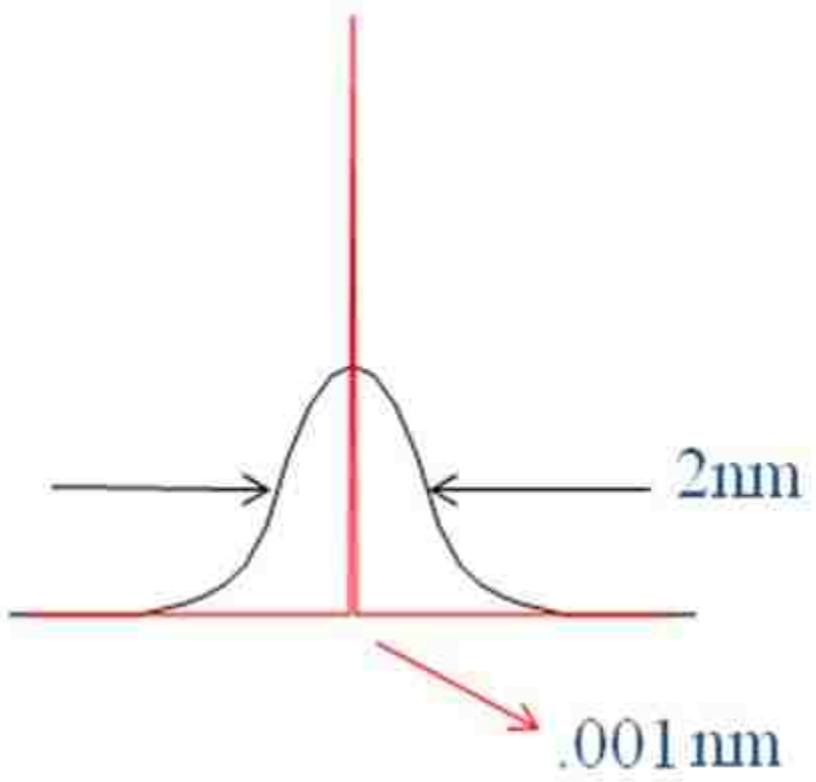

Figure 1.1 Diode laser spectral width versus atomic absorption spectral width

The addition of the buffer gas to the gain medium is an issue that needs to be investigated when designing a DPAL, as well as determining the most beneficial ratio of the buffer gas and the alkali metal. Adding a buffer gas to the gain medium has positive and negative results. A positive result is the greater overlap of the pump and absorption spectral widths. Another positive result is the advantage of spin mixing achieved when adding a buffer gas. This will be discussed in more detail when discussing the physics of how the alkali laser works in chapter 2. A negative result is if there is too much buffer gas, the absorption spectral width can inhomogeneously pressure broaden too much, leaving less overlap than the maximum achievable. Another issue is the high pressure

needed to get optimal spectrum overlap is on the order of a few atmospheres [13]. With extremely high pressure systems such as these, problems such as thermal loading which causes the beam quality to deteriorate, the use of thick windows for a high pressured cell, and the loss of energy through these thick optics due to absorption are introduced, just to name a few. Although this is a pathway that some research has gone, there are more issues than positives with this route and so low pressure is desired.

If the alkali atoms are given adequate energy, usually provided by heating, then the atoms combine together and produce dimers, molecules of the same atom in pairs. Producing these dimers helps the atoms relax and share electrons. This covalent bonding keeps the molecule neutral, which allows the excited molecules to relax rovibrationally. Rovibrational relaxation is a way for excited molecules to lose some energy by vibrating and rotating. Unfortunately this also adds to the complexity of the system because it adds the rotational and vibrational structure on the electronic transitions. The physics is presented in Chapter 2 in order to provide a better understanding of this molecular phenomenon.

Producing optically pumped dimer lasers is not something innovative. Even producing alkali dimer lasers such as Li_2[14], Na_2[15], and K_2[16] have been completed and reported on. These lasers used pump lasers such as rare gas ion lasers (krypton ion or argon ion lasers) to produce a laser emission. These types of pumping lasers are expensive which makes them undesirable. Some of these dimer lasers are also heated up to temperatures as high as 1300 K to create a suitable dimer population to lase [17]. High temperatures and reactive elements such as the alkali metals are also not desired as they

can cause extreme reactions with the ambient air. One issue that was mentioned frequently was the issue of self absorption. This usually happened due to the high thermal population in the lower laser levels. Self absorption also becomes a strong loss mechanism for excited bands in more complicated molecules [17]. This could potentially be an issue for the Cs_2 and will have to be considered.

Research on cesium was done for a couple of straightforward and intriguing reasons. One reason is that cesium is the heaviest of all the stable alkali metals. Using the cesium dimer will ensure we can get the most energy out of the system because it has the densest set of vibrational and rotational sub energy levels if successful. Another reason cesium was studied was because there is a good absorption window that overlaps the 780 nm region. This is interesting because this is a common emission wavelength for commercial diode lasers. The lasers at these wavelengths are much cheaper than the rare gas ion lasers that are currently being used to produce alkali dimer lasers [17]. Another intriguing reason is that with the cesium dimers in the cell, there is no need for a high pressure buffer gas. This happens because of the allowable rovibrational relaxation. Most alkali lasers have an inert buffer gas included in the gain material to help with broadening as well as a hydrocarbon gas to help with spin mixing. With all these interesting opportunities Cs dimers seem to offer, the following research was pursued to see if Cs dimers would be the next breakthrough in DPAL technology.

1.2 Goals

The goal of this research was to determine if Cs is indeed a good candidate for the next push in alkali dimer metal vapor laser research. There are three main objectives that

needed to be addressed to determine if Cs dimers would be a suitable gain medium. A few other questions came up as the research started and will be included in the goals of this project. The main goals were:

1. Find out if Cs_2 can be a suitable gain material for alkali lasers
2. Find a suitable enclosure for cesium that allows higher temps of 180 C to be reached
3. Find a solution to stopping the material from reaching the windows and corroding the anti-reflection coating

There were four questions that were determined useful to help solve the first goal. These questions are as follows:

1. What is the optimal pumping wavelength?
2. What will be the lasing wavelength(s)?
3. What is the optimal Cs_2 concentration?
4. What is the minimum gain length required?

These questions will be the structure of this master's thesis and the great effort to answer these questions was the work that was completed. In the following chapters the theory, the physics, and the calculations will be discussed. Then the discussion of the experimental set up will follow. After that, the data collected and a discussion of the results will be provided. Finally, a summary and future work needed to continue this research will be presented.

CHAPTER 2 - THEORY AND EXPERIMENTAL SETUP

Since Cs_2 can absorb and emit at many wavelengths, preliminary experiments and theoretical calculations needed to be completed in order to answer this thesis' main questions. A discussion about the theoretical calculations will be presented followed by the experimental set up. Due to the multiple rotational and vibrational energy levels of the Cs dimer, their energy levels needed to be calculated. These levels are typically calculated using Morse Potential theory [18]. Once the Morse potentials are calculated, the next important piece of information is calculating the probability of the molecules moving from one transition to another; this is solved by calculating the Frank Condon Factors. Using the Morse Potentials and the Frank Condon Factors, theoretical estimates can be made to predict which transitions are most likely to occur. This provides insight into solving two of the five questions that were presented earlier. This information also helps put together the theoretical simulations of what the Cs dimer emission spectra could possibly look like. In addition, laser calculations were computed to provide basic information about how much power to expect from the laser and how efficient the laser could be. The information was also used to determine how long the gain length needed to be as well as the operational temperature for the optimal density of Cs dimers. As the first

tests for the cesium cell were conducted, the cesium corroded the anti-reflective coating of the laser cell windows causing the cell to be ineffective. A solution to this problem was found by utilizing heat pipes. An overview on heat pipe theory will also be covered in coming sections.

2.1 Nomenclature

Before discussing the physics of how a Diode Pumped Alkali Lasers (DPAL) laser works, a brief overview of spectroscopy nomenclature will make terms understandable and easy to follow along. As was mentioned in Chapter 1, and can be seen later in Figure 2.7, dimer potential energy structures are much more complicated than just single atom energy structures. Dimers are molecules with two of the same atoms. Unlike the traditional solid state laser systems where we have discrete energy levels, the dimer molecular energy states are not as discrete, but rather have multiple sub-level energy levels due to the rotational and vibrational energies associated with the dimer molecule. The following is a reasonable approximation on calculating both the vibrational and rotational energies but a more rigorous and mathematical model can be followed in reference [19].

Once two atoms combine to form a molecule, a potential energy well is formed. This potential well limits where the molecules with a certain radial distance between each atom are allowed to be. The expression that represents the total potential energy (U) is given by

$$U = -\frac{A}{r^N} + \frac{B}{r^M} \quad \text{EQ 1}$$

where r is the atom separation, N and M are small integers, and A and B are parameters associated with the attractive and repulsive forces, respectively. As can be seen in Figure 2.1, as the atoms draw closer and closer together, the repulsive forces increase causing the system to require energy to put them closer together. This is confirmed by the exponential growth to the left of the curve. If the atoms are pulled apart, there is an attractive force that will force the atoms to stay together, and after a certain distance, this attractive force is broken and the atoms are far enough away to separate and no longer generate forces upon each other. This is shown on the right side of the curve in Figure 2.1.

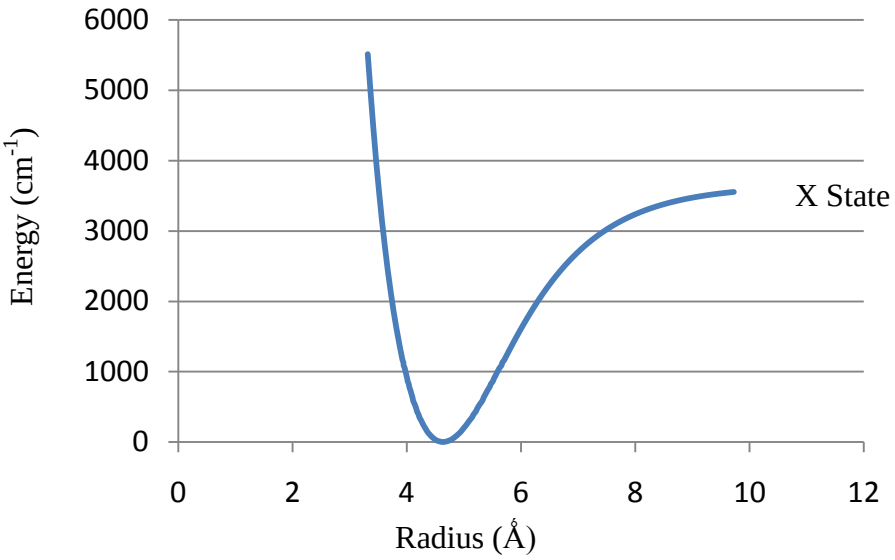

Figure 2.1 Example of potential energy well

Each molecule has multiple electronic states. The lowest energy state, where most of if not all of the molecules reside in at room temperature, is called the ground state.

This is also denoted as the X-State. All the ascending electronic states are labeled with subsequent letters. The dimer molecule not only generates these potential wells in the potential energy graph, but they also induce rotational structure as well as vibrational structure and will be shown in the following sections.

2.1.1 Rotational Energy of Molecules

Rotation of a diatomic molecule (Cesium Dimer) is limited to only two rotational degrees of freedom as seen in Figure 2.2a. These degrees are limited to the axis perpendicular to the molecular axis. If we set ω to be the angular frequency of rotation around one of the axis, then the rotational kinetic energy of the diatomic molecule can be written as

$$E_{rot} = \frac{1}{2} I \omega^2 \qquad \text{EQ2}$$

where I is the moment of inertia usually written as

$$I = \mu r^2 \qquad \text{EQ3}$$

r is the atomic separation, and μ is the reduced mass of the molecule. This can be written as

$$\mu = \left(\frac{m_1 m_2}{m_1 + m_2}\right) \qquad \text{EQ4}$$

Here m_1 and m_2 are the masses of the atoms, which in our case are the same. The magnitude of the angular momentum is the moment of inertia multiplied by the angular momentum. Since these calculations are in the realm of quantum mechanics, the magnitude of angular momentum values have to be multiples of $\hbar$ to be allowed.

$$I\omega = \sqrt{J(J+1)}\hbar \qquad \text{J=0, 1, 2, 3…} \qquad \text{EQ5}$$

where *J* is a non negative integer called the rotational quantum number. Therefore the allowed values for the rotational energy are achieved by combining EQ5 and EQ2 giving us EQ6.

$$E_{rot} = \frac{\hbar^2}{2I}\big(J(J+1)\big) \qquad \text{J=0, 1, 2, 3…} \qquad \text{EQ6}$$

The rotational energy of the molecule depends on the moment of inertia and is a quantized number. Setting $E_1 = \frac{\hbar^2}{2I}$, an example of allowed rotational energy levels of a diatomic molecule are graphed below in Figure 2.2b.

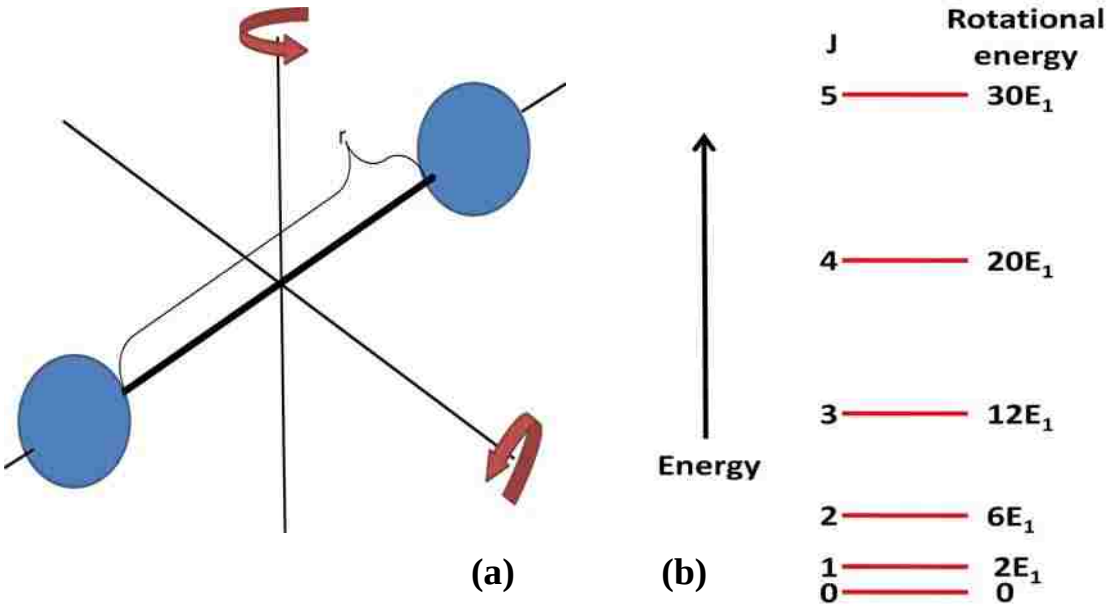

Figure 2.2 (a) Graphical representation of a diatomic molecule with 2 rotational degrees of freedom, (b) Examples of allowed rotational energy levels

2.1.2 Vibrational Energy of Molecules

When a dimer forms, vibrational energies are also created and limited to where these energy levels can form. Since the molecule is sharing some electrons and the atoms are bonded to one another, there is some flexibility that can be modeled in classical dynamics as springs. If disturbed, the molecule can vibrate and receive vibrational energy. The molecule can also absorb energy that can be transferred to vibrational energy, changing the way the molecule is vibrating. Looking again at a diatomic molecule (Cesium Dimer), a model can be derived as two atoms connected with a spring. This can be seen in Figure 2.3a. With a spring constant k, classical dynamics models the frequency of vibration (*f*), as

$$f = \frac{1}{2\pi}\sqrt{\frac{k}{\mu}} \qquad \text{EQ7}$$

where μ is the reduced mass of the molecule. Again, solutions to this system has quantized energy levels allowed like the rotational allowed energy states and is expressed as

$$E_{vib} = \left(v + \frac{1}{2}\right)hf \qquad \text{v=0, 1, 2, 3…} \qquad \text{EQ8}$$

where *v* is an non negative integer called the vibrational quantum number. Something to notice is even at v=0 there is a residue vibration, even if the molecule is not excited. The final expression for the allowed vibrational energy levels is achieved by combining EQ8 and EQ7 to acquire

$$E_{vib} = \left(v + \frac{1}{2}\right)\frac{h}{2\pi}\sqrt{\frac{k}{\mu}} \qquad \text{v=0, 1, 2, 3…} \qquad \text{EQ9}$$

By setting $E_0 = \frac{h}{2\pi}\sqrt{\frac{k}{\mu}}$, an example of allowed vibrational energy levels of a diatomic molecule are graphed in Figure 2.3b. Note that unlike the rotational energy levels, the vibrational levels are evenly spaced apart.

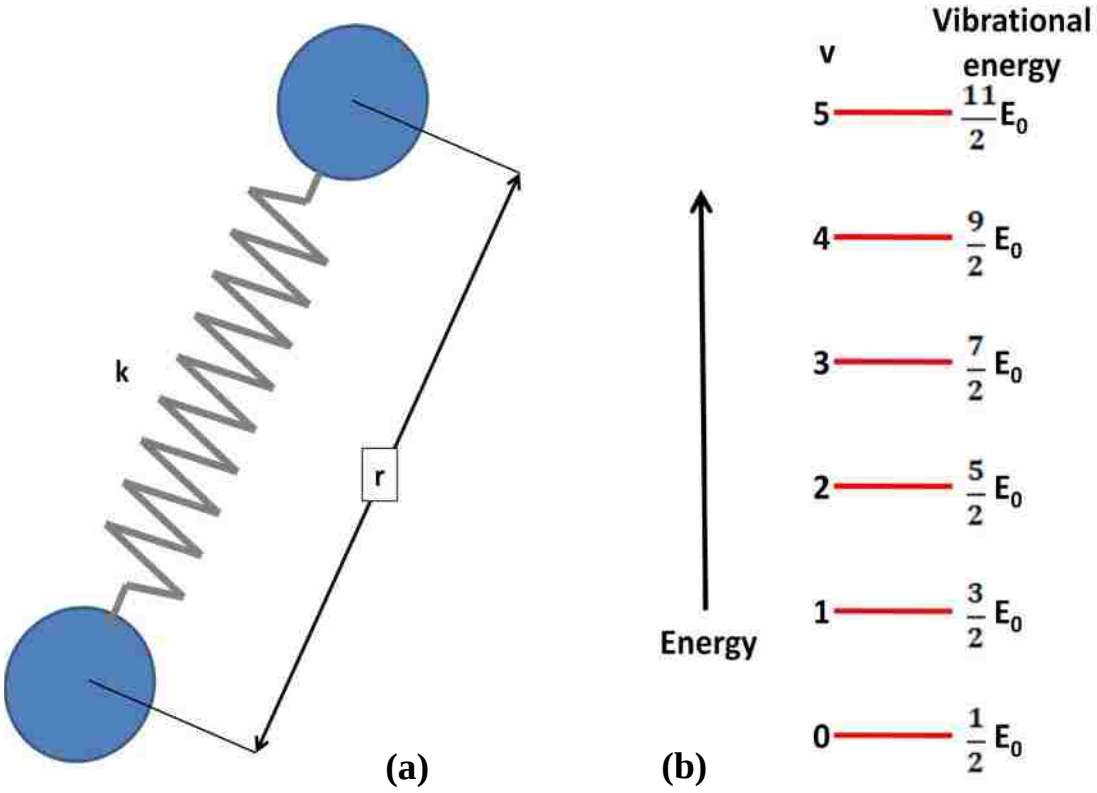

Figure 2.3 (a) Spring model representation of a diatomic molecule, (b) Example of allowed vibrational energy levels

The actual energy calculations for the vibrational and rotational levels are not as simple as stated but by using a more refined but complicated approach, better approximated vibrational and rotational levels can be achieved. All of the vibrational and rotational energy levels were calculated using Excel. To distinguish between the different

molecules, there are vibrational and rotational constants that are known for all the elements. Once a brief literary search was completed, these constants were inputted into the energy equation and the vibrational and rotational levels were outputted.

Once both the vibrational and rotational sub levels are plotted together in a potential energy level diagram, the complexity of the system is seen in Figure 2.4. Just looking at an energy level diagram, it would seem like there is an area of allowed energy states, but looking at the graph's potential well filling, it can be seen that the spacing between energy levels is very small. The spacing between the vibrational sublevels of the ground state of Cs_2 is 42 cm^{-1} and the first rotational sublevel of the ground state of Cs_2 is .01 cm^{-1}. The spacing for the rotational sublevels grows bigger between each step. These are relatively small energy differences between each vibrational and rotational level. If we would compare this to say a carbon dioxide laser, the vibrational spacing's are about 2100 cm^{-1}. Figure 2.4 is a plot of just the first 30 vibrational and rotational sublevels. An expansion of this plot to include all of the sublevels would be overwhelming to grasp.

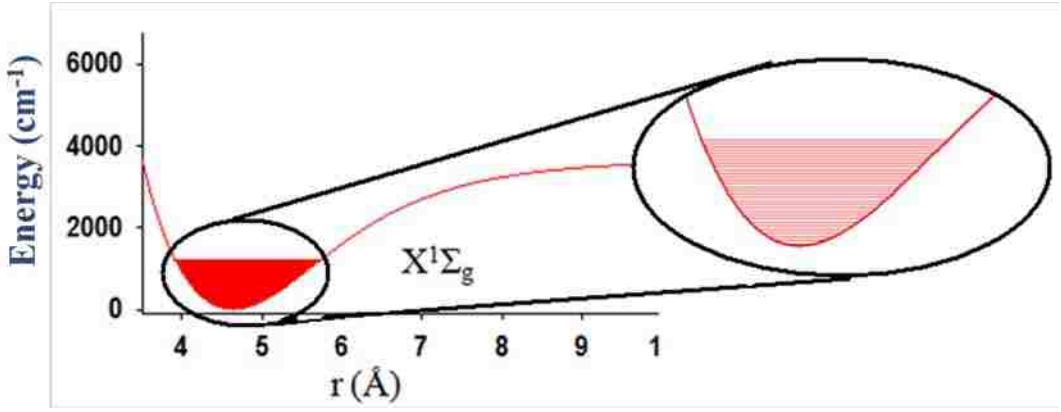

Figure 2.4 Zoom in image of vibrational and rotational energy levels on the ground state of Cs_2

2.1.3 Selection rules and branching types

There are three main types of branching, *P*, *Q*, and *R* branching states that happen in molecular spectroscopy. These rotational and vibrational allowed energy transitions occur for each electronic transition. So for example, there is a J=0 for both the ground state and the lowest excited state A. A molecule can go from the ground state vibrational level 0 to an excited A state rotational level 0. This is called a Q branch line and is shown in Figure 2.5. If a molecule goes from a higher rotational level to a lower rotational level in an upper excited state, this would be called a P branch line. And the last option would be if a molecule goes from a lower rotational level to a higher rotational level, and would then be called an R branch line. Examples of each type of branch level are shown in Figure 2.5.

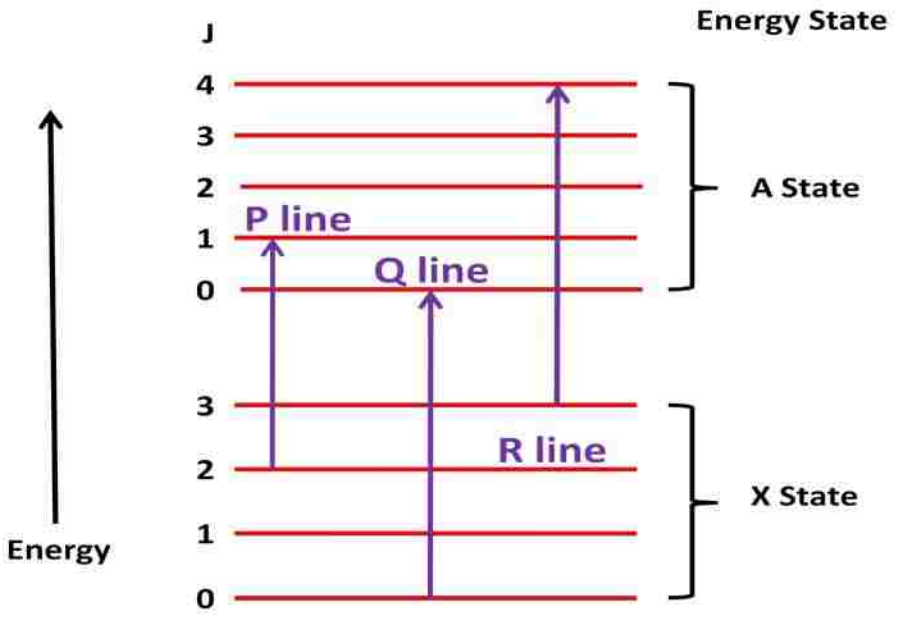

Figure 2.5 Examples of different branch level transitions

The selection rules on the other hand are based on mathematical models that theorists and scientists have developed to try to physically explain the well known spectral results from the early experiments. Since there is no theory that can explain exactly how these quantum energy levels work, an exception can be found to almost every rule. The main rules will be discussed and assumed when calculations are carried out. The selection rules are as follows for diatomic molecules in the same electronic state.

$$\Delta v = \pm 1 \qquad \text{EQ15}$$

Where EQ15 states that the vibrational quantum number of a dimer molecule can change by ± 1, but not ± 3 or ± 4. The second rule is:

$$\Delta J = \pm 1, 0 \qquad \text{EQ16}$$

Where EQ16 states that the rotational quantum number of a dimer molecule can change by ± 1, or 0, but nothing more. The last rule is:

$$J = 0 \not\leftrightarrow J = 0 \qquad \text{EQ17}$$

Where EQ17 states that transitions between electronic states with J=0 is forbidden. These are the selection rules that were followed to calculate transitions suitable for lasing. The next topic of discussion is how to calculate the probabilities of going from one state to another, called the Frank-Condon Factors.

2.1.4 Franck-Condon Factors

Franck-Condon factors are important in the study of diatomic molecules because it explains the intensities of vibrational and rotational transitions. These factors are well known in spectroscopy and the quantum mechanics behind the transition of a molecule due to the absorption or emission of a photon is understood. The Frank-Condon Factor principle states that the probability of an electronic transition depends on how much overlap the two vibrational waveform potentials have. The more the waveforms overlap each other the more likely the specific electronic transition is going to happen. Not only do the waveforms have to overlap well with each other, but the molecules need to have their nuclei vibrating in a similar fashion. This leads to vertical transitions in an energy diagram and no horizontal movement, because in a classical sense, electron orbital's can be readjusted much faster than the slower vibrational motion of the nucleii. In Figure 2.6, from the v″=0 ground state, the most likely transition into an excited state would be into v′=2 since it is vertically above the ground state.

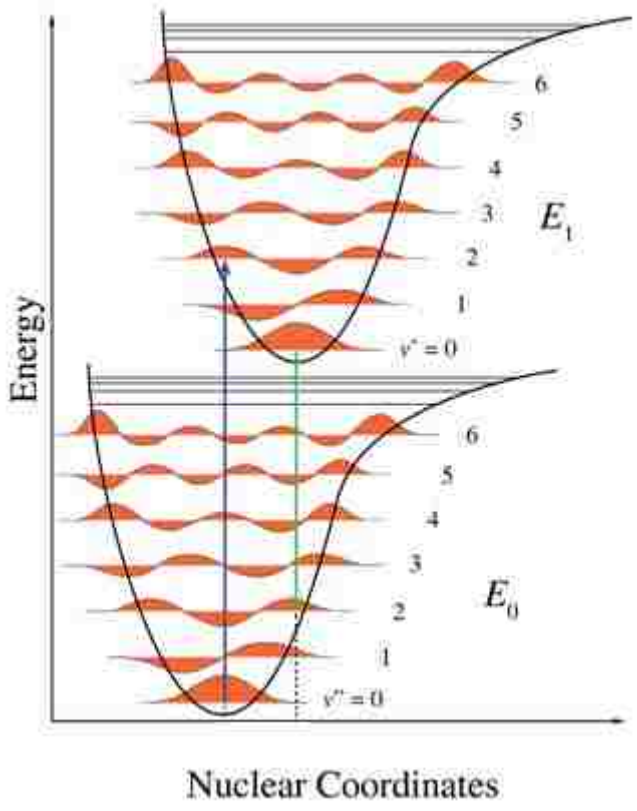

Figure 2.6 Examples of dimer transitions [20]

The same goes for the transition from the excited state v′=0 to the ground state v″=2. The Franck-Condon Factor is a rule that is applicable to both the absorption and emission of a dimer molecule.

The first 90 vibrational levels of both the X ground state and the B excited state were calculated for Cs_2. Professor Mark Masters from Indiana-Purdue University was kind enough to send us a program that calculated all the Franck-Condon Factors for dimer molecules. The spectroscopic vibrational and rotational constants were found by a literary search, and then they were plugged into the program as variables. The program also asked how many vibrational levels it should calculate for both the ground state and

the excited state B. The most the computer could calculate before freezing was 90 so I calculated 90 levels. They were then put in a 3-D graph to help visualize where the best pump probe measurements needed to be. Although the graph is very overwhelming and the detail is lost when looking at all the vibrational levels at once, zooming in to a select area of interest makes the graph very helpful. The 3-D graph is shown below in Figure 2.7.

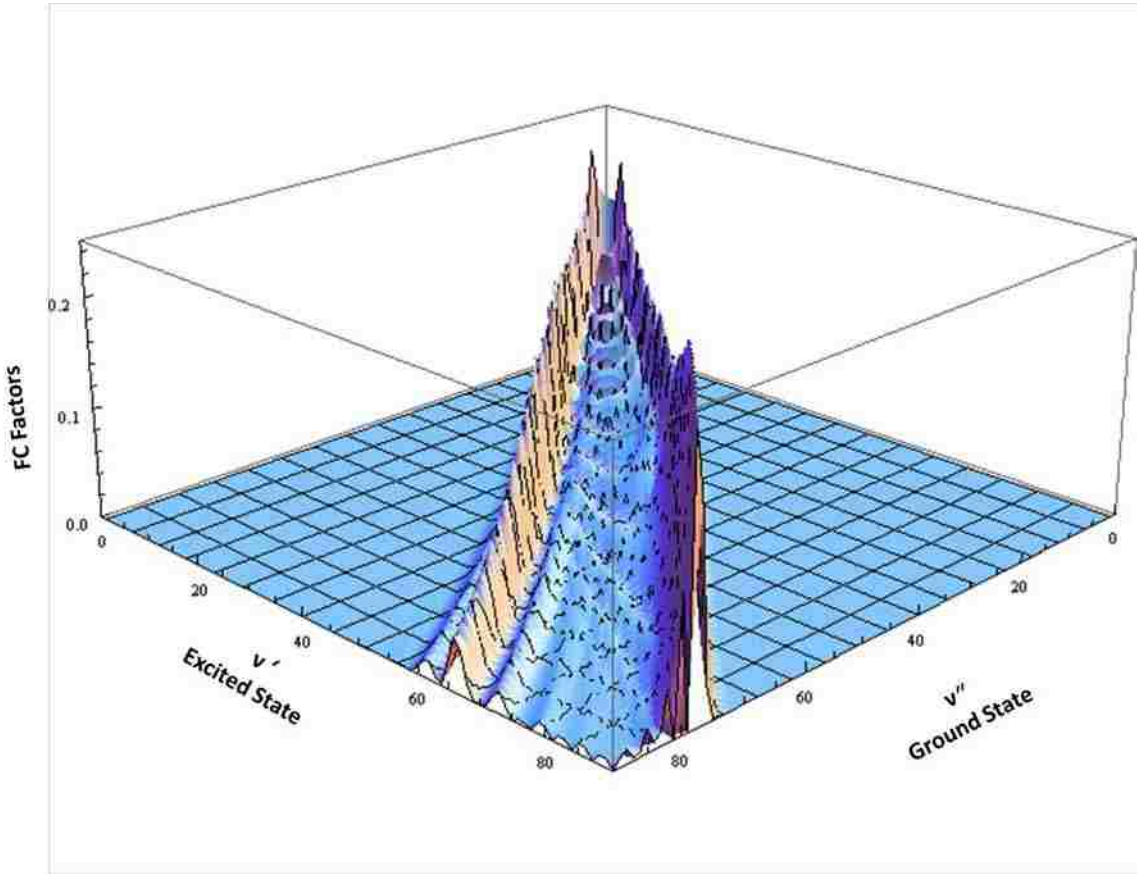

Figure 2.7 3-D graph of Frank Condon Factors for the first 90 states of the ground X state and excited B state.

If the 3-D image is zoomed in for example to see the ground vibrational states of 15 to 50, and the excited vibrational states of 25 to 35, as seen in Figure 2.8, an example

of a pump probe measurement can be given. If the laser pumps the vibrational level 18, the best transition to excite, the one with the highest FCF (Frank Condon Factor), would be the excited vibrational state 30. When looking for a good lasing state, a transition that has a high FCF would be the best choice. By moving along the other ridge, if the molecule rovibrationally relaxed a level, say excited state 29, the molecule be perturbed by stimulated emission and relax down to the ground vibrational level 41. This satisfies both the desire for a large FCF transition as well as the most probable transition where there are no molecules on that ground state level due to thermal occupation. The energy level graph can be seen in Figure 2.8b.

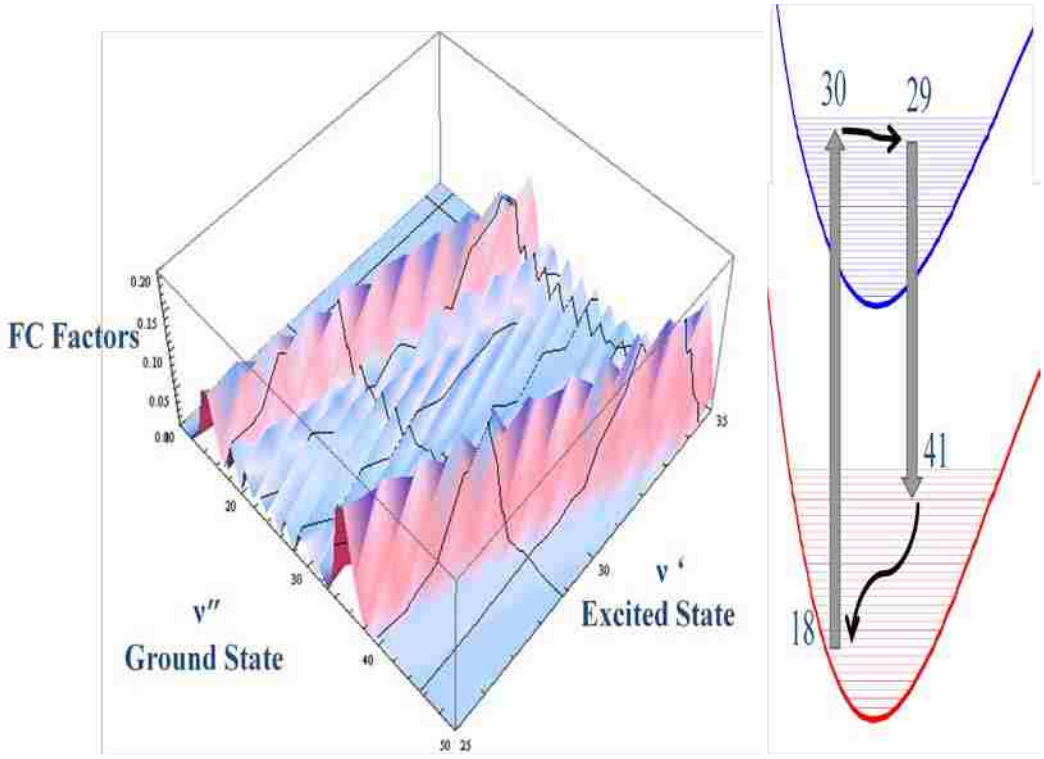

Figure 2.8 (a)Zoomed in 3-D graph of Frank Condon Factors pump probe graph (b) energy level representation of example potential pump probe measurement

2.2 How an Alkali Dimer Laser Works

This section touches upon how a simply designed alkali dimer laser works. First, an optical pump source is used to create a population inversion into a high vibrational level of the excited state. Since there are many “sub bands”, traditionally, the most efficient way of exciting a specific energy level would be optically pumping with a narrow-band source, most likely a laser. The final objective would be to pump the alkali using a narrowband diode, making the laser a DPAL (Diode Pumped Alkali Laser). The pumping is labeled as 1 in Figure 2.9. Then, rovibrational relaxation causes the molecules to move down the potential well. This relaxation can be caused by atoms running into themselves, or inert gas that has been added to help broaden the absorption. An inert buffer gas is added because without it, the molecule would be excited up to a higher energy level, and then directly relax back down to the ground state giving off the same wavelength that had been absorbed, which results in very low absorption. Consequently, using cesium dimers as a gain medium also cuts down the need of adding as much buffer gas. The cesium dimers will run into each other inside the cell and relax the electrons to an energy level desired for lasing. The relaxation is denoted as 2 in the Figure 2.9. Next, there is lasing down to a high vibrational level in the ground state that isn’t thermally excited. Lasing down to a high vibrational sub level is usually done because there is a population inversion between the excited level in the excited state compared to the lower energy state. This is denoted in the Figure as number 3. In the last step, rovibrational relaxation takes the atom back to the lower ground state level that it was excited from in

the beginning so the process can start all over again. This is denoted in the Figure 2.9 as number 4. This is how a simple alkali dimer laser operates.

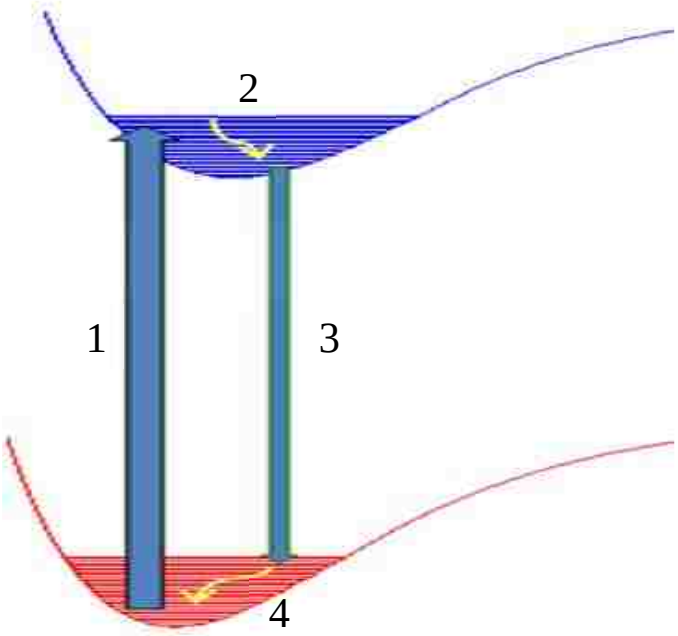

Figure 2.9 Example of an alkali dimer laser operation

2.3 Cesium Dimer Simulations

Once all the previous terms such as vibrational and rotational allowed energies, Morse Potentials, and the Frank Condon Factors for the different ground and excited states were calculated, they were used to plot some simulations of what the cesium dimer would emit. An example can be seen plotted in Figure 2.10. This plot was created by using the FCF's and inputting the information into a program called Sigma Plot. From

there the FCF's were given a Doppler width, and then the data points were exported and plotted in Excel.

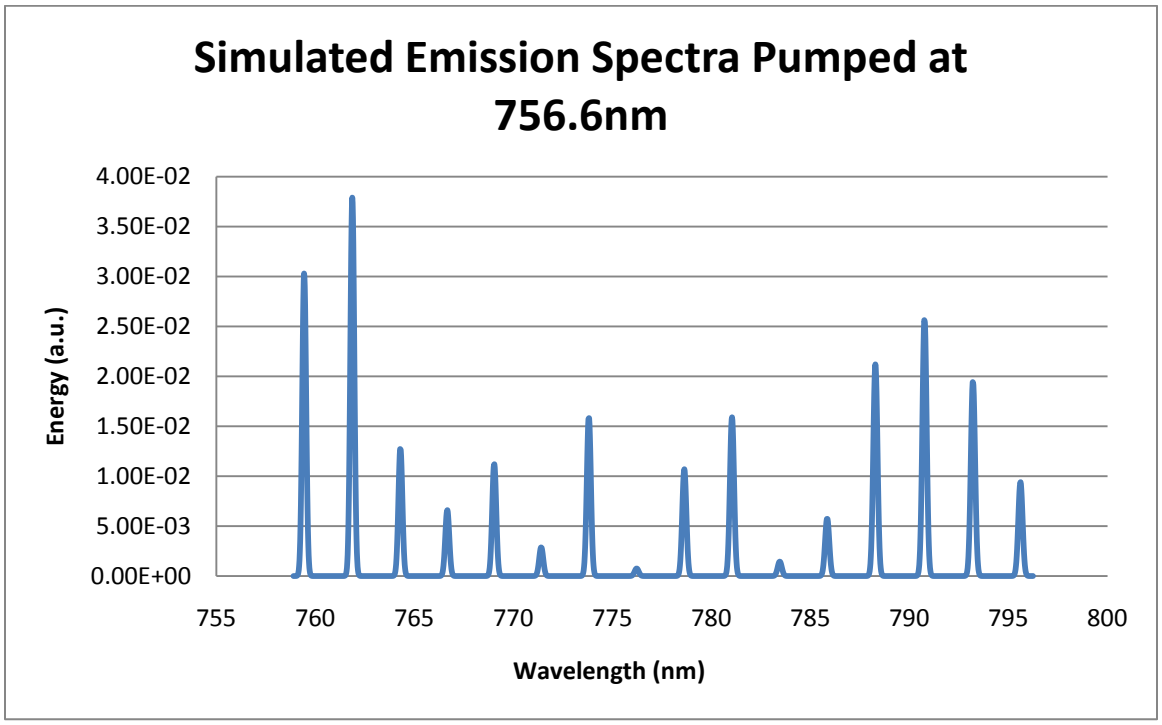

Figure 2.10 Plotted results of stimulated emission from calculations being pumped at 756.6 nm

When looking at the graph, we can see there are many different emission wavelengths available from ~760nm to 800nm. By looking at the intensity it is possible to identify which transitions are most likely to occur. When making these graphs, a Doppler width was added to give the spectra peaks a finite width. The Doppler spread was chosen because of the low pressure used, and was calculated based on the desired experimental temperatures. These graphs will be used to compare our experimental spectra and note if indeed the cesium dimer behaves the way it is predicted to behave. When comparing both spectra's, the simulation and experimental data had to be

normalized to certain value depending on the pump wavelength, and could then be compared. After calculating the simulated emission spectra, estimates on the laser emission were done. Additionally, a few calculations were done to predict, one of which was to determine how large to make the cesium cell to achieve the maximum output.

2.4 Laser Calculations

In order to see gain on the pump/probe measurements, calculations of number density, absorption cross section, and gain length are desirable. Once these parameters are calculated, they can be used to optimize the output of the potential gain of the pump/probe measurements.

2.4.1 Number Density

The path taken to calculate the number density of cesium dimers in the cell and in the heat pipe was as followed. The controllable parameters were the temperature of the cell, and in the heat pipe case, how big the cell volume was. Since the pressure in the cell could not be measured, the vapor pressure curve of Cs_2 was used to calculate the vapor pressure inside the cell. The vapor pressure equation was given by Dr. Benedict [21] was as follows:

$$\log P = 18.22054 - \frac{6064.472}{T} + 9.016 \times 10^{-5}(T) - 3.45395 \log T \quad \text{EQ18}$$

Where P is pressure in mmHg, and T is temperature in Kelvin. Once the pressure is calculated, and utilizing the ideal gas law, the number of moles in the cavity can be found. Then dividing by the volume and multiplying by Avogadro's number, we can find the number of molecules we have of cesium. Rearranging the ideal gas law gives:

$$n = \frac{PV}{RT} \quad \text{EQ19}$$

Where P is the pressure, V is the volume of the cell, R is the gas constant of Cs (69.4), T is the temperature, in Kelvin, and n is the number of moles. The volume was calculated to be about 60 ml assuming the cell length of the heat pipe is 12 cm from one cooling block to the other. The final density of molecules was 4.8×10^{14} molecules/cm^3.

2.4.2 Absorption Cross Section

Once the density of molecules was calculated, the next step was to calculate the absorption cross section. Since the absorption cross section is wavelength dependant, there were no specific publications of absorption cross sections by other research associates. There were however a few publications on the absorption coefficient, which was used to calculate the absorption cross section. First, the absorption coefficient was obtained for the wavelength and temperature intended on running the experiments found in this paper [22], and used it to calculate what was missing:

$$\ln \frac{I}{I_0} = \alpha \times x \quad \text{EQ20}$$

where I is the intensity of a light source after going through a medium, I_0 is the original intensity from the same light source before going through the medium, α is the absorption coefficient, and x is the length of material the light goes through. A diagram can be seen in Figure 2.11.

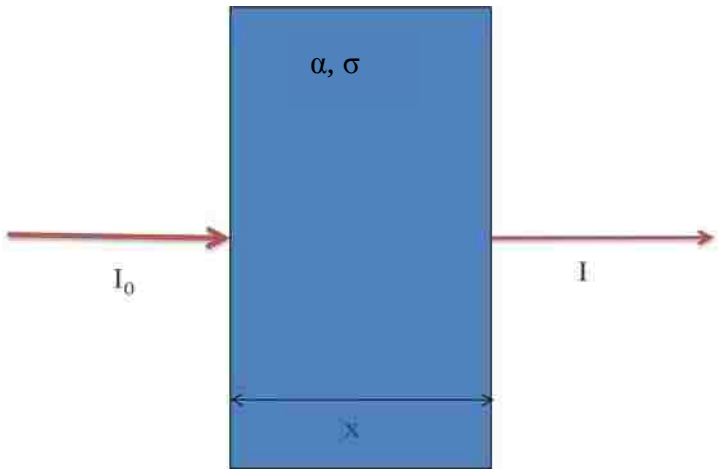

Figure 2.11 Diagram of the Beer-Lambert Law

Substituting the information for the right side and solving for the left, the absorption cross section is solved with the following equation:

$$\ln\frac{I_0}{I} = \sigma \times L \times C \qquad \text{EQ21}$$

where σ is the absorption cross section, L is the length of the cell, and C is the concentration or density of molecules in the volume. Solving for the absorption cross section gives 5.9 x 10^{-16} cm^2/molecule. This will be compared to the experimental value in a later chapter. Now the length of the cell needs to be estimated to make sure the correct length of a gain cell is used.

2.4.3 Gain Length

The gain length was estimated using the Beer-Lambert law. The assumption here was to try to get as much pump power absorbed as possible. By looking at the equation:

$$\ln\frac{I}{I_0} = \sigma n L \qquad \text{EQ22}$$

the free variables are the absorption cross section(σ), the density of molecules(n), and the gain length(L). In reality, the glass cells used had a distinct length associated with them. The remaining free variables were the density of molecules and the absorption cross section. These both could be changed by changing the temperature but only to a certain extent. An example is given in Figure 2.9.

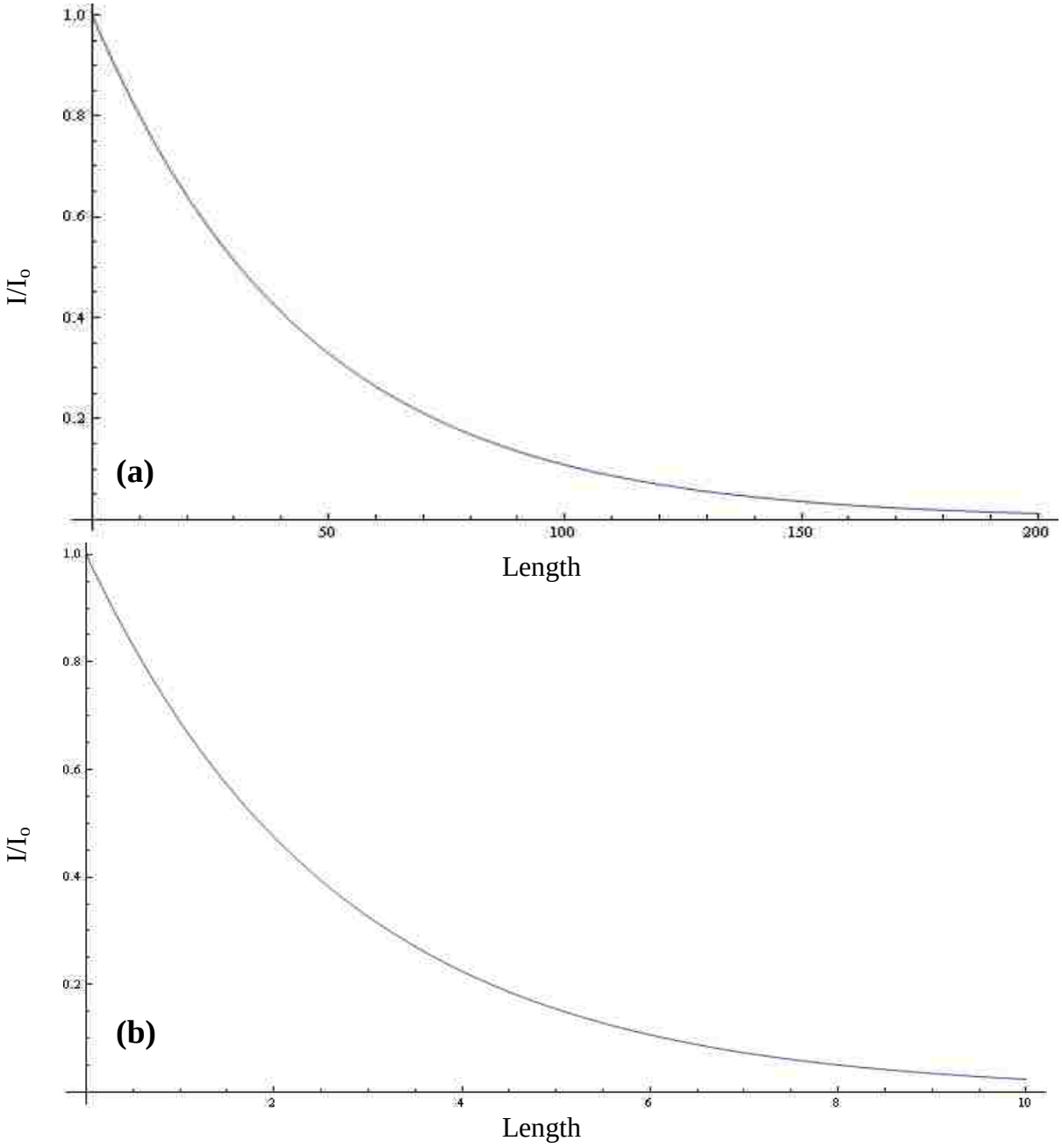

Figure 2.12 Plotted I/I_0 versus gain length of (a), cesium cell at 240 C and (b), cesium cell at 320 C.

Looking at Figure 2.12a, if it was desired to get 50% absorption of the pump laser, this simple calculation estimates that the gain length of the cell should be ~34 cm long at 240 C. If the temperature is raised to 320 C, the absorption gets stronger as shown in Figure 2.12b where the same 50% absorption is estimated at ~1.8 cm. Other thermal issues will be discussed in later sections.

2.5 Device Design

As mentioned earlier, there were two different cesium cell containers used in this research. At first, a glass cell made from Spectrocell with a few milligrams of cesium was filled. As the research prolonged, it seemed desirable to raise the temperature beyond the heat and pressure the cell could handle. It was then decided that a better container for the cesium was needed and research began on finding a solution. In the end a heat pipe was chosen, and the following is a discussion on the positives and negatives of both the glass cell and the heat pipe.

2.5.1 Glass Cell

The glass cell was purchased from Spectrocell and was filled with a few milligrams of cesium. The cell windows were made out of sapphire, and were coated with antireflection coatings for the wavelength range of 650-1050 nm. The cell was also 7.62 cm long and its small size was beneficial because of the completed laser's need to be small as well. Another advantage was that the cell was already filled up and ready to go when it was received. Because the cell was sealed, the pressure inside in the cell was known by the temperature. This was also how the density of molecules was known at

each pressure. The sapphire windows had antireflection coatings to maximize the output emission. There were also negative issues associated with the glass cell as well. One of the biggest issues was that the cell was pressure limited. The cell could only be taken up to a certain temperature before the pressure would puncture the cell. The glass cell also had a temperature limit before the glass would deform. The cesium collecting on the windows would react with the antireflective coatings creating black crystals that ruined the cell. There were some precautions taken to try to keep the cesium off the windows, such as heating the ends of the cell to a higher temperature than the middle, but eventually after time, the cesium would reach the windows and collect on them. Another issue was that because the cell was small, there was a small gain length. Looking at Figure 2.9, it can be seen that running the cell at temperatures of 250 C would not be enough to see gain from the glass cell. Another issue is the cost of purchasing these cells. Once the cell is damaged, there is no way to fix the cell; a new cell had to be ordered. Another issue of the glass cell is of its “one time use”, meaning once it was filled, it couldn’t be refilled. The cost of replacement was the full cost of the cell. After a few cells had been damaged, looking at an alternative replacement was explored. The final decision was to build a heat pipe.

2.5.2 Heat pipe

The idea of using a heat pipe for a laser cavity was suggested since it has been used for a long time as a heat conductor. The physics behind the heat pipe that was designed will be discussed and then benefits from the heat pipe will be given. Negative issues with the heat pipe will be discussed at the end.

The design for using a heat pipe in our research is shown in Figure 2.12. The heat pipe was composed of a stainless steel pipe, liquid material (Cs), and a metal grating to be used as a wick. The heat pipe is heated from the middle and the Cs forms a vapor. This is noted as 1 in Figure 2.12. The vapor flows away from the source of heat and moves from the middle towards the ends to be cooled as noted as 2 in Figure 2.12. The ends are cooled with cooling blocks and to speed up the condensation process they are set up to be very cold, >20 C. As the material condensates on the mesh in the cell, the liquid Cs is drawn towards the middle of the cell from the heat by capillary forces and noted as 3. Once the material makes it back in the middle, it is evaporated and the process is repeated. The only limiting factor on the temperature maximum on the heat pipe is due to container material.

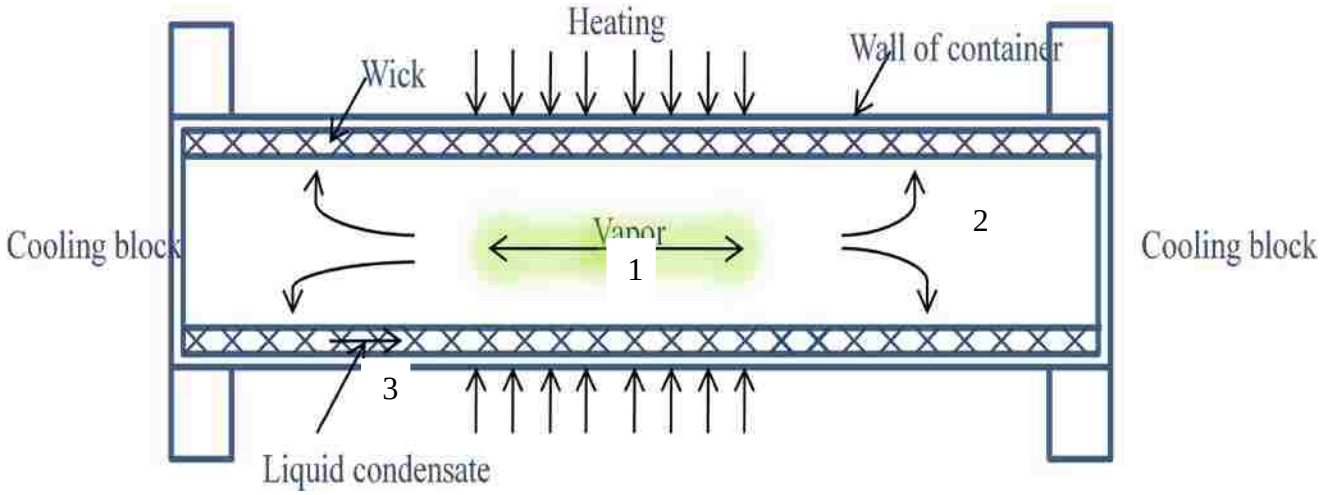

Figure 2.13. Heat pipe used in experiments

Since our windows are kept at room temperature it is imperative that cesium deposition on the cell walls does not occur. This was enforced by adding another set of

cooling blocks near the windows. The inner set of cooling blocks were set to 20 C, the freezing point of cesium. The outer set of cooling blocks were set at 12 C, to make sure none of the cesium vapor went out and deposited on the windows. This set up worked very efficiently and to date there has been no deposition of cesium on the heat pipe windows. Another advantage over the glass cell is that this heat pipe can be taken to the limit of the heaters, 375 C, as compared to the glass cell's limit of 220 C. This designed heat pipe can take temperatures up to 1200 C. There are many advantages of using a heat pipe instead of the glass cell. One reason is that the temperature of the cesium in the cell can be taken much higher than allowable in the glass cell. The hotter the temperature, the more cesium dimers are made until a limit is reached and the dimers receive enough energy to break apart, cracking temperature. The thermal disassociation of cesium dimers is ~500 C [23]. Since our heaters only allow up to 375 C, there is no worry about breaking up the dimers. Another advantage of using the heat pipe is that the windows of the heat pipe are kept at room temperature without worry about condensation of cesium on the windows. With the glass cell, care had to be taken so that the ends would always be at a higher temperature than the rest of the cell, otherwise the cesium would stick to the windows. Another advantage of the heat pipe is that the cell length was adjustable. Depending on where we place the inner cooler blocks, we can change the cell length from 12 cm to 1cm. There is a final length of 12 cm though that can't be changed unless a bigger heat pipe is built. Another advantage was its reusability and the ease of refilling. Although there was never a need to refill the heat pipe, the heat pipe could be opened and

filled with different gases and different alkali metals with ease. A picture of the heat pipe can be seen in Figure 2.13.

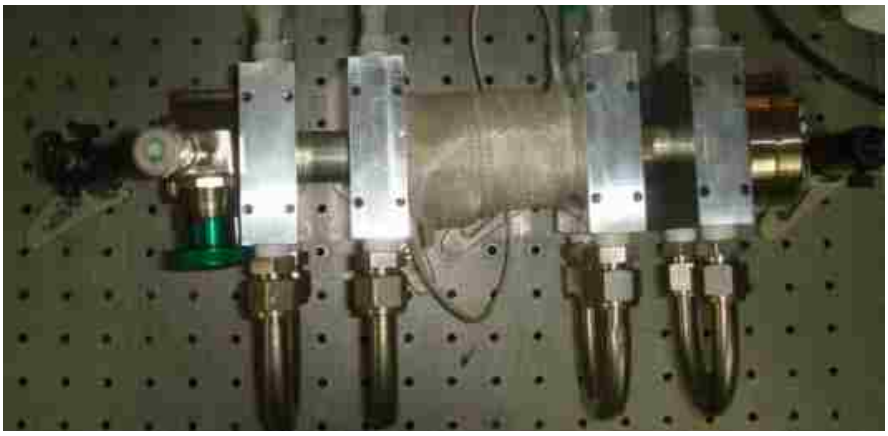

Figure 2.14 Picture of heat pipe used in experiments

Although the heat pipe had many advantages, there were also some disadvantages compared to the glass cell. The most noticeable is that the heat pipe is bulkier. Where the glass cell is about 7.6 cm long and 1 cm thick, the heat pipe is 30 cm long and 7.6 cm thick. This does not include the cooling blocks though, which would make the size even bigger. Another issue is that because we were running a heat pipe in a certain regime, there had to be a Cs test done after turning on the heat pipe each time to make sure the heat pipe was running correctly. This test was done by passing a laser with a certain wavelength through the heat pipe, and detecting Cs_2 dimer emission spectra. Although the test was very quick, the test wasn't necessary for the glass cell. Another issue with the heat pipe that will be discussed later is the fact that there was a temperature gradient throughout the cell. Although it was assumed that the temperature remained the same

throughout the cell, it actually changed drastically from the middle of the cell to the first set of cooling blocks.

Since cesium reacts heavily with oxygen, there were specific steps that needed to be taken to fill up the heat pipe without having any contaminants or reactions. Once the heat pipe was built, it was heated up to about 120 C and put on a vacuum pump and pulled down to 10^{-8} Torr. Once the heat pipe is clean, meaning all the water and other particles have been sucked out and heated up, it is put in a nitrogen purged glove box. This is where the cesium is stored to prevent it from reacting with the oxygen in the air. Cesium is taken with a depositing spoon and placed in the center of the heat pipe. 2.5 grams of cesium was deposited inside the heat pipe and then the heat pipe was sealed up again. Then the heat pipe was taken out of the glove box and placed on the fill station to pull the nitrogen out of the cell. A few purges were completed to make sure none of the cesium gets pulled into the system. Once the nitrogen is pulled out, 2 Torr of helium was added to the cell to broaden the absorption transitions slightly. Once that was completed, the cesium heat pipe was ready to be used. Figure 2.14 shows the glove box and fill station set up.

Figure 2.15 Picture of (a) Nitrogen purged glove box and (b)fill station

Now that all the calculations and theoretical assessments have been made, discussion of the experimental set ups will be talked about as well as the tests that were completed. Discussion of why each experiment was done, and what questions they were trying to answer will be given as well.

CHAPTER 3 - DATA AND MEASUREMENT

3.1 Measurements

In looking to answer the first main goal of this thesis, finding out if Cs_2 can be a suitable gain material for alkali lasers, a few questions were mentioned earlier that needed to be answered:

I. What is the optimal pumping wavelength

II. What is the lasing wavelength

III. What is the optimal Cs_2 concentration

IV. What is the minimum gain length required

Analysis and experiments were completed to solve each of these problems. Since each experiment had its own unique parameters specific to each experiment, they will be discussed separately and all pieces of equipment will be discussed. There were also some measurements done with both the glass cell and the heat pipe and they will be mentioned as well.

Laser induced florescence was used to find an optimal pump frequency of the system. The results of this were then compared to the calculated spectral emissions as explained in Chapter 2. For finding a suitable lasing wavelength, traditional pump probe double resonance measurements were done. This experiment had quite a few hurdles during its implementation. Explanations as well as solutions will be given in detail later in the chapter. Finally, an explanation about the heat pipe measurements that were taken and the corrected method after noticing some inconsistencies between the simulations and the experimental values will be presented. Utilizing these experiments, the last two questions of finding the optimal dimer concentration and the minimum gain length required for lasing will be discussed in a later chapter. All of these tools and lasers were available courtesy of Air Force Research Laboratory's (AFRL) Center of Excellence (COE).

3.2 Fluorescence Measurements

The laser induced florescence was used to solve one of the sub questions of finding an optimal pump frequency for Cs_2. The results of this experiment were then compared to the calculated spectral emissions as explained in Chapter 2. The experimental set up is shown in Figure 3.1.

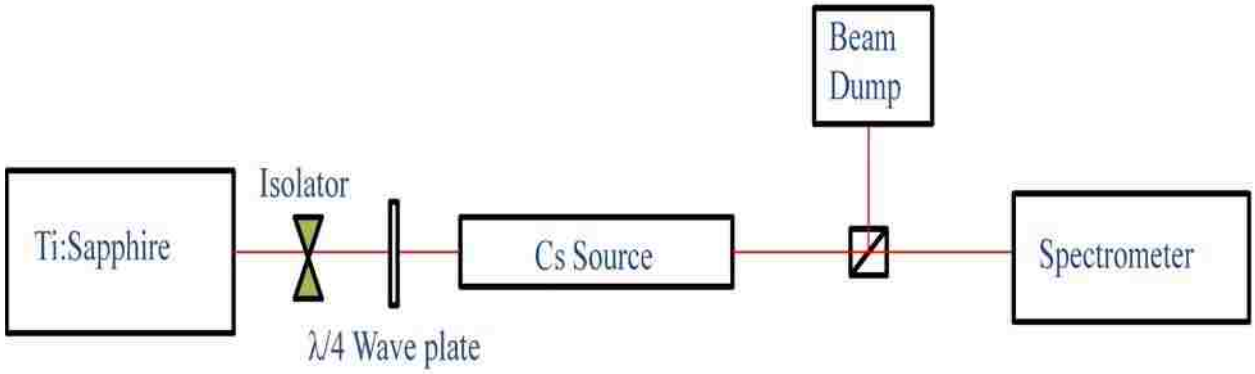

Figure 3.1 Florescence measurement set up diagram

In the fluorescence measurements, a Coherent Verdi V-18 green pump laser from an optically pumped semiconductor emitting at 572 nm was used to seed a Titanium Sapphire (Ti:Sapphire) laser made by Sirah. The Verdi was pumped to produce approximately 5 watts. This laser excited a sapphire crystal doped with titanium that emitted out a tunable wavelength range of 700-900 nm which was controlled by a grating. The lasers output was continuous wave, and had a max power of 5 watts. In the experiments this laser was outputting power from the range of 30 mw to 300 mw.

The laser light was then passed through an isolator to prevent the power from going back into the laser, and then passed through a quarter wave plate to polarize and

separate the laser light from the output emission of cesium, and finally went into the Cs_2 cavity.

The cavity consists of a glass cell with sapphire lenses on each end to allow the laser light to pass through freely. Since cesium is an alkali metal, it is very reactive with oxygen and water. The cell was filled in a nitrogen filled glove box. Care was taken during the filling to keep it free of oxygen. After filling the cell with the desired amount of cesium, ~milligrams, it was pulled out and the nitrogen was pulled from the cell by pumping it out. Then after all the nitrogen was pulled, the cell was seared shut. The first layer is a metal casing to create an oven like effect. Before the metal casing was put over the cell, a thermo couple was attached to the glass cell to detect its temperature. There were 3 openings in this metal casing, two of them were at the ends of the cavity so the laser light can pass freely, and an additional small hole at the top of one of the edges so observations can be made inside the cell during the experiments. A picture of the glass cell is shown in Figure 3.2.

Figure 3.2 (a) side view with both laser beam entrance and observation hole. (b) cell wrapped in metal "oven", evenly wrapped heater rope, and insulated with fiberglass rope.

A photo detector was usually put up against the top hole in the metal casing seen in Figure 3.2a, to see what wavelengths were generated inside the cell. An ocean optics USB4000 photo detector was placed at the observing hole which showed what was happening in the cavity. This detector had a spectral range of 600 nm to 1400 nm. This photo detector was used for alignment and detection of cesium and cesium dimers. This photo detector had a fiber optic attached which gave good flexibility. Heat rope was evenly wrapped over the entire metal cavity. The cell cavity was then wrapped in a fiberglass insulation rope to insulate it and mitigate heat dispersion. The cell was heated to 245 C to excite the cesium and produce dimers. As the laser beam travels through the heated cell, cesium dimers absorb the Ti:Sapphire laser light, become excited, and then emit at their different wavelengths. The output cesium dimer radiation is reflected by a polarizing beam splitter and the cesium dimer output is captured by a monochromator. Since the emission of the cesium dimer spanned from 750 to 1800 nm, two different monochromators were used to record the data. For the beginning spectra, mainly 750-850 nm, a Spect-10 monochromator built by Princeton instruments was employed. The output was captured, graphed, and processed using WinSpec. Once we reached the end of the spectrum for the Spect-10, a more IR sensitive monochromator was used. A SpectraPro 2300i IR monochromator was used to analyze wavelengths from about 800nm-1800nm. This was placed at the same location as the Spect-10, and the same test was performed. The light was coupled into a fiber that was connected to the monochromators.

One sensitive issue to this experiment was the positioning of the fiber head of the spectrometer with respect to the incoming radiation. Since the polarizing beam splitter is not completely efficient, some of the output of the Ti:Sapphire would bleed through and saturate the camera giving unreliable and artificial emission spectra. After a few experiments, it was noticeable when the camera was reading the cesium dimer output, compared to the Ti:Sapphire laser. When the camera was reading the cesium dimer output, the spectra showed peaks every few nanometers, but when the camera was reading the laser input, the spectra either didn't show up at all, or big gaps would saturate the camera. This was solved by adjusting the camera if signs of light saturation hit the fiber head.

In other experiments to determine if the output spectra were from Cs_2, solutions such as using filters and wavelength dependant mirrors were employed. An example of the output spectra is shown in Figure 3.3. Notice that pumping at 754 nm excites the spectrum from ~762 nm to ~810 nm. The transitions appearing after 800 nm are from the excited A state of the cesium dimer. Therefore pumping into the excited B state also allows some of the excited A state transitions to happen. This will be discussed later as a potential hindrance of overlapping bands. The losses of pumping to the excited B state and having some excited A states become excited could be detrimental to seeing gain in the system. There are over 20 recorded emission spectrums like Figure 3.3 provided in Appendix 1. All transitions that were stronger than the noise floor were noted and kept as potential pumping or lasing wavelengths. All of the strong emissions were recorded and saved as potential attractive pumping wavelengths.

The results from this experiment, the peak emissions of Cs_2 recorded would be used as potential pumping wavelengths for a future pump probe measurement to try and detect gain. This future experiment will be discussed later in the chapter.

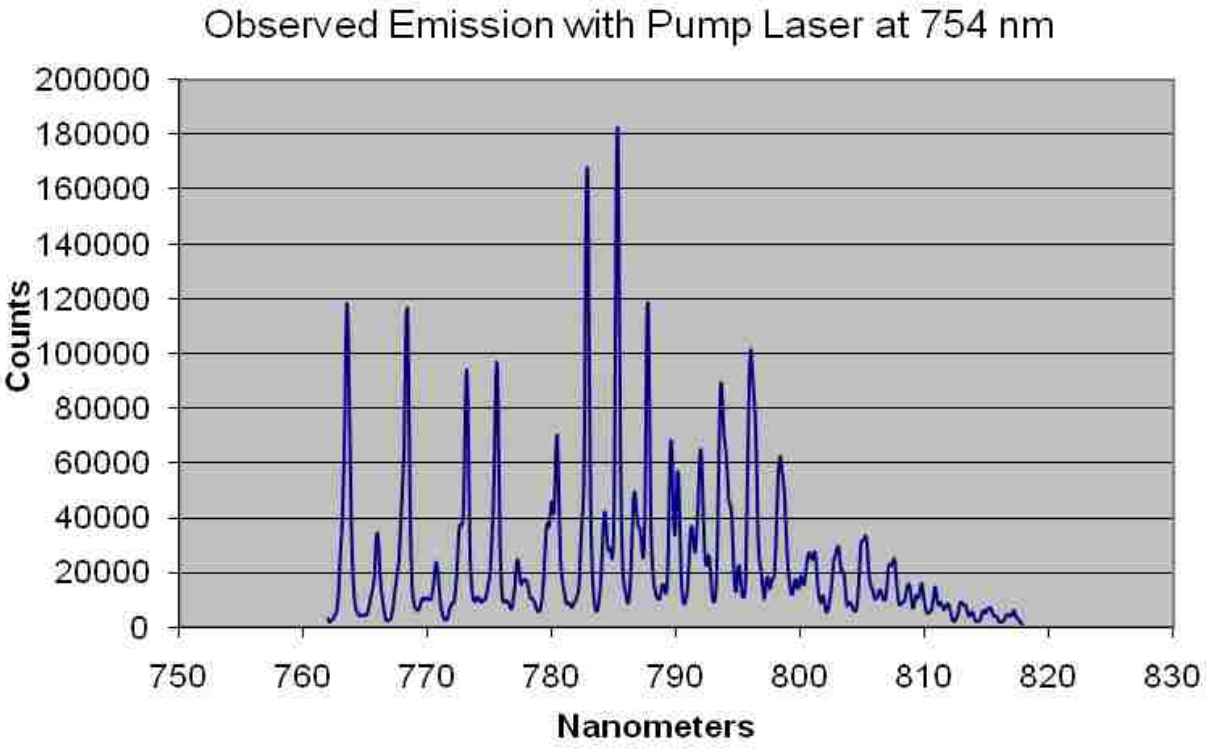

Figure 3.3 Emission Spectra of Cs_2 pumping at 754nm

Another interesting experiment that was run was to pump the cesium dimer with a more powerful laser to investigate if the spectrum changed or had a different preference of emission. The laser chosen was a yttrium aluminum garnet (YAG) pumped dye laser. The YAG crystal was excited by flash lamps and created a green 532 nm laser emission that pumped dye which had variable spectra depending on the dye pumped through the system. The wavelength range is 545 to 900 nm depending on the type of dye supplied.

The dye that was chosen was Exciton LDS 751, which had a wavelength range from 714 nm to 790 nm. The output laser would be a pulsed output, about 20 mW at 10 Hz. The pulse duration was about 8 ns and this resulted in an average peak power of 250,000 watts. Once the dye was chosen, there were a few sensitive steps that were done to get the type of dye needed. First the old dye circulator needed to be cleaned of the old dye. This was done by flushing the system with methanol a few times and running the methanol throughout the laser dye cells. Then using a scooper, the dye powder was put on a very sensitive scale and about .07 grams were taken out. Since the wavelength is solvent dependant, the type of solvent was determined. The wavelength is also dependant on the concentration of the solvent and this was noted. This dye was mixed with 500 ml methanol which gave the specs given previously. Once the dye was thoroughly mixed it was cycled through the dye cells for about 15 minutes and then the laser was warmed up to use.

Using this laser as a single pump source was not sufficiently on long enough to be recorded by the photo detector. There was no way to sync both the photo detector and the dye laser together so the photo detector could record when the YAG pumped dye laser was pulsing. In the end, we saw the same dimer output by overlapping both the YAG pumped dye laser and the Ti:Sapphire laser and pumping at the same wavelengths. With this overlap of both lasers at the same wavelength, we could see the stronger transitions, but overall the spectrum was very similar to the output of when the Ti:Sapphire was pumping alone. Another thing to note was that each time spectra were measured, the peaks intensity relative to one another weren’t always the same, although the same

transitions occurred. This was attributed to the cesium dimers not always absorbing the same amount of energy.

In conclusion to this experiment, the results were very similar to the previous experiment with just the Ti:Sapphire laser pumping the Cs_2 dimer. Although the YAG pumped dye laser excited higher levels, the wavelength peaks were the same as the previous experiment.

Once these measurements of both pumping Cs2 with the Ti:Sapphire laser and the YAG pumped dye laser with the Ti:Sapphire laser were completed, comparison of the simulated spectra and the experimental spectra was investigated. Looking at Figure 3.3, it can be seen that the overlap of both the experimental and simulated emission of Cs_2. Although the peaks have great overlap, the specific amplitudes on each peak are not the same. Slight discrepancies can be explained by calculation simplifications and not using all the possible states allowed. The simulation emission of Figure 3.4 was calculated using one rotational level per vibrational level although there are multiple rotational levels per vibrational level.

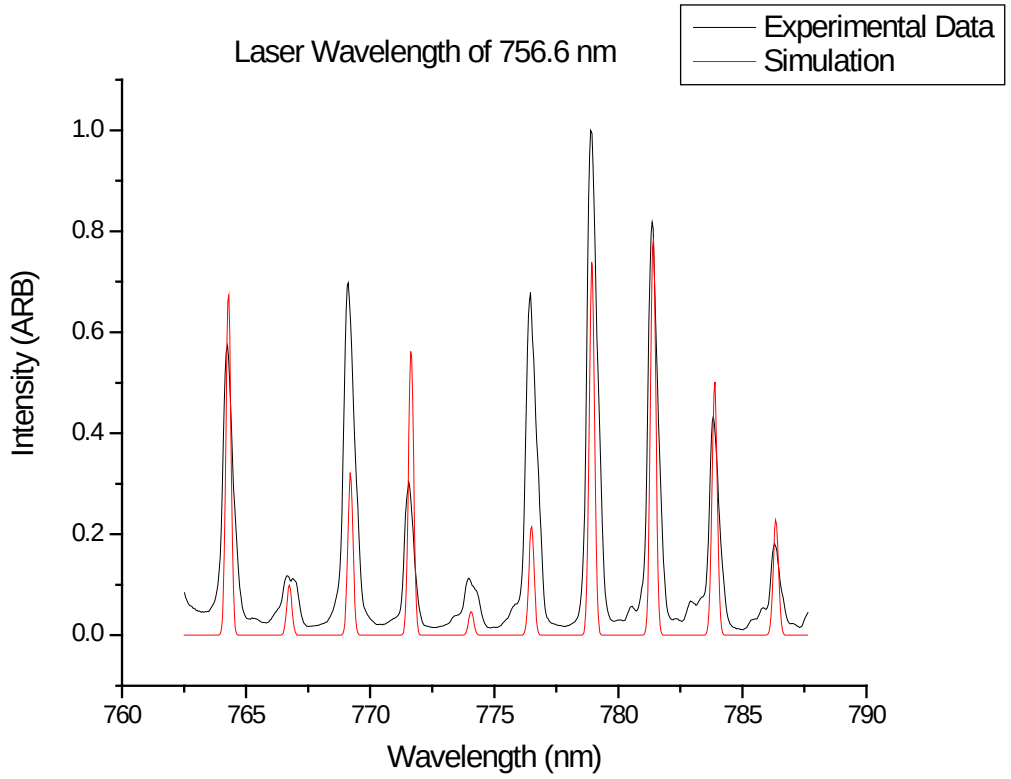

Figure 3.4 Overlap of simulated Cs_2 emission and experimental Cs_2 output emission

3.3 Pump Probe Measurements

The pump probe measurements were by far the most enduring measurements of this thesis. This measurement also would help finalize the questions of what pump wavelength should be used and what lasing wavelength will the cesium dimer lase at. Theoretically, the pump laser would be used to excite the molecules up into the excited B state of the cesium dimers. Then through rovibrational relaxation, the molecules will relax down to a lower vibrational state. From there they will fall down from the excitement of the Ti:Sapphire laser to a high vibrational level in the ground state. Then the molecules will rovibrationally relax to the lower vibrational ground states and the process can be repeated over and over again. This can be seen in Figure 3.5.

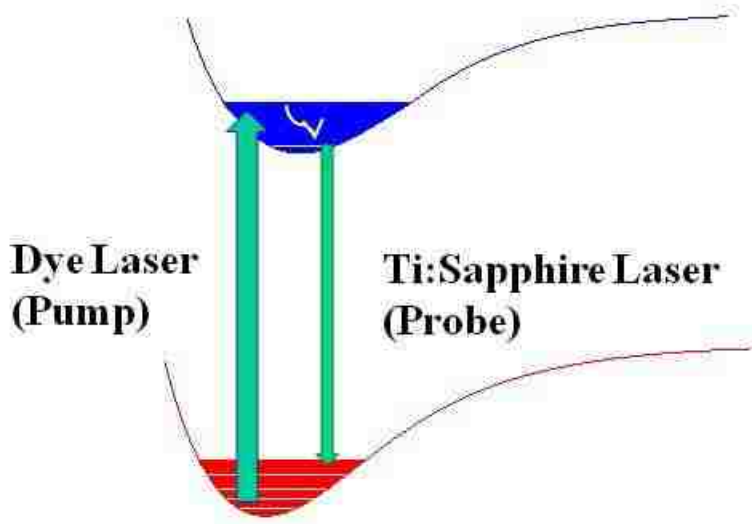

Figure 3.5 Visual for pump probe experiments

The Ti:Sapphire laser is set up to go through the same optics as shown in Figure 3.1, but the quarter wave plate has been removed so the Ti:Sapphire laser light can pass through the polarizing beam splitter. Then the Ti:Sapphire laser light is coupled into the cesium cell and passes through another beam splitter where there is no interference. The laser light from the Ti:Sapphire continues through and reaches the photo detector to be recorded. The YAG pumped dye laser is set up to go through some optics for alignment purposes, into the same first beam splitter and then into the cesium cell. After the cell there is another beam splitter that sends the YAG pumped dye laser light to a beam dump and the cesium emission passes through to the photo detector. The photo detector was a silicon detector with a response from 400 nm to 1000 nm. The detector, a Thorlabs DET 210 was connected to a Tektronix DPO 4032 digital phosphor oscilloscope and the data was collected and displayed. A diagram of the set up is pictured in Figure 3.6.

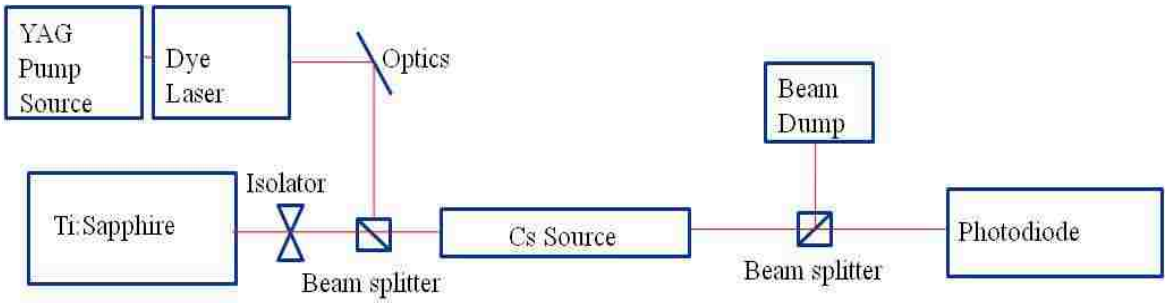

Figure 3.6 Diagram of pump probe experiments

If the pump laser (YAG) excited a state that relaxed to the level the probe laser was pumping at, and the excited molecule emitted its photon with the probe laser (Ti:Sapphire) wavelength and relaxed back down to the ground state, the photo detector would detect a pulse and it could be said that the cesium dimer can be made to lase at those transitions. Since the photo detector was constantly reading the power from the Ti:Sapphire laser, the pulse would have to be larger than the power seen by the Ti:Sapphire.

This experiment had many crucial details such as alignment of the lasers, overlapping of the lasers on one another, and the alignment of the photodiode. If any one of these parameters were not precisely done, the experimental results would not be credible and the experiments would have to be redone. A Melles Groit helium neon continuous wave laser was used for alignment purposes. This laser was used to help do all the optics alignments because of its output in the visible range. This laser proved invaluable for the rough alignment of both higher powered lasers used. The power outputted was 5 mW and emitted at 632 nm.

The most crucial alignment was of the lasers going through the heatpipe at the same location. This was measured by placing a marked note card in front of the cesium cell and having the lasers hit the same point. After a few experiments it was noticed that although the lasers went inside the cell at the same location they didn't end up overlapping each other other than in the center. Pump probe measurements rely on exciting the same area of molecules and if there is no overlap there will be no gain measurement made.

Another important alignment was making sure both lasers followed the same path through the cell. This was done by placing iris's both in front of the cell and after the cell. By having both lasers go through 2 different irises, it follows the theorem of only one line can pass through 2 points. As experiments continued, detecting gain was still unsuccessful.

Another issue that was found was beam divergence of the pulse laser. This was remedied by putting a plano-convex lens with a focal length of 75 cm and focusing the beam inside the cesium cell. A longer focal length ensured that there was a small beam waist throughout the cesium heat pipe or cesium cell. Since gain was not seen on any of the calculated or experimental transitions, a second pass of the pump laser was suggested.

The easiest way to get a second pass through the cesium cavity was to put a reflecting mirror at the location of the beam dump and adjust the mirror until it overlapped the original pump pulse beam. This was completed and the test was reiterated. Although there was a slight difference, the divergence of the pump laser pulse was so

great that it was no longer being absorbed only by the original molecules from the first pass of the pump laser.

After going through many different possible transitions, it was decided to probe through all the transitions looking for anything interesting or that could have been missed. At one point during the experiment, there was a pulse being recorded at a specific transition. After doing a few tests, it was determined that it was a coincidence and the pulse was a combination of absorption and bleaching of the pump source. One test done to determine if a possible gain site was indeed a real transition was by changing the pump and probe wavelengths. When the pump and probe were taken off the transition, the gain pulse should disappear which it did. Another test was to make sure that the output power was greater than the input power. After trying to measure the difference in power, it was determined that a definite measurement wasn't available due to the pulsed power of the pump laser. This output power fluxuated at each pulse, and the pulse that was thought to be gain was small. An alternate route was to measure the probe power without any cesium vapor. The temperature was taken down and the probe laser power was measured relative on the oscilloscope. Once the probe laser power was measured, it was seen that the output had less power than what was being inputted into the cesium cell.

After tracking all the possible issues, it was noted that the probe laser was indeed being absorbed. When the pump laser operated many of the molecules were already excited from the probe laser and the pump laser passed through unabsorbed to the detector. This was the pulse seen on the oscilloscope.

On another testing day, as the pump laser was scanned through the different pump wavelengths, a large peak was seen on the oscilloscope when the pump laser was put at 742 nm. This situation will be discussed in Chapter 5. The output was indeed gain, but it was not produced by the cesium dimer; rather from the cesium atoms excited in the vapor. The output wavelength was 455.5 nm and 459.3 nm depending on the pump wavelength.

In conclusion, there were no gain measurements successful with Cs_2 molecule. Although there were many different adjustments made to try to detect gain, all efforts resulted in no gain detected. Although there indeed was gain detected by the experimental setup, the gain was from the cesium atom and will be discussed in Chapter 5. Although it was thought that gain would be detected, it wasn't seen due to self absorption and heat pipe issues as will be discussed in Chapter 4.

3.4 Heat Pipe Measurements

As soon as the heat pipe was designed there were a few tests that needed to be completed in order to verify if it could replace the glass cell that was previously being used. The heat pipe was taken up to the operating temperature of the glass cell, approximately 220 C, and the Ti:Sapphire laser was sent through the heat pipe and the emission spectra documented. Once it was seen that the heat pipe could create cesium dimers the other experiments were completed. Tests were carried out to verify the repeatability of creating cesium dimers and they proved successful.

Another test was to see what temperature needed to be reached in order to reduce the cesium dimer density. In this experiment, the temperature was increased by 5 C and

the Ti:Sapphire laser light put through the heat pipe and the emission output was recorded. The transition that the laser was running at was 754 nm, which was not absorbed by the cesium atoms. This is important to note because if this wavelength was absorbed by the cesium atoms, what would be assumed as absorption by the cesium dimers would in fact be absorption of the cesium atoms. The power output of the Ti:Sapphire laser was measured at the beginning of the experiment where the laser output was recorded below 150 C. As the temperature was raised past the dimer creating temperature, 220 C, the absorption of the laser light increased. This was predicted since Cs_2 should absorb more and more of the laser light as more dimers are created due to the raise in temperature. It is assumed once the dimers started breaking up the absorption should decrease. This disassociation temperature was never reached with our heat pipe, and no definite temperature could be recorded.

Another test was to see how cold the cooling blocks could be made while still having a significant number of cesium dimers to detect cesium dimer emission. As the temperature of the cooling blocks was lowered, a laser would be passed through the cell to verify that there were cesium dimers in the cell by observing the cesium emission. The multiple peak cesium dimer emission was noted and the temperature would be taken lower. Although the inner cooling blocks were taken down to 15 C, after a few days of having the heat pipe run at this temperature, the cesium would freeze on the inner cooling blocks and there would not be any cesium to heat up to form the cesium dimers. It was then noted that although the heat pipe could be run at lower temperatures, 20 C was the

optimum temperature for running the inner cooling blocks of the heat pipe and 12 C was the optimum temperature for running the outer cooling blocks.

An interesting observation about the cesium glass cell was that the temperature to form cesium dimers would be 190 C, but with the heat pipe dimers formed at a higher temperature, 220 C. This was overlooked at first, but will be discussed as a possible issue with the heat pipe in chapter 4. Since there was a change at what temperature the dimers started forming, the measurements of the dimer emission spectra and the pump probe measurements were redone. The dimer emission spectra correlated for both the cesium glass cell and the heat pipe, but just at a higher temperature.

After running into some issues with absorption of the probe laser completing the pump probe measurements, a few absorption experiments were completed. The experimental setup can be seen in Figure 3.7. The Ti:Sapphire was passed through the heat pipe and the output from the Ti:Sapphire was measured both before and after the heat pipe labeled 1 and 2 in Figure 3.7.

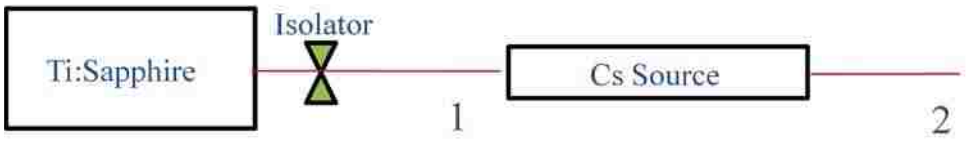

Figure 3.7 Experimental setup for absorption experiments

Experiment was completed a few times on different days and different pump wavelengths to find out why gain wasn't being detected. It was also used to determine the density of Cs_2 molecules in the cell.

The results can be seen in Figure 3.8. These results show the trend that as the temperature goes up, the absorption of the pump laser increases. The reason why the

green and purple tests are lower than the blue and the red tests is because those tests were done before the laser could full stabilize their output. All of the rest of the tests were given ample time for warm up and stabilization. Loss through the heat pipe was also recorded and measured to be about 30% due to reflections. Another thing to note is throughout the wavelengths tested for absorption, at higher temperatures, mainly over 300 C, absorption increased irrelevant to pump wavelength.

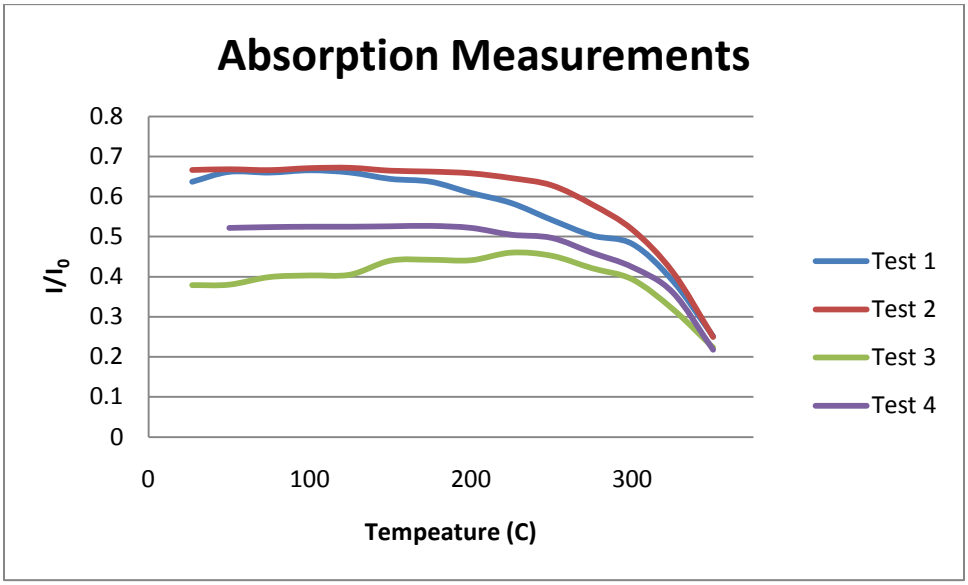

Figure 3.8 Absorption results showing as the temperature goes up, the absorption increases

In the next chapter issues with both the heat pipe and the cesium dimers that hindered our ability to measure any potential gain from the system will be described and discussed.

CHAPTER 4 - ISSUES WITH CS_2

Although the calculations suggested that gain should be reached at a few transitions, no gain was observed in the setup mentioned previously. The biggest issues were the temperature gradient within the heat pipe and the overlap of the cesium dimer energy bands. The temperature gradient makes the true gain length of the cell relatively unknown, which then affects the amount of cesium dimers in the vapor that gives an inaccurate number density, which is most likely much smaller than what was being calculated.

4.1 Heat pipe Issues

The heat pipe was checked many times to make sure there was cesium dimer emission after running the pump probe measurements and detecting no gain. Since the cesium dimer output was easy to see, it was assumed that the heat pipe was working correctly and there were no issues with the heat pipe. Since no successful gain measurements were made, the heat distribution in the heat pipe needed to be investigated.

In the experiment proposed, it was decided to ramp the heat pipe up and measure the temperature of the heat pipe cell at different locations to see the heat distribution of

the pipe. Three thermocouples were used and the locations of each are shown in Figure 4.1. As the temperature was raised, the temperature nearest the first cooling block (TC3) was around half the temperature of what the heat controlling middle (TC1) thermocouple was reading.

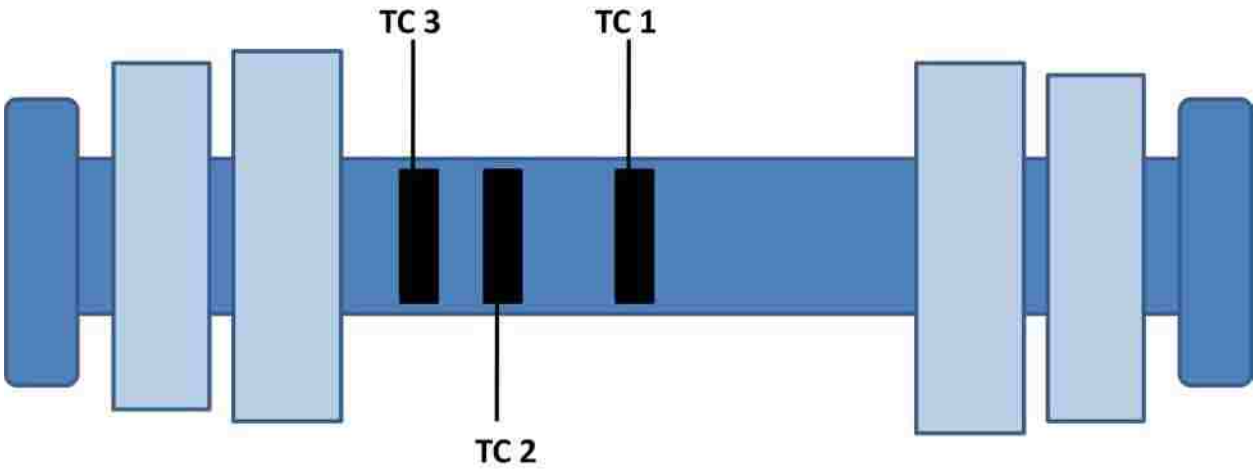

Figure 4.1 Locations of thermocouples on heat pipe measurement

Temperature readings ranged from 120 to 190 C. Figure 4.2 shows the output of each of the thermocouples as well as the average reading of all the thermocouples. TC1 was the thermocouple being used as feedback for the heater rope. But looking at TC3, the max temperature does not even break 100 C. This makes all the estimated gain lengths inaccurate since the temperature is not constant throughout the cell. The number density of the cesium dimers is calculated depending on the pressure. Since the temperature is not the same throughout the cell, the actual temperature gradient inside the cell affects the pressure. If the density is the average of the temperature gradient in the center of the heat pipe, then the highest temperature the cesium dimers can reach is 281 C. At that

temperature, the gain length required to get 50% absorption of the pump laser would be ~ 22 cm. With the heat pipe having a gain length of 12.2 cm, this 50% absorption cannot be reached.

Something interesting to note is when doing absorption cross sections, which rely on cesium dimer concentrations, it was calculated to observe an absorption cross section of 5.9×10^{-16} cm^2/molecule. It was measured to be 7.7×10^{-16} cm^2/molecule, which is close to the original calculation although, after realizing a smaller Cs_2 vapor concentration due to the temperature gradient, the new dimer concentration of 2.9×10^{13} molecules/cm^3 should be in the cell which leads to an absorption cross section of 3.6×10^{-18} cm^2/molecule.

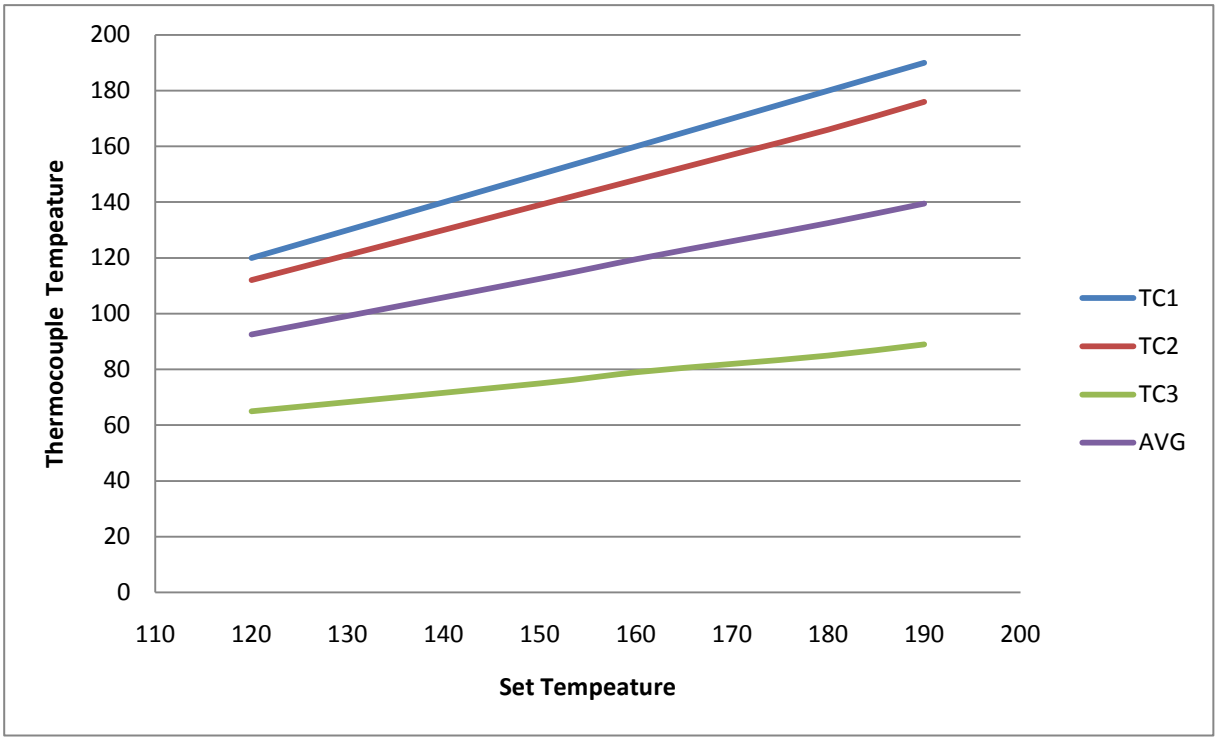

Figure 4.2 Plot of different temperature measurements on the heat pipe

Another issue that was discovered near the end of this research was the change in absorption depending on the temperature of the heat pipe. At all the important pump probe transitions that were calculated, it was recorded that the probe laser was being absorbed. This is an issue because the probe laser was at a wavelength that was at a higher energy that shouldn't be absorbed. These transitions were calculated based on probabilities of molecular occupation using Boltzman statistics, and FCFs of that transition. Since there was absorption being recorded, this hindered our ability to detect possible gain. Although the high vibrational ground state levels are calculated as having a low probability of having any population, the transition could be populated due to unknown lifetimes at each energy level. There is also the issue of absorbing from the ground state to the A state, as was seen in the fluoresce measurements shown in an earlier experiment. Although there is a possibility of gain to be detected, self absorption hinders the emission.

Another problematic discovery was that the threshold temperatures for detection of cesium dimers would change after time. In Chapter 3, it is discussed that dimers were created ~220 C and as the temperatures went up, so did the intensity of the emission spectra of the cesium dimers. In later tests, the dimer creation temperature had changed to ~260 C. Figure 4.3 shows a measurement done where the peak emission changed from 220 C to a higher temperature of 260 C.

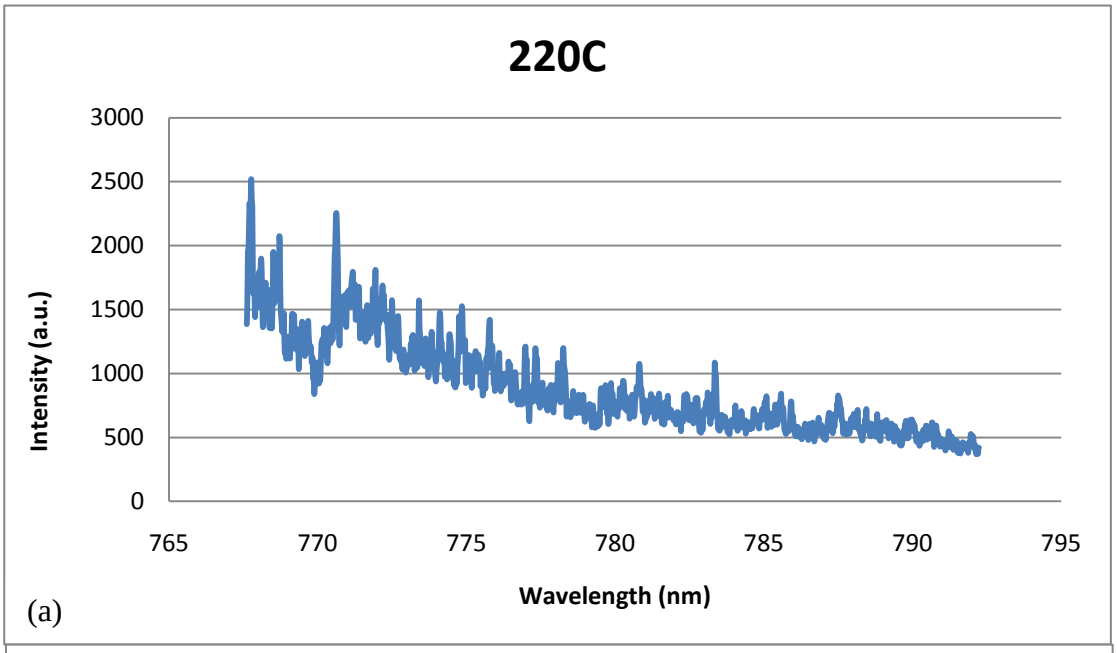

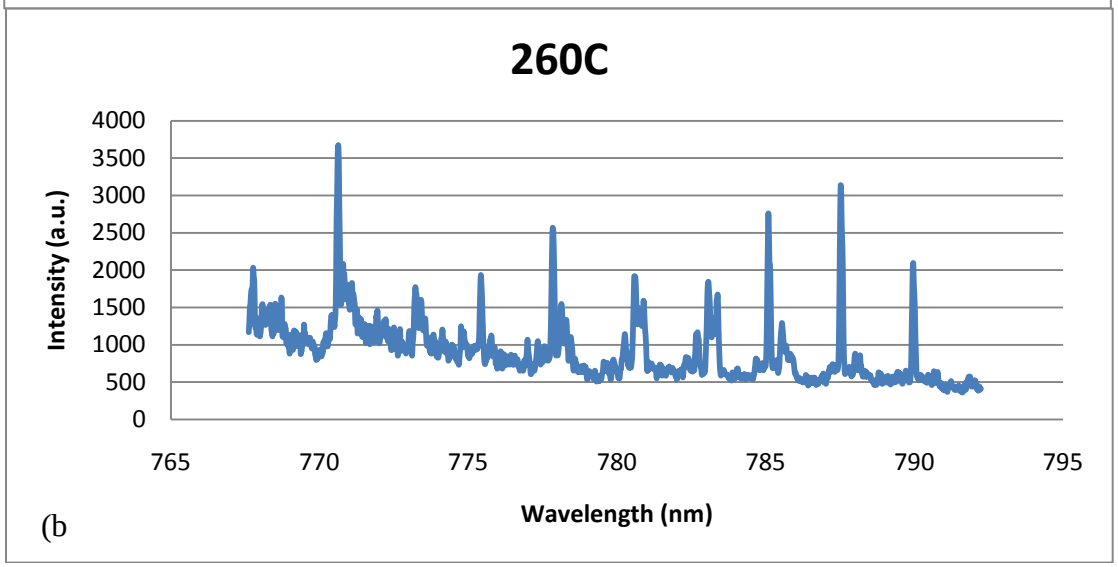

Figure 4.3 Graphs of Cs_2 emission output at (a) 220 C and (b) 260 C

This change is most likely due to the fact that the temperature associated with the temperature throughout the heat pipe was not correct. The temperature measured in the middle of the glass cell was allowed to be used since the cell was small, but the temperature was not the same with the heat pipe, and a higher temperature had to be met

by the heat pipe center before there was a big enough dimer concentration to see cesium dimers emission.

4.2 Multiple Cs_2 Absorption Band Overlaps

Another issue that is detrimental in finding suitable gain transitions is the fact that the cesium dimer bands overlap each other. This can be seen in Figure 3.3 with emission coming from the A excited state, 800 nm and longer. Although the pump emission was pumping the B excited state of Cs_2 because of the overlap of bands, the A excited state was populated as well but these lower lying excited states were ignored during the experiments. When looking for possible issues that are hindering the gain measurements, it was mentioned by many other researchers that band overlaps hindered possible measurements and caused uncertainty. D.H. Sarkisyan mentioned that he was having trouble measuring and calculating variables for Cs_2 because "of the substantial overlapping of bands and band systems of Cs dimers" [24]. M. Lapp also describes his problem of not being able to calculate these overlaps of the spectra due to the unavailability of the line-width data measurements [25]. Further interest in the overlap of Cs_2 bands can be looked at in a paper by F. W. Loomis and P. Kusch titled, "The Band spectrum of Caesium" [26]. Although there was no intensive investigation of band overlaps due to time restraints, this could be a possible issue that hindered the detection of any gain in the system.

4.3 Cesium Dimer Concentration Measurements

While doing optimal cesium dimer concentration measurements, it was seen that each test resulted in different final temperatures. The way the optimum concentration was detected was by changing the temperature of the heat pipe and recording the cesium dimer emission. The emission that gave the highest peak was determined to have the optimum concentration. There were no trends that were noticeable; the optimal temperature would change monthly. Appendix 2 shows a test resulting in a maximum cesium dimer temperature at 235 C. Figure 4.4 shows the emission spectra at (a) 235 C that can be compared to (b) 260 C. Although the biggest peak on the plot is highest at 235 C, there are many more transitions occurring with the temperature at 260 C. Recalling the discussion about the temperature needed to break apart the dimers is ~500 C, it is assumed the closer the cesium is taken to 500 C the more dimers are produced. This however does not seem the case between each cesium dimer optimal temperature experiment. Possible reasoning for why these tests were not repeatable could be due to the fact the heat pipe temperature wasn't constant throughout more of the heat pipe. Another issue could be that at the higher temperatures, the lack of emission could be due to self absorption.

Figure 4.4 and Figure 4.3 are different emissions due to different pumping wavelengths and different adjustments due to the photo detector and shouldn't be compared to each other.

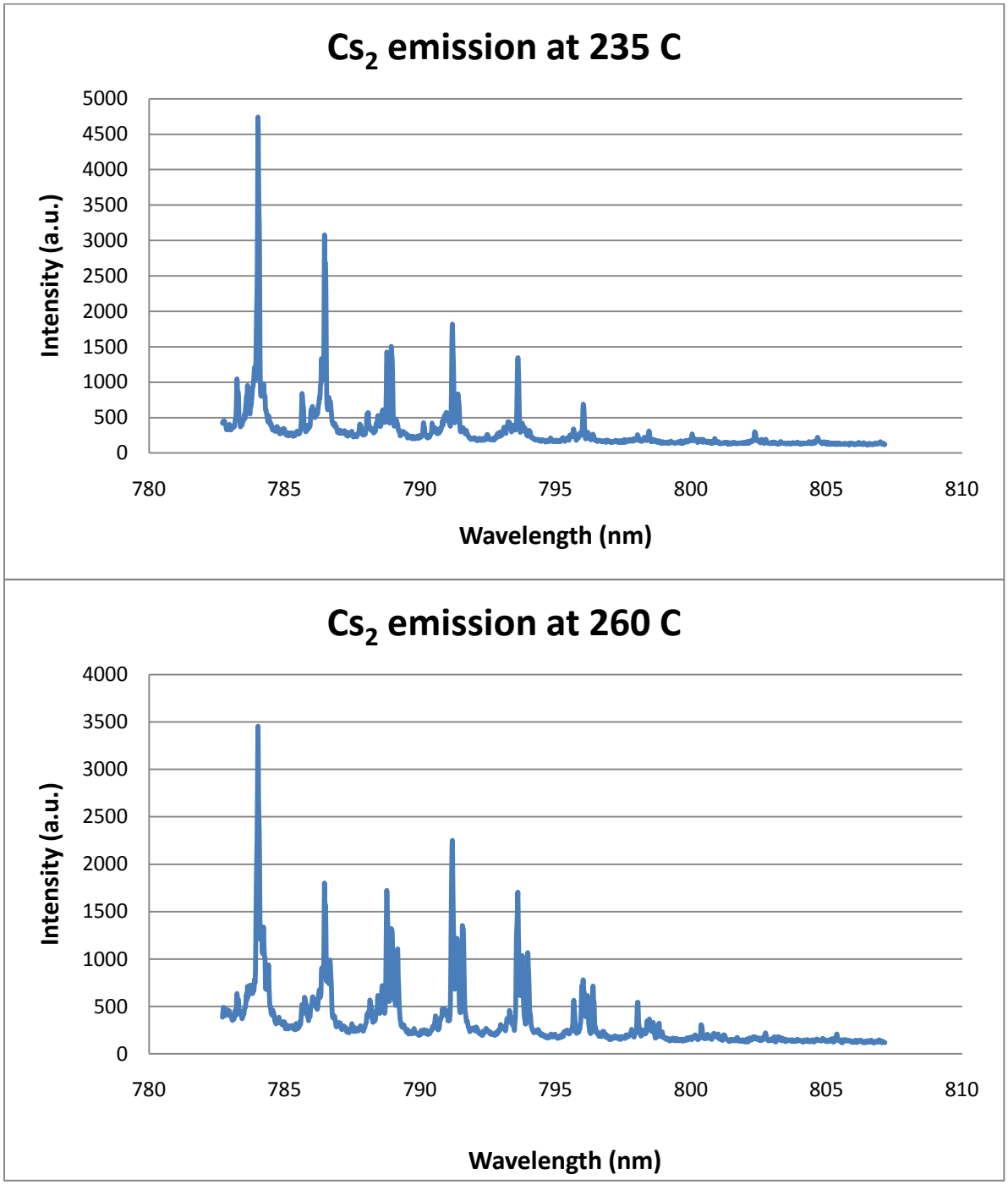

Figure 4.4 Graphs of Cs_2 emission output at (a) 235 C and (b) 260 C

4.4 Simulated Cs_2 emission spectra issues

While doing the simulations for the Cs_2 emission spectra, there were some irregularities that came up depending on what pump wavelength was employed. It can be seen in Figure 3.3 in Chapter 3, there was good overlap of simulated emission done by known values in literature and the experimental emission when excited by a Ti:Sapphire laser. With different pump wavelengths though, the amount of overlap changed considerably. Looking at Figure 4.5, it can be seen that the overlap between the simulation and experimental data was not very good. Not only are the amplitudes different, but the peaks are not even at the same areas.

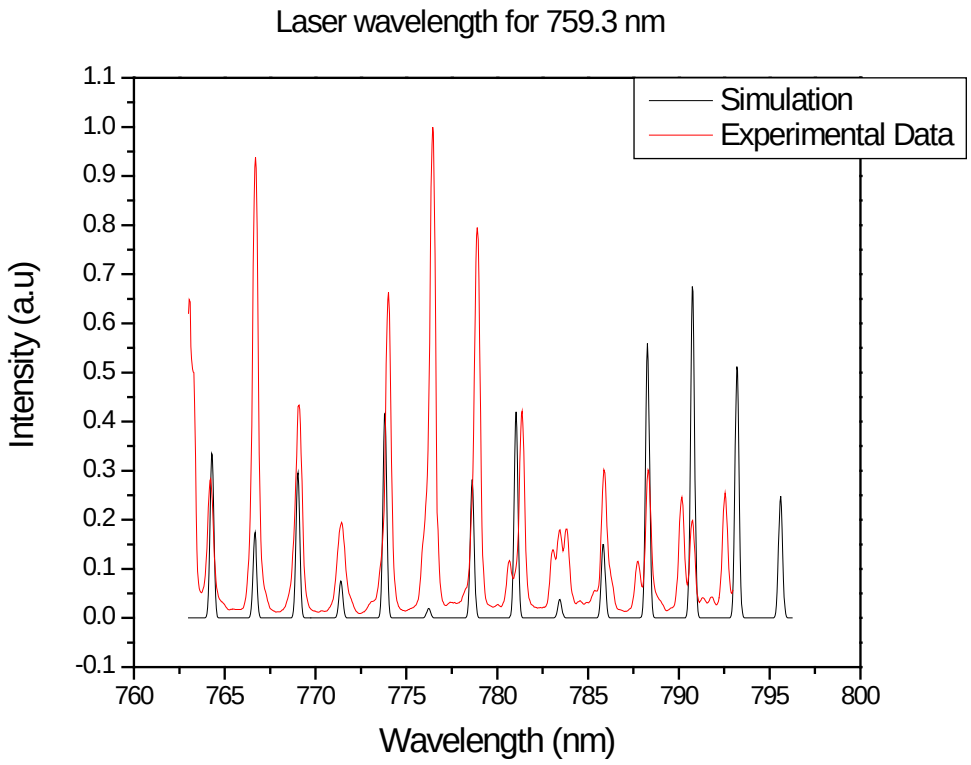

Figure 4.5 Overlap of simulated Cs_2 emission and experimental Cs_2 output emission showing very little similarities.

Although the calculations could predict emission to a degree, the simulated emissions weren't necessarily correct. There could be different reasons for this unfavorable result, the main ones being that either the cesium dimer does not follow the same rules during this transition due to excited state mixing, or that the emission simulations were miscalculated. The simulated emissions need to be redone to make sure the output is on the same transitions as the experimental measurements. Due to time constraints, further investigation couldn't be completed, and will hopefully be looked at by another student continuing the research.

4.5 Summary

Even though calculations suggested that gain should have been detected at a few transitions, the gain was unobservable. This could have been due to many different issues, and the most important issues were discussed. Issues with the heat pipe temperature gradient, the true gain length of the cell which affects how the density is calculated, cesium dimer band overlap, and simulated emission issues all could contribute to reasons why gain was not observed during these experiments. In the next chapter, discussion of an interesting observation during the experiments is explained as well as future experiments to exploit this phenomenon is discussed.

CHAPTER 5 - INTERESTING PHENOEMON WITH CS MOLECULE

While scanning for ideal pump probe transitions, strong gain was detected by the Cs atom, prompting further investigation. The wavelengths that demonstrated substantial gain were plotted and compared to possible calculated transitions. They fit well with experiments, which further confirm which transitions are being utilized. One wavelength in particular was interesting due to the high gain of emission and lack of self absorption. It will be looked at for possible use as an optical parametric oscillator (OPO).

5.1 Experimental results

The experimental set up was the same as the traditional pump probe measurements and can be seen in Figure 5.1. The YAG pumped dye laser was the pump laser and pumped the cesium atoms at 742 nm. At first the Ti:Sapphire laser was going through the cesium heat pipe, but after detecting the wavelength, it was determined that the Ti:Sapphire wasn’t needed to produce the blue emission. In the end there was just a pump laser and no probe laser required for emission.

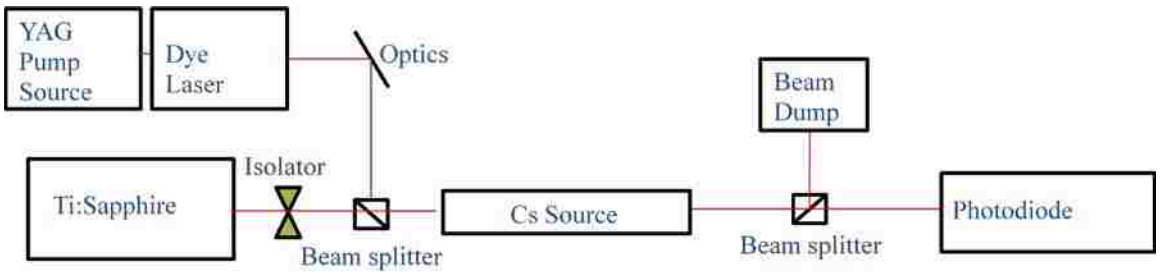

Figure 5.1 Set up for pump probe measurements for the cesium atom

As pump probe measurements were being made, a few of the transitions were emitting in the blue wavelengths. When pumping 742 nm, strong emission of 455.5 nm and 459.3 nm were detected, other radiation transitions were emitted as well but to a smaller degree. The transition was investigated and all the emission transitions were recorded. All of the transitions can be seen in Appendix 3. Figure 5.2 shows a graph representing all observed emission wavelengths.

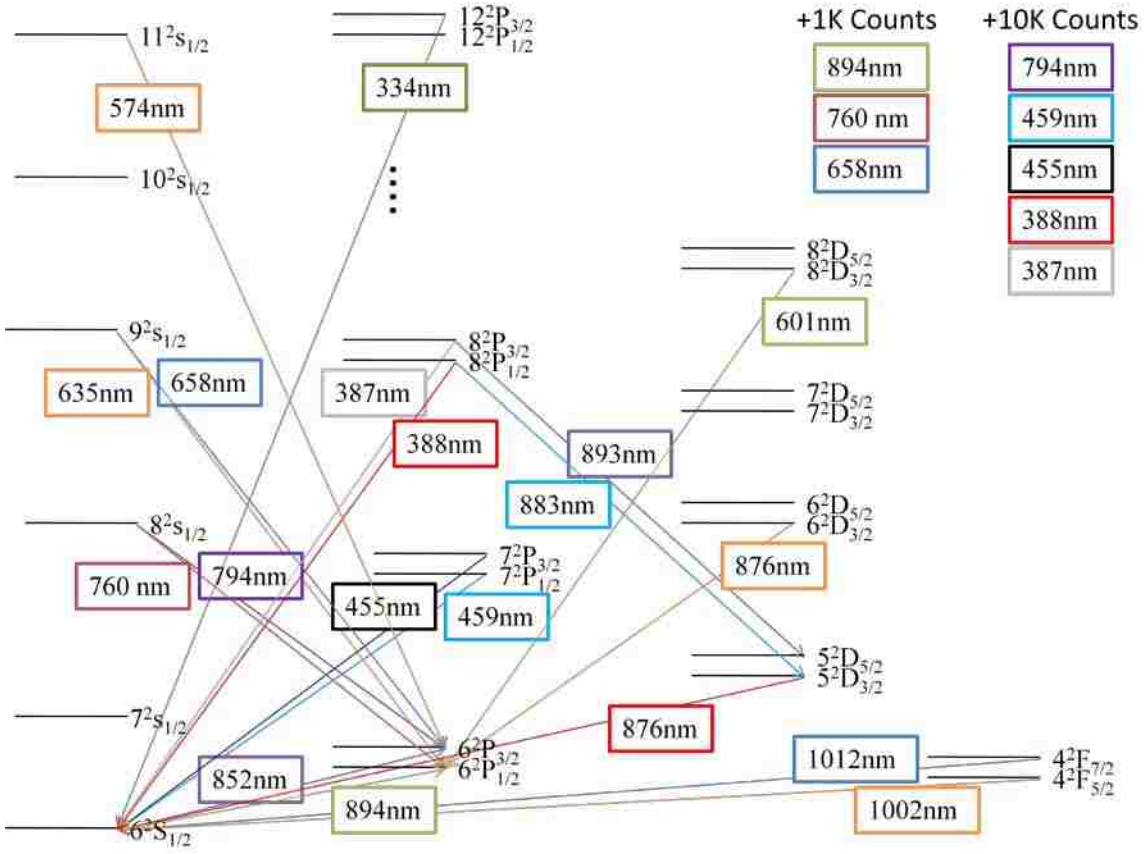

Figure 5.2 Emission transitions of pumping Cs with a pulsed 742 nm pump laser. Relative emission wavelengths are noted in top right corner.

After doing a quick literary search, it was determined that these are all possible transitions of the cesium atom. Although 459.3 nm hasn't been reported in previous research, it was seen very strongly in these tests. There were also a few wavelengths that emitted from the cesium dimer, but they were such a low output that they will not be discussed here. The particularly interesting wavelength emissions (455, 459 nm) are those that have more energy than the pump energy from the laser (742 nm). The possible mechanism of producing this phenomenon is the non-linear effect of four-wave mixing or muliphoton absorption as seen with slight emission of 334 nm.

5.2 Four-wave mixing

Four-wave mixing is a non-linear effect realized by Issac Abella in 1962[27] and the process begins when a molecule absorbs a photon and goes into a virtual state, a state not normally available but created in this non-linear effect. While there, it absorbs another photon taking it to an even higher excited state above what would be possible with one photon absorption. Once excited the molecule will release a photon to lower its energy on a resonance, and release another photon to go back down to the ground state. Figure 5.3 shows an arbitrary example of how the phenomenon observed in the lab is produced if it is indeed from four-wave mixing.

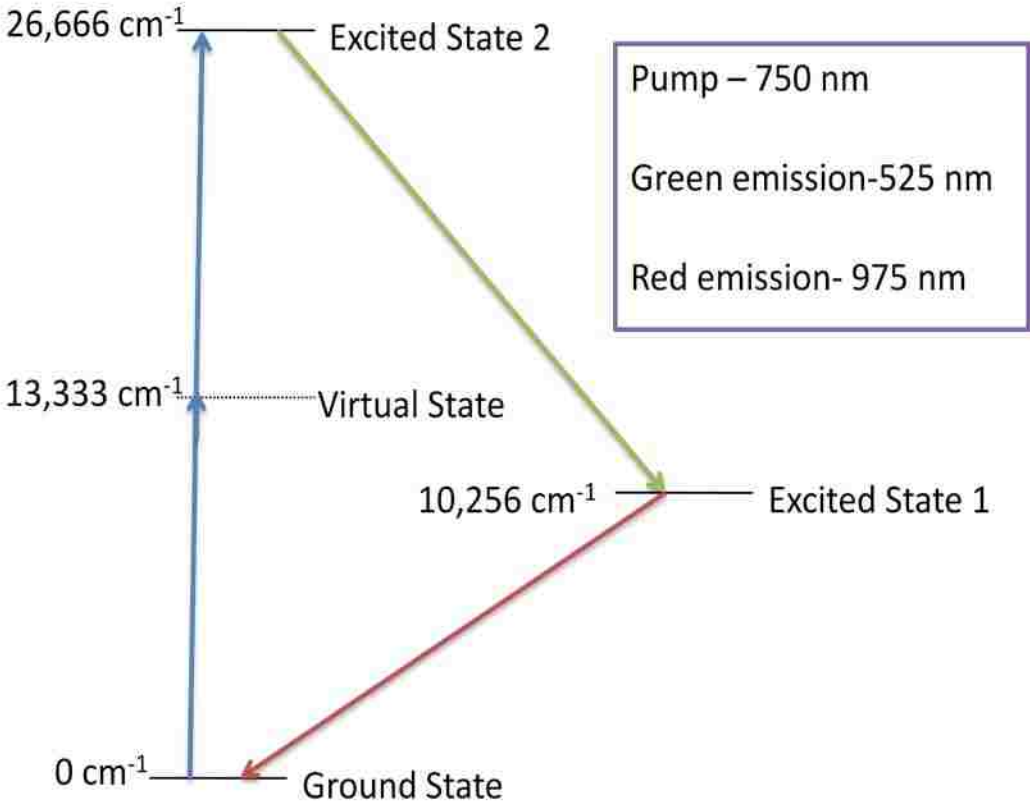

Figure 5.3 Arbitrary example of two photon absorption with a "virtual" state

If there is a real resonance near the location of the virtual state, then the system can be considered four-wave mixing with resonance enhancement. If this is indeed the case, then the energy level representation of what is happening in the experiment can be seen in Figure 5.4. The graph is not representative of exact energy levels, and although the 9S state and the 7D state are at different energy levels, they are relatively close energy levels enough for both states to absorb the multiphoton absorption. Both absorption transitions occur because detection of both corresponding IR wavelengths of 1020 nm and 1011 nm are detected.

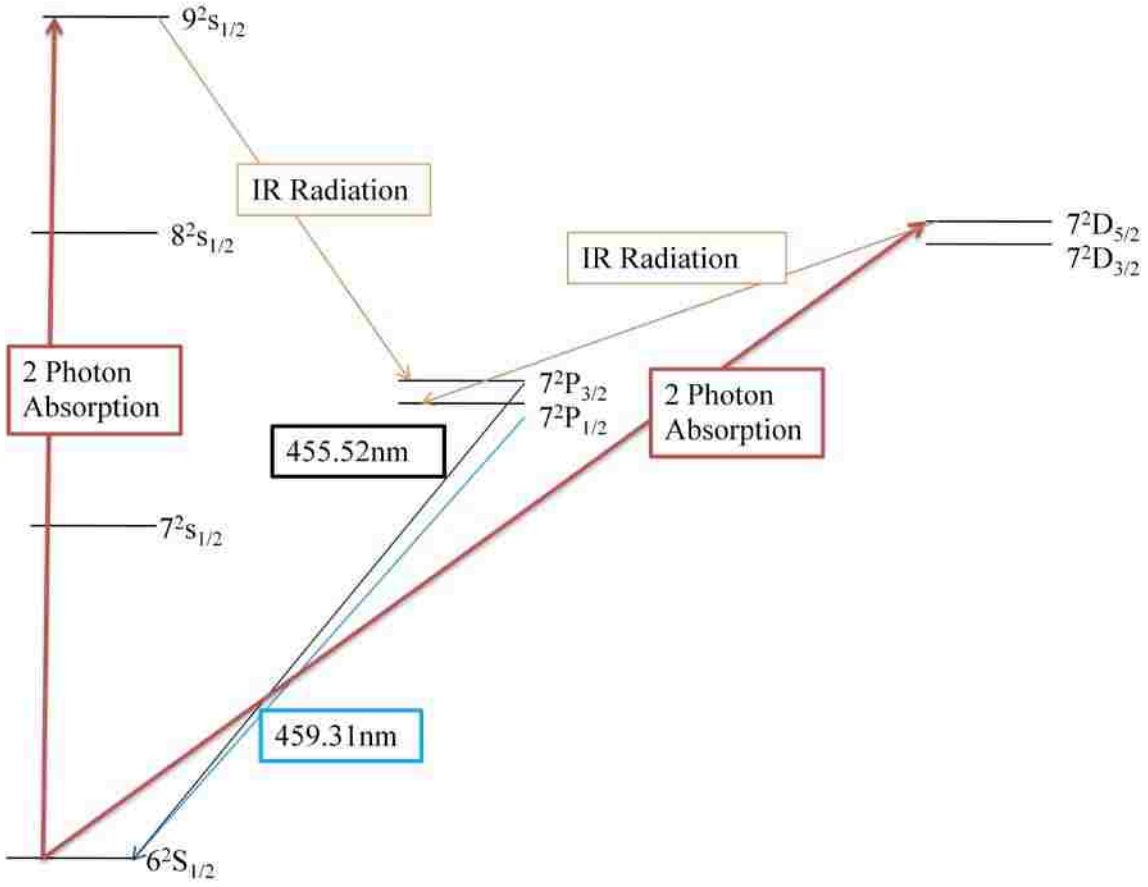

Figure 5.4. Energy diagram of pumping Cs2 at 742 nm and emitting at 455 nm.

An experiment was set up to verify if indeed the output is a nonlinear four wave mixing phenomenon, as well as checking transitions to find out if there is any resonance enhancement. In the experiment, the spectral width was measured of the 455 nm wavelength emission. This was done by recording the wavelengths where the pump laser could be tuned to while still observing 455 nm emission. The experimental set up can be seen in Figure 5.5.

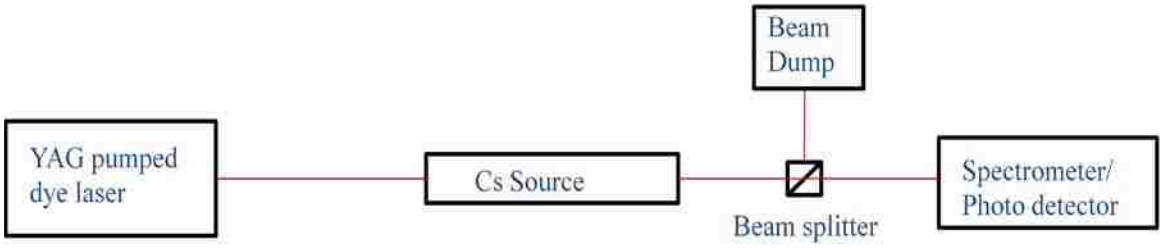

Figure 5.5 Experimental set up for spectral width measurements

A YAG pumped dye laser sends 742 nm pulsed radiation into the cesium cell and the laser output that is not absorbed by the cesium molecules is sent to the beam stop. The emission from cesium goes through the beam splitter and is detected by either the photo detector read by an oscilloscope for intensity or the spectrometer to detect what wavelength the emission is at. The blue intensity is recorded and then curve fitted to measure the area under the curve. Once the area is calculated, it is plotted to determine the spectral width.

After determining the spectral widths they were compared at different temperatures. The temperatures were varied to see if the spectral width was temperature dependent. The results are located in Appendix 4. The spectral width of the blue transition at 320 C was ~ 0.124 nm. Although it seems like the spectral width changed depending on temperature, it is most likely due to the area approximation methods of curve fitting rather than real changes in spectral width. The spectral width at 320 C is shown in Figure 5.6.

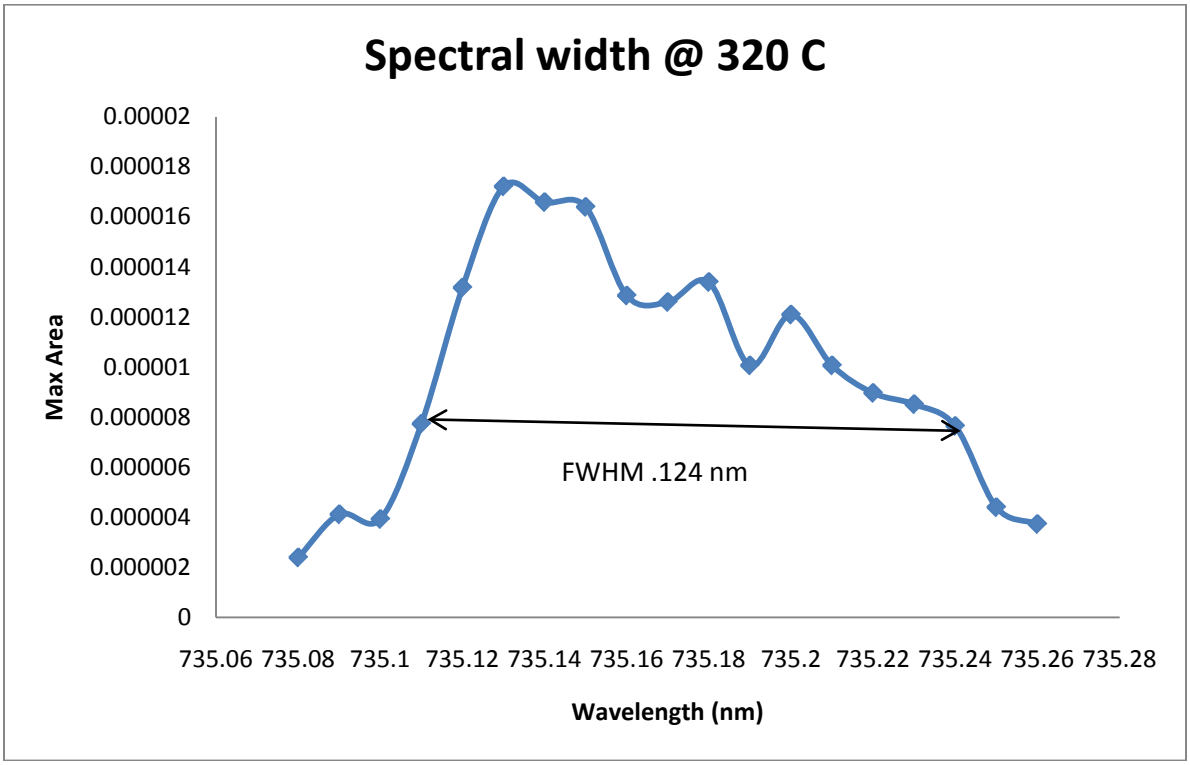

Figure 5.6 Spectral width determined by integrating the curve fit of the intensity emission of 455 nm output transition at 320 C.

There is interest in this non linear multiphoton absorption and emission phenomenon due to the possible use of producing an optical parametric oscillator. By using the cesium as the nonlinear object inside the OPO, it might be possible to create OPOs without the use of non linear crystals usually associated with them.

5.3 Optical Parametric Oscillator

An optical parametric oscillator is of interest to the research community due to its emission of wavelength transitions that are usually unavailable [28]. It is very similar to a laser, but receives its gain from parametric oscillation in a non linear crystal instead of

stimulated emission. There are both continuous and pulsed systems, but pulsed systems are less complicated to achieve with higher powered systems, due to high intensity. This causes less damage to the nonlinear optical material and the mirrors than a continuous high intensity OPO would cause [29].

Research would need to be done to determine what wavelengths the cesium atom could produce, as well as the power output achievable. Although a few preliminary tests were completed to try to create an OPO at the current wavelengths observed, the limited amount of time and pulsed laser beam size did not allow for any impressive results. Although the OPO experiment was not successful, by looking at Figure 5.6, a resonance is observed confirming our instincts. The OPO experiment would have been the best way to prove the four wave mixing phenomenon. These concerns provide opportunities for future work in the area. The interest is still existent, and further OPO research using the cesium dimer will be completed by another student. This will be discussed further in detail in the future work section in the next chapter.

CHAPTER 6 - SUMMARY AND FUTURE WORK

6.1 Accomplishments

An overview of the research and results will be given as well as a brief discussion of future work. There were a few issues that needed to be solved, and although not all had a positive result, all were solved to the best of my ability. It has been shown in the presented work that to solve the 3 main questions given in Chapter 1, many different experiments had to be done.

- Finding a suitable enclosure to replace the glass cell to achieve higher temperatures over 200 C was done by using a heat pipe. The heat pipe could reach a temperature of 281 C.
- Finding a solution to stopping Cs from reaching the windows and corroding the anti-reflection coating was done by using the heat pipe design as well as adding a set of cooling blocks to cool the cesium back into a liquid state. There has been no corrosion so far and the heat pipe has been running for over 4000 hours.
- Calculating the Frank-Condon coefficients of the first 90 levels of the vibrational levels of the excited B state and ground state of Cs_2.
- Recorded Cs2 emission spectra from 750 nm to 800 nm. This data can be used as experimental data to compare different or more sophisticated modeling and simulations.

6.2 Conclusions

Research was completed to determine if Cs_2 could be used as a gain medium for diode pumped alkali laser research. When finding a suitable enclosure to reach higher temperatures in excess of 200 C, the heat pipe design was used. Although it was thought the heat pipe could reach temperatures as high as 375 C, the gradient inside the heat pipe had an overall temperature around 140 C and the max temperature the heat pipe could reach in the set up was 281 C. This was still over the desired temperature but now there is a new desire to reach even higher temperatures due to a theoretically higher cesium dimer number density. Finding a way to regulate the temperature of the heating can easily fix this and temperatures could theoretically reach up to 600 C before any damage to the heat pipe would occur.

The heat pipe design was also a very efficient way of keeping the cesium material from reaching the outer windows and corroding the anti-reflection coating. The cooling blocks kept the cesium from reaching the windows even after running the heat pipe for over 4000 hours.

As for the main goal of finding out if Cs_2 could be a suitable gain material for alkali lasers, there were four questions that needed to be answered. Spectroscopic measurements were completed to determine ideal pumping wavelengths, as well as calculating the Franck Condon Factors to find the highest overlap probability for each transition. Pump probe measurements were completed to try to find a lasing wavelength, and gain lengths and absorption cross sections were calculated. Detecting gain was ultimately unsuccessful due to issues examined in Chapter 4.

Frank Condon coefficients were calculated and the results compliment the previous Frank Condon coefficients calculated for Cs_2. Although all previous work examined only calculated the first few levels, this comprehensive collection has all 90 Frank Condon coefficients for the ground X and excited B states which can be used by other research facilities interested in them.

The results from this work tend to make the final decision of using Cs_2 as a gain medium for future DPAL research as not a very good candidate. This result is tentative for the wavelength range of 750 nm to 800 nm. If there is interest at another wavelength range, this research shouldn't exclude Cs_2 from being investigated further.

6.3 Future Work

There are still other experiments that can be investigated to further the understanding of cesium dimer research. These experiments will most likely be completed by another student that is interested in cesium dimer research. One of the most important issues to tackle would be finding a suitable enclosure where temperatures can be taken up higher than 400 C while maintaining a longer gain length. This will need to be done by finding a better way to evenly heat the heat pipe cell. A potential solution to this problem might be done by expanding the heat pipe length. The longer the heat pipe, the longer one can have a constant temperature over a longer range before the temperature gradient changes towards the cooling blocks.

Further research could also be done on investigating if the cesium molecules could be used to produce an OPO. Finding a laser or other higher energy powered source to have the cesium emit the blue 455 nm continuous wave instead of pulsed should make it easier to produce.

Another issue that would need to be addressed is finding a more precise way of measuring the pressure inside these heat pipes to get a better determination of the actual cesium dimer concentration. By knowing the cesium dimer concentration and the appropriate gain length, more accurate gain calculations can be made, which would lead to better understanding about the nature and direction of further research using cesium dimers as a gain medium.

The final issue that needs to be looked at in more detail is the Franck Condon Factor calculations. A more sophisticated model needs to be used where there are more rotational levels calculated per vibrational level to get a better overlap on prediction of the cesium dimer spectra. This also factors into the gain calculations and pump probe measurements, so advancements in this area would help out multiple areas of interest.

REFERENCES

1. K. Howard, S. Lawson, and Y. Zhou, Welding Aluminum Sheet Using a High-Power Diode Laser, Welding Journal, May 2006, pg 101-110.
2. Los Alamos National Labs, “How LIFE Works”, https://lasers.llnl.gov/about/missions/energy_for_the_future/life/how_life_works.php
3. Peter Michaud, “Gemini's Laser Vision Reveals Striking New Details in Orion Nebula”, http://www.gemini.edu/index.php?q=node/226, March 22, 2007.
4. Hecht, Jeff. “A New Generation of Laser Weapons is Born”, Laser Focus World, April 2010.
5. Boeing, “Boeing begins flight tests and laser firings for laser gunship program” http://www.boeing.com/news/releases/2006/q4/061012b_nr.html
6. Encyclopedia of Laser Physics and Technology, Beam Quality, http://www.rp-photonics.com/beam_quality.html
7. Encyclopedia of Laser Physics and Technology, Thermal Lensing, http://www.rp-photonics.com/thermal_lensing.html
8. Yam, Marcus. “Sony Develops Powerful Laser for 1Tb Optical Disk” Toms Hardware US, July 26 2010.
9. Boris V. Zhdanov, Adam Stooke, Gregory Boyadjian, Adam Voci, and R. J. Knize, "Rubidium vapor laser pumped by two laser diode arrays," Opt. Lett. 33, 414-415 (2008)
10. Zhdanov, B.V.; Sell, J.; Knize, R.J.; , "Multiple laser diode array pumped Cs laser with 48W output power," *Electronics Letters* , vol.44, no.9, pp.582-583, April 24 2008

11. Raymond J. Beach, William F. Krupke, V. Keith Kanz, Stephen A. Payne, Mark A. Dubinskii, and Larry D. Merkle, "End-pumped continuous-wave alkali vapor lasers: experiment, model, and power scaling," J. Opt. Soc. Am. B 21, 2151-2163 (2004)
12. B.V. Zhdanov, T. Ehrenreich, R.J. Knize, Highly efficient optically pumped cesium vapor laser, Optics Communications, Volume 260, Issue 2, 15 April 2006, Pages 696-698, ISSN 0030-4018, DOI: 10.1016/j.optcom.2005.11.042.
13. Yujin Zheng, Minoru Niigaki, Hirofumi Miyajima, Teruo Hiruma and Hirofumi Kan, “High-Efficiency 894-nm Laser Emission of Laser-Diode-Bar-Pumped Cesium-Vapor Laser”, Appl. Phys. Express 2 (2009) 032501
14. H. Welling and B. Wellegehausen, “Optically pumped continuous alkali dimer lasers,” in Springer Series in Optical Sciences, vol. 7, Laser Spectroscopy III. New York: Springer-Verlag, 1977, pp.365-369.
15. B. Wellegehausen, S. Shahdin, D. Friede, and H. Welling, “Continuous laser oscillation in diatomic molecular sodium,” Appl Phys., VO. 13, pp. 97-99,1977.
16. B. Wellegehausen, H. Welling, K. H. Stephan, +d H. H. Heitmann, presented at the 10th Int. Quantum Electron. Conf., Atlanta, GA, 1978.
17. Wellegehausen, B.; , "Optically pumped CW dimer lasers," *Quantum Electronics, IEEE Journal of* , vol.15, no.10, pp. 1108- 1130, Oct 1979. URL: http://ieeexplore.ieee.org/stamp/stamp.jsp?tp=&arnumber=1069897&isnumber=22990

18. A. D. Smirnov, “Calcuations of Molecular Constants for the Ground Electronic States of Alkali Metal Dimers Based on Combined Potential Energy Curves”, Russian Journal of Phy Chem., Vol 76, No. 2, 2002, pg. 224-230.
19. Bernath, Peter F., “Spectra of Atoms and Molecules”, Oxford University Press, 1995.
20. Mark M. Somoza, Lehrstuhl für Physik Weihenstephan, Technische Universität München, Vöttinger Straße 40, 85350 Freising, Germany
21. R. P. Benedict, “ Investigation of diatomic cesium as a laser medium by absorption and florescence spectroscopy”, Dissertation, AFIT, June 1977.
22. S. Vdovic, D. Sarkisyan, G. Pichler, Absorption spectrum of rubidium and cesium dimers by compact computer operated spectrometer, Optics Communications, Volume 268, Issue 1, 1 December 2006, Pages 58-63, ISSN 0030-4018, DOI: 10.1016/j.optcom.2006.06.070.
23. D.H. Sarkisyan, A.S. Sarkisyan, A.K. Yalanusyan, “Thermal Disassociation of Cesium Dimers”, Applied Physics B:Lasers and Optics, Vol 66, 1998 pg. 241-244.
24. D.H. Sarkisyan, A.S.Sarkisyan, A.K. Yalanusyan Thermal dissociation of cesium dimers, Appl. Phys. B. 241-244 1998.
25. M. Lapp, L. P. Harris, Absorption cross sections of alkali-vapor molecules: I. Cs2 in the visible II. K2 in the red, Journal of Quantitative Spectroscopy and Radiative Transfer, Volume 6, Issue 2, March-April 1966, Pages 169-179, ISSN 0022-4073, DOI: 10.1016/0022-4073(66)90035-5.
26. F. W. Loomis, P. Kusch, The Band Spectrum of Caesium, Phys. Rev. Volume 46, Issue 4, pg 292-301, Aug 1934.

27. I.D. Abella, Phys. Rev. Lett. 9 (1962), p. 453.
28. T. Tanimura, D. Akamatsu, Y. Yokoi, A. Furusawa, M. Kozuma, Opt. Lett. 31, 2344 (2006).
29. Encyclopedia of Laser Physics and Technology, Optical Parametric Oscillators, http://www.rp-photonics.com/optical_parametric_oscillators.html

APPENDIX 1

This appendix has all the experimental output of the florescence experiments completed by pumping the cesium vapor and recording the emission. The pumping wavelengths were scanned from 750 nm to 800 nm.

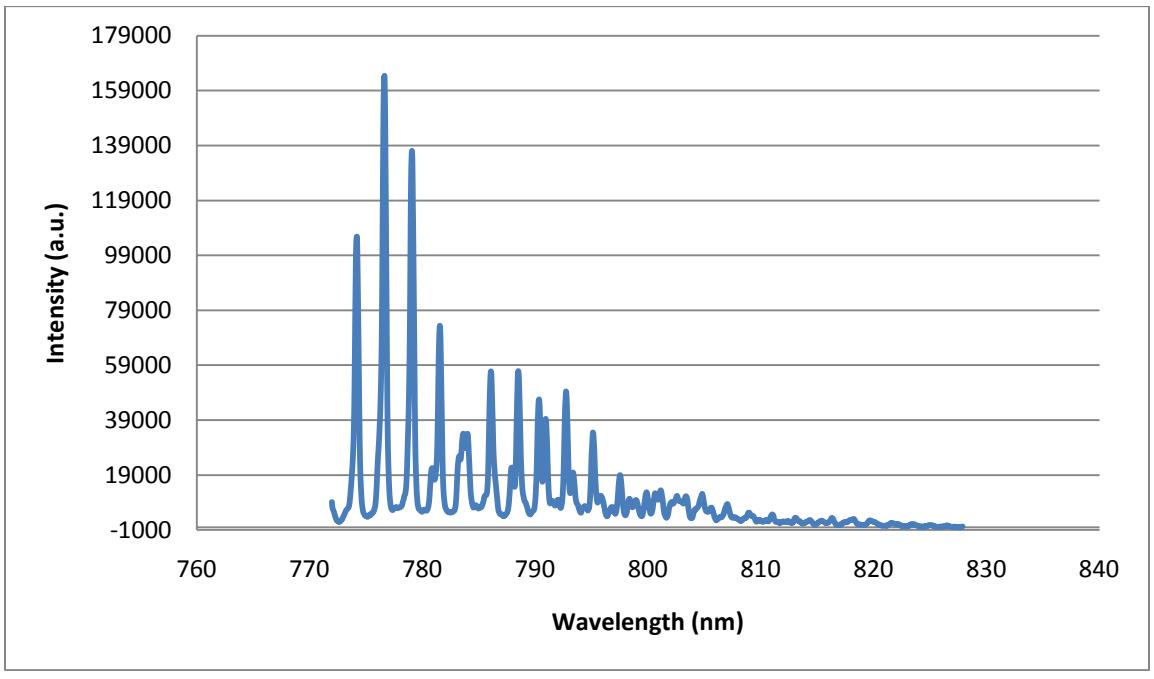

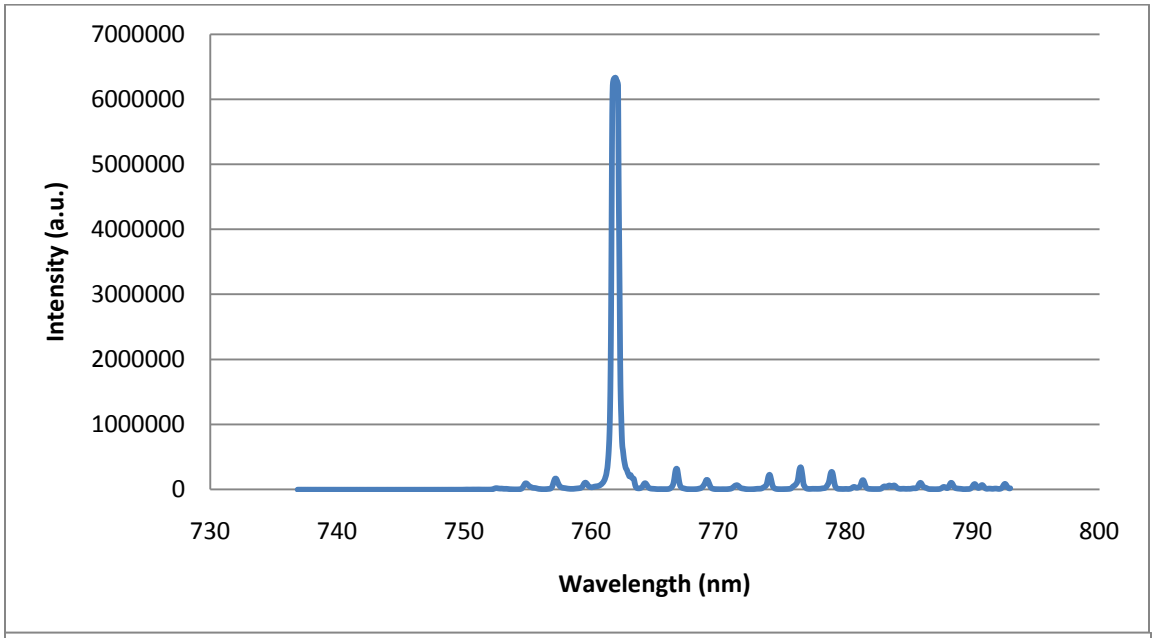
7000000
6000000
5000000
4000000
3000000
2000000
1000000
0
Intensity (a.u.)
730
740
750
760
770
780
790
800
Wavelength (nm)

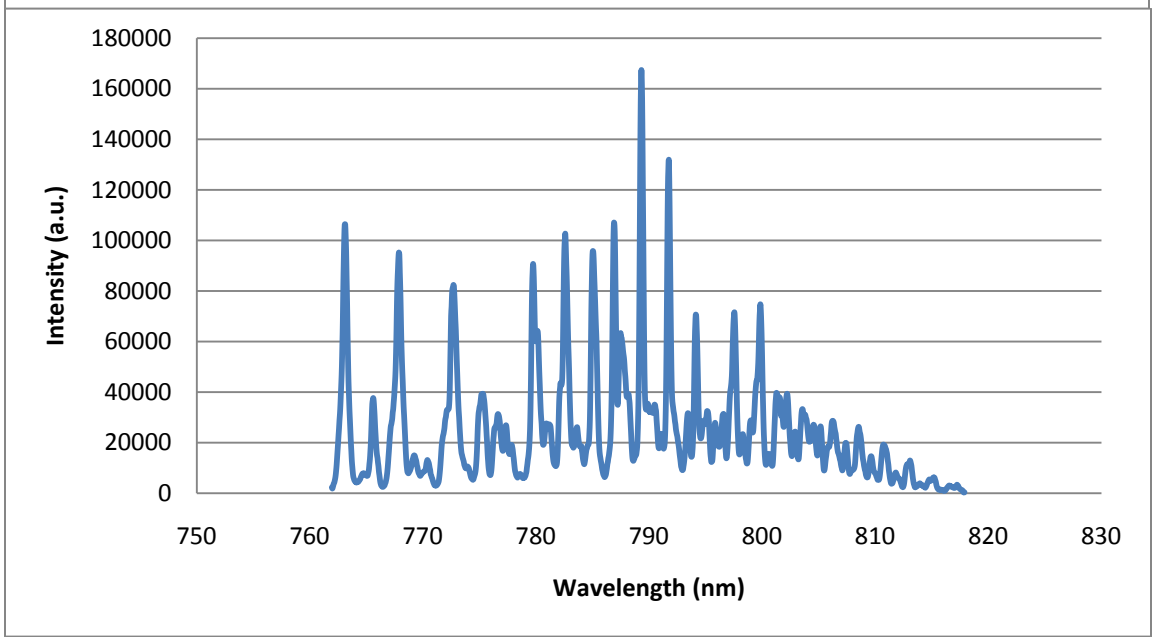
180000
160000
140000
120000
100000
80000
60000
40000
20000
0
Intensity (a.u.)
750
760
770
780
790
800
810
820
830
Wavelength (nm)

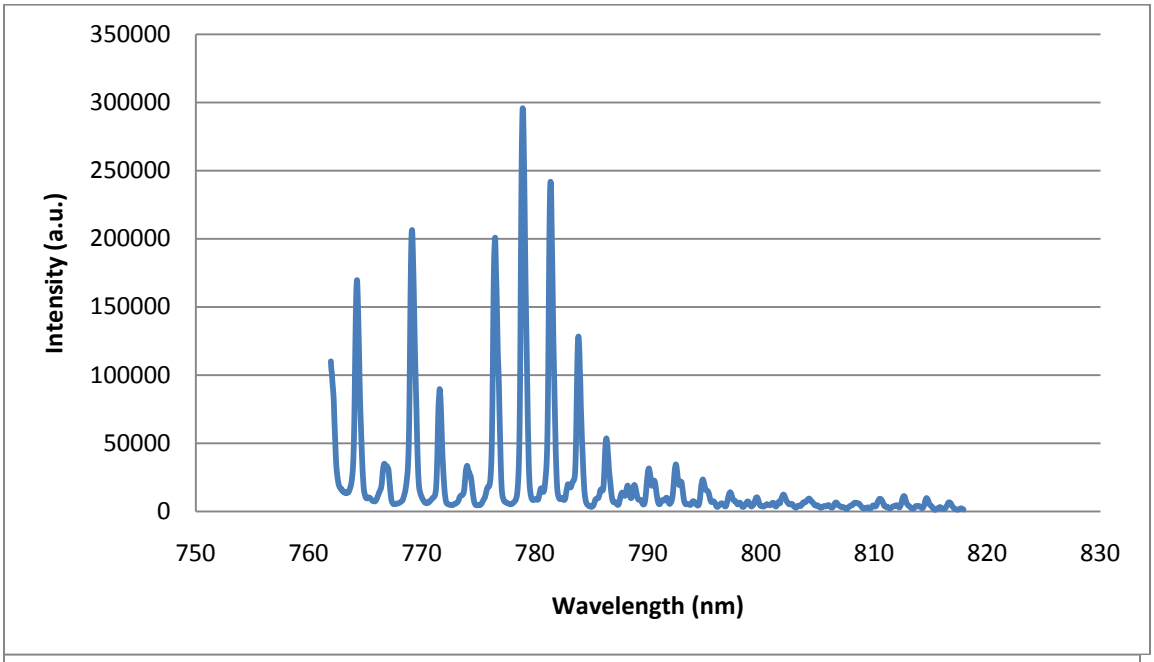
350000
300000
250000
200000
150000
100000
50000
0
Intensity (a.u.)
750
760
770
780
790
800
810
820
830
Wavelength (nm)

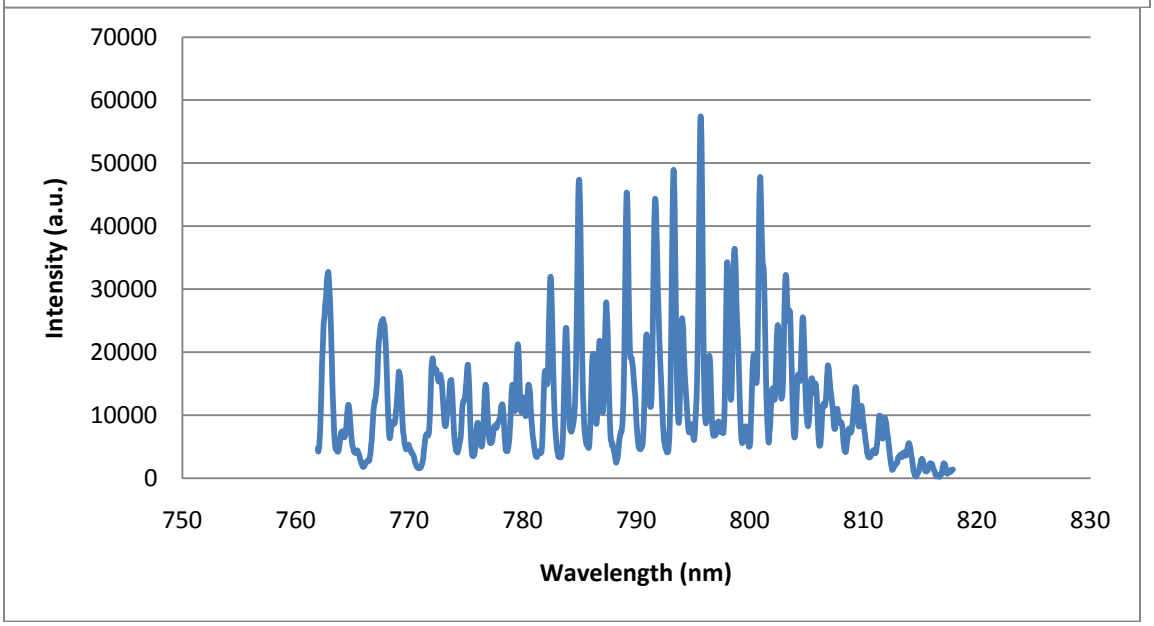
70000
60000
50000
40000
30000
20000
10000
0
Intensity (a.u.)
750
760
770
780
790
800
810
820
830
Wavelength (nm)

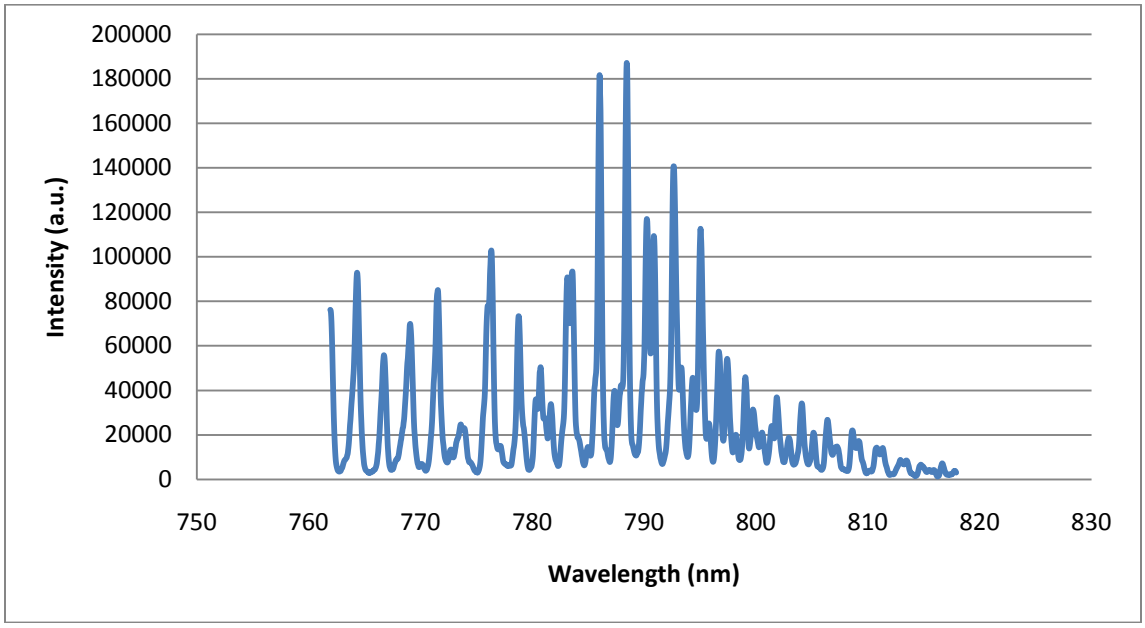
200000
180000
160000
140000
120000
100000
80000
60000
40000
20000
0
Intensity (a.u.)
750
760
770
780
790
800
810
820
830
Wavelength (nm)

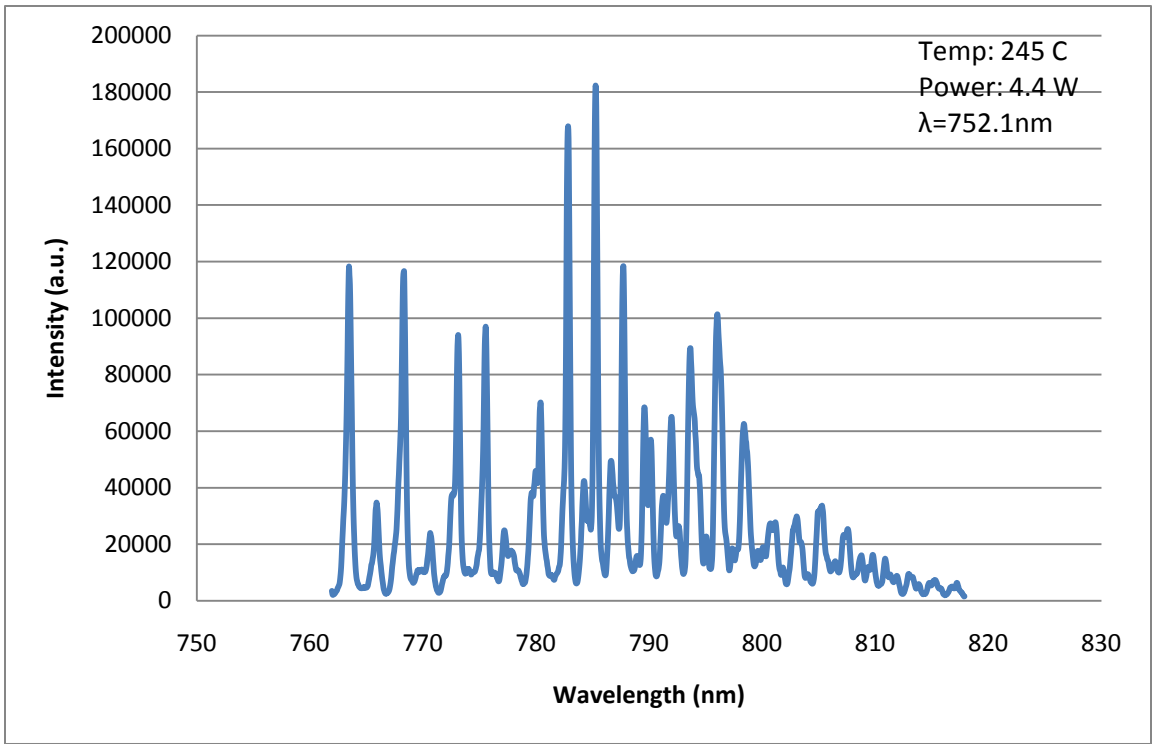
Temp: 245 C
Power: 4.4 W
λ=752.1nm
200000
180000
160000
140000
120000
100000
80000
60000
40000
20000
0
Intensity (a.u.)
750
760
770
780
790
800
810
820
830
Wavelength (nm)

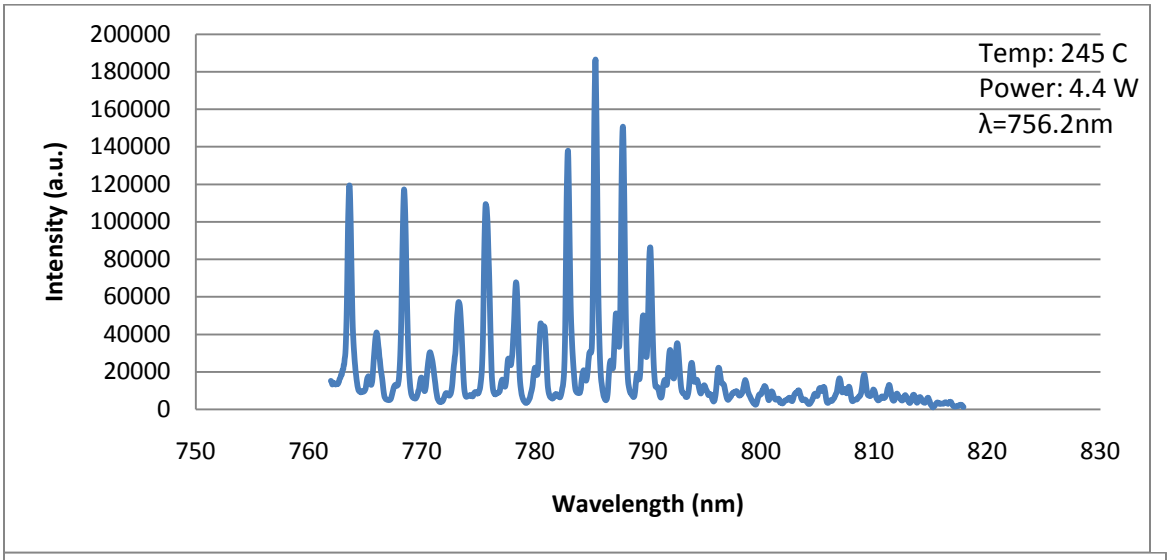
Temp: 245 C
Power: 4.4 W
λ=756.2nm
Intensity (a.u.)
200000
180000
160000
140000
120000
100000
80000
60000
40000
20000
0
750
760
770
780
790
800
810
820
830
Wavelength (nm)

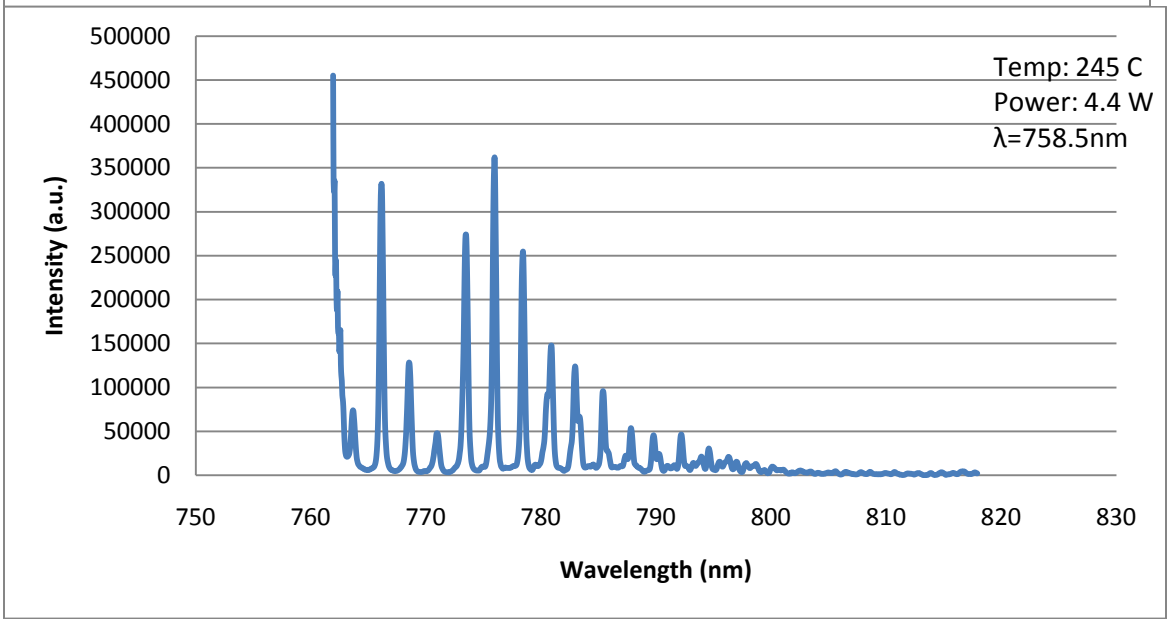
Temp: 245 C
Power: 4.4 W
λ=758.5nm
Intensity (a.u.)
500000
450000
400000
350000
300000
250000
200000
150000
100000
50000
0
750
760
770
780
790
800
810
820
830
Wavelength (nm)

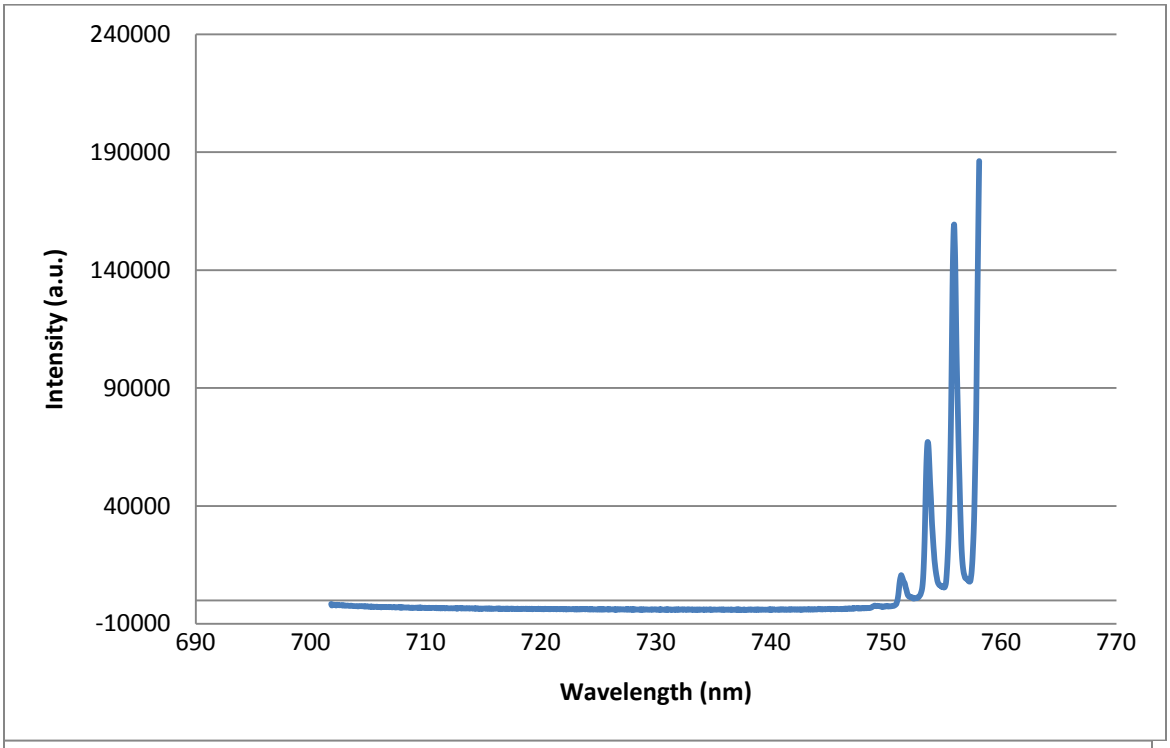
240000
190000
140000
90000
40000
-10000
Intensity (a.u.)
690
700
710
720
730
740
750
760
770
Wavelength (nm)

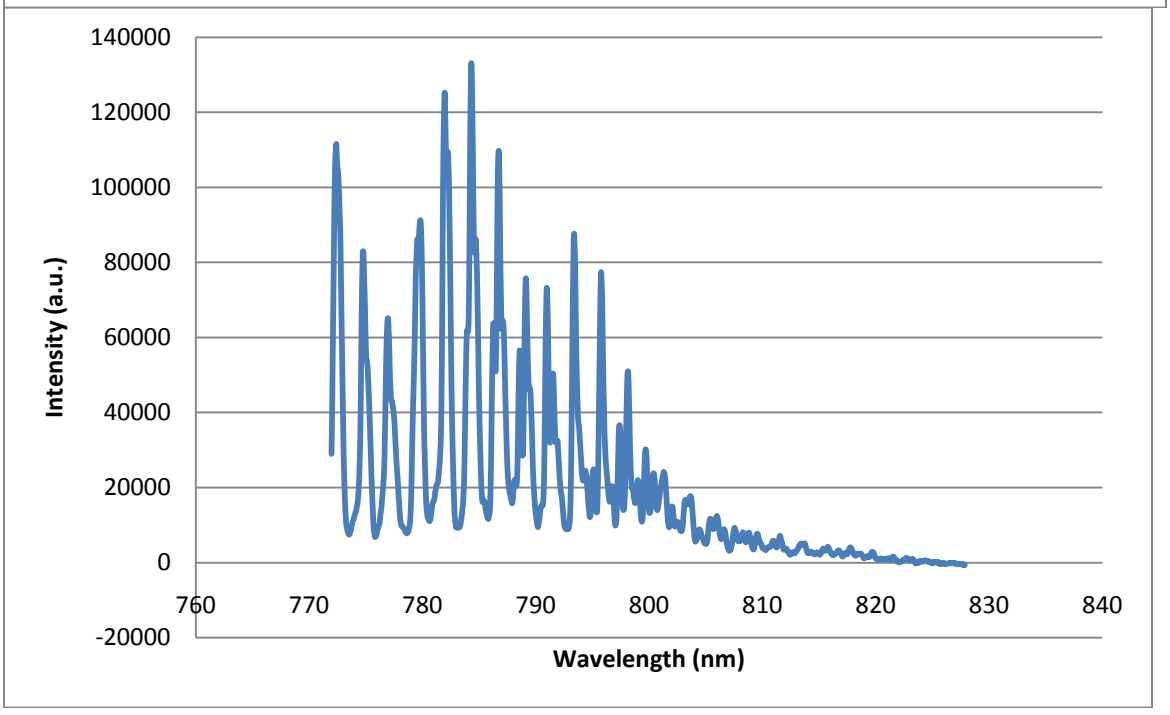
140000
120000
100000
80000
60000
40000
20000
0
-20000
Intensity (a.u.)
760
770
780
790
800
810
820
830
840
Wavelength (nm)

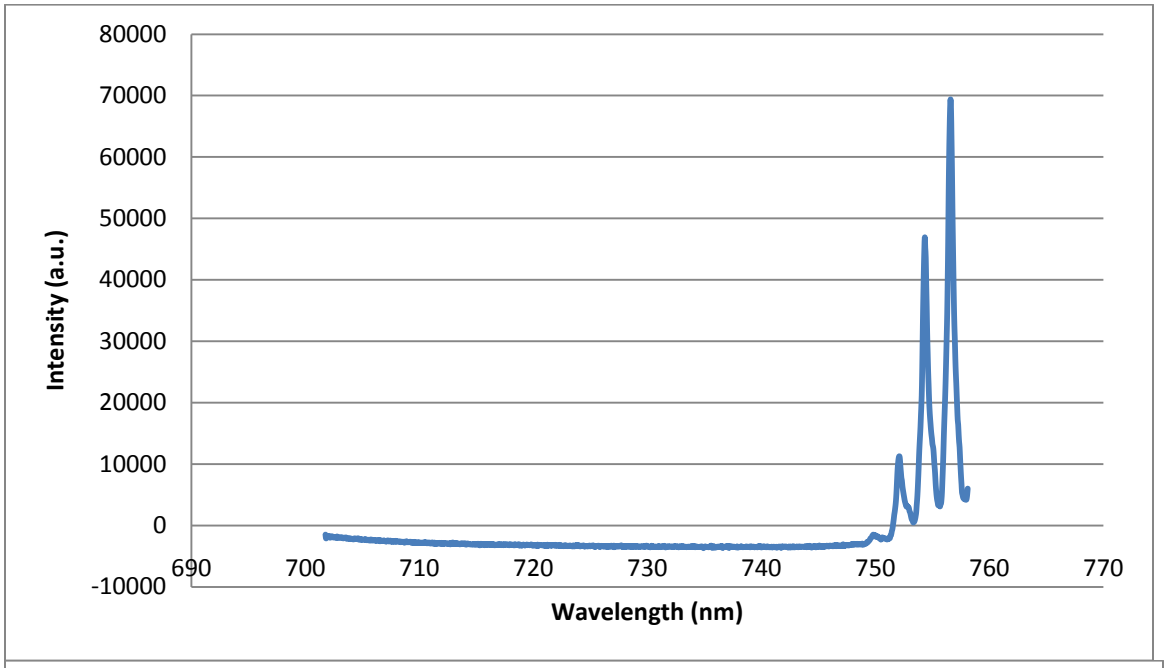
80000
70000
60000
50000
40000
30000
20000
10000
0
-10000
Intensity (a.u.)
690
700
710
720
730
740
750
760
770
Wavelength (nm)

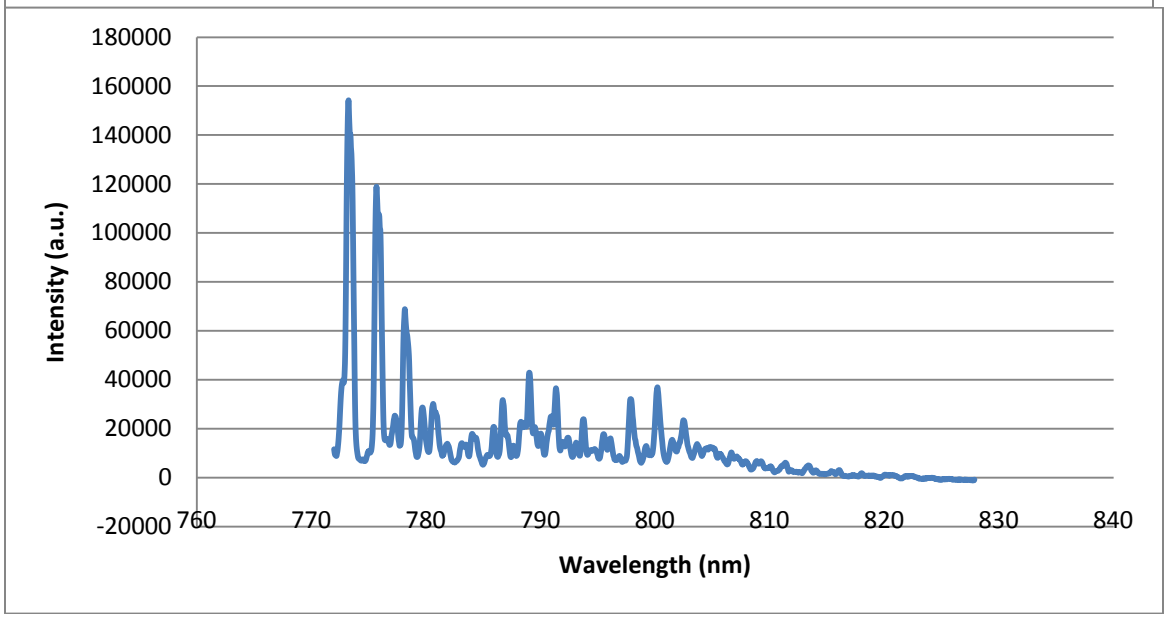
180000
160000
140000
120000
100000
80000
60000
40000
20000
0
-20000
Intensity (a.u.)
760
770
780
790
800
810
820
830
840
Wavelength (nm)

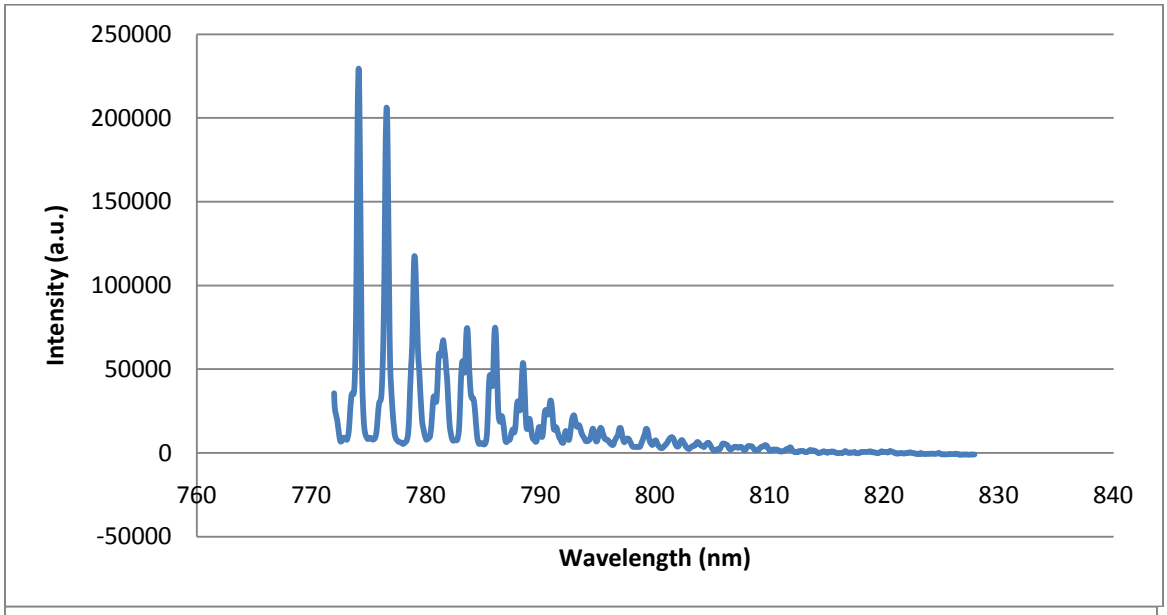
250000
200000
150000
100000
50000
0
-50000
Intensity (a.u.)
760
770
780
790
800
810
820
830
840
Wavelength (nm)

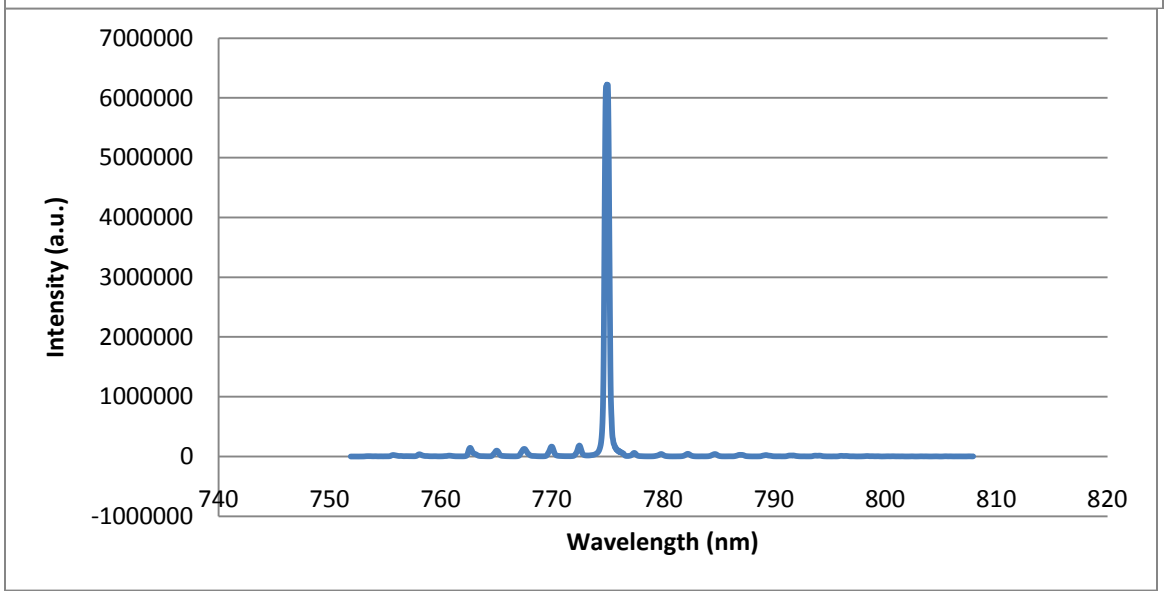
7000000
6000000
5000000
4000000
3000000
2000000
1000000
0
-1000000
Intensity (a.u.)
740
750
760
770
780
790
800
810
820
Wavelength (nm)

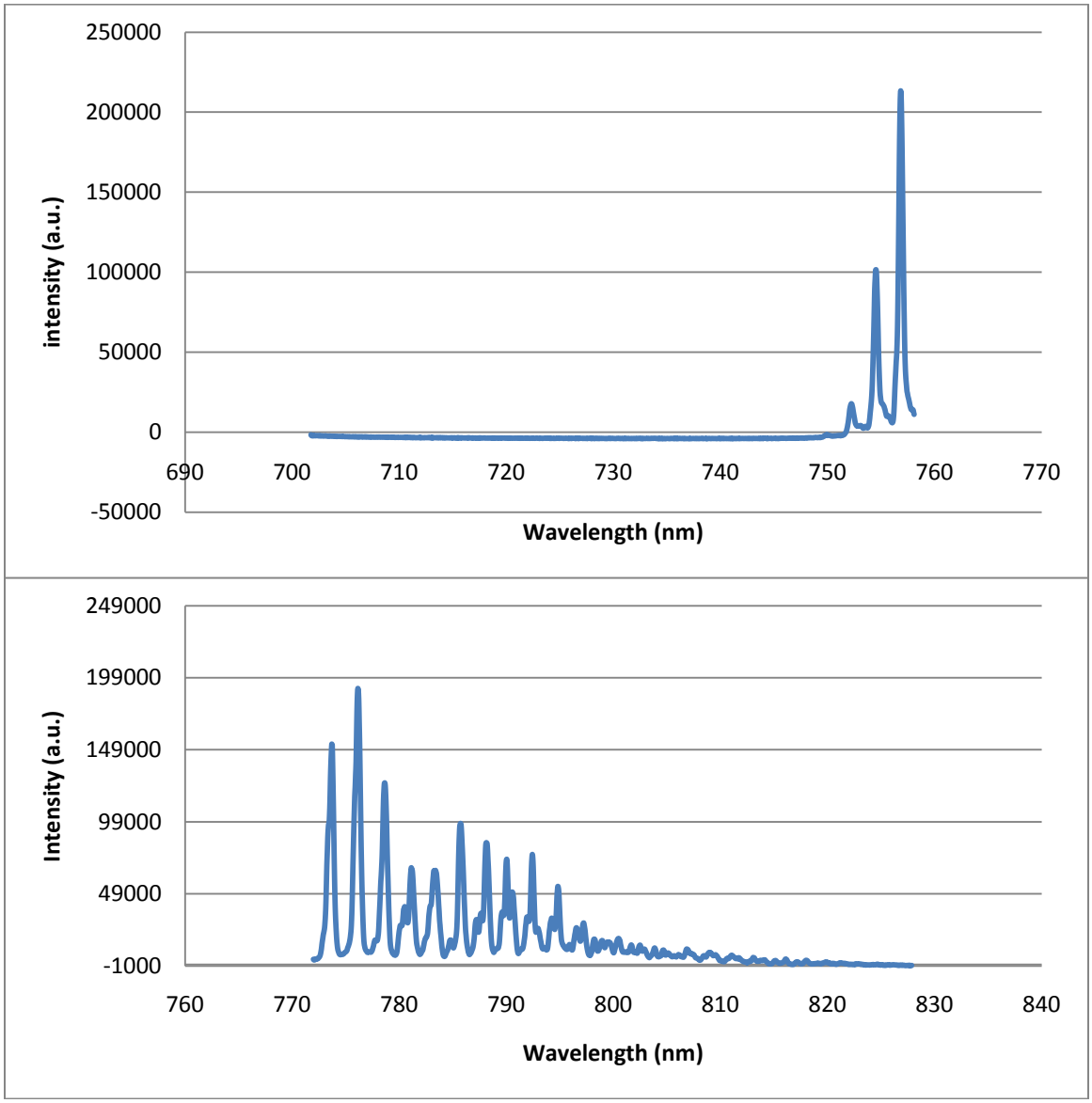
250000
200000
150000
100000
50000
0
-50000
intensity (a.u.)
690
700
710
720
730
740
750
760
770
Wavelength (nm)
249000
199000
149000
99000
49000
-1000
Intensity (a.u.)
760
770
780
790
800
810
820
830
840
Wavelength (nm)

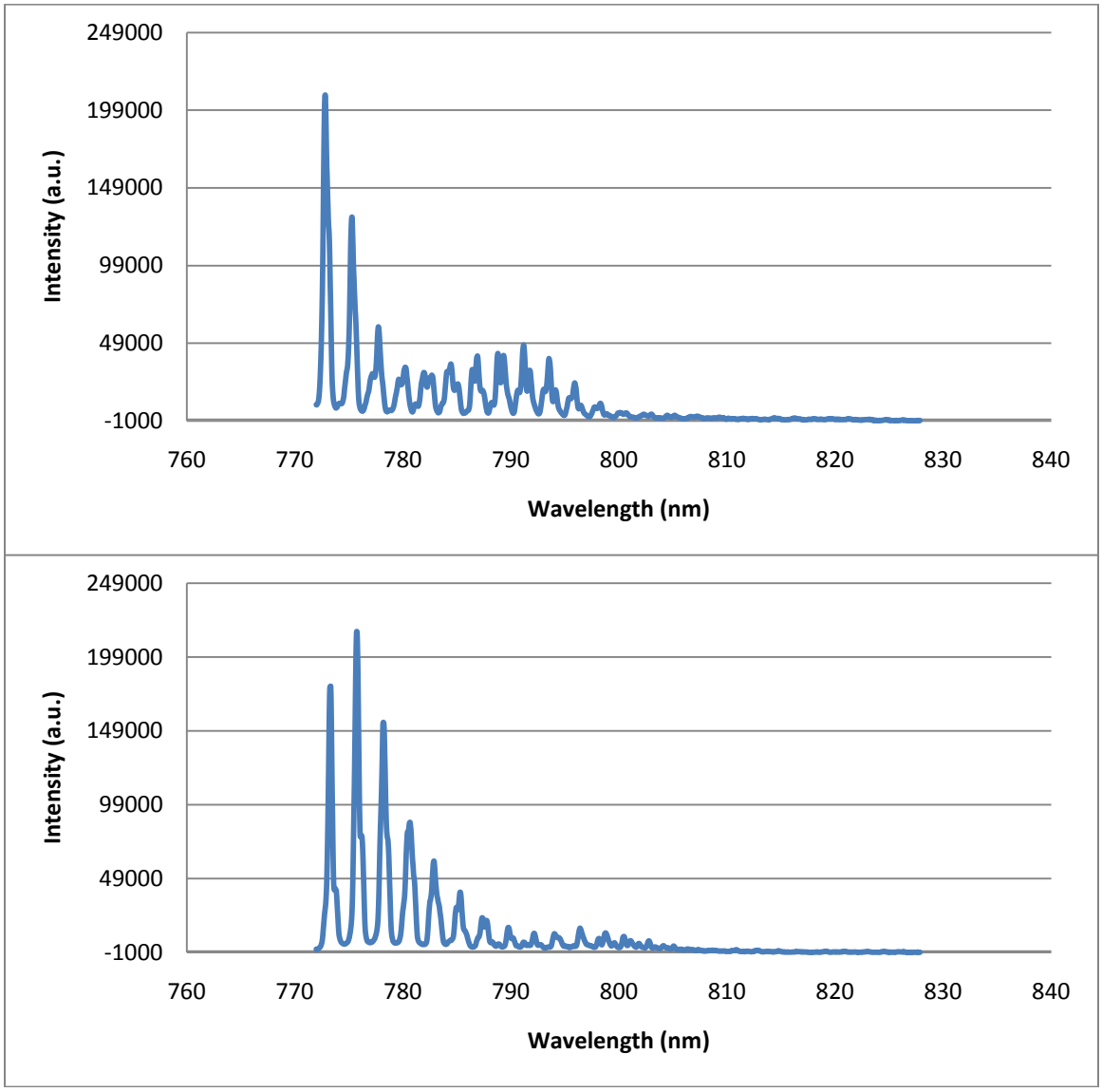
249000
199000
149000
99000
49000
-1000
Intensity (a.u.)
760
770
780
790
800
810
820
830
840
Wavelength (nm)
249000
199000
149000
99000
49000
-1000
Intensity (a.u.)
760
770
780
790
800
810
820
830
840
Wavelength (nm)

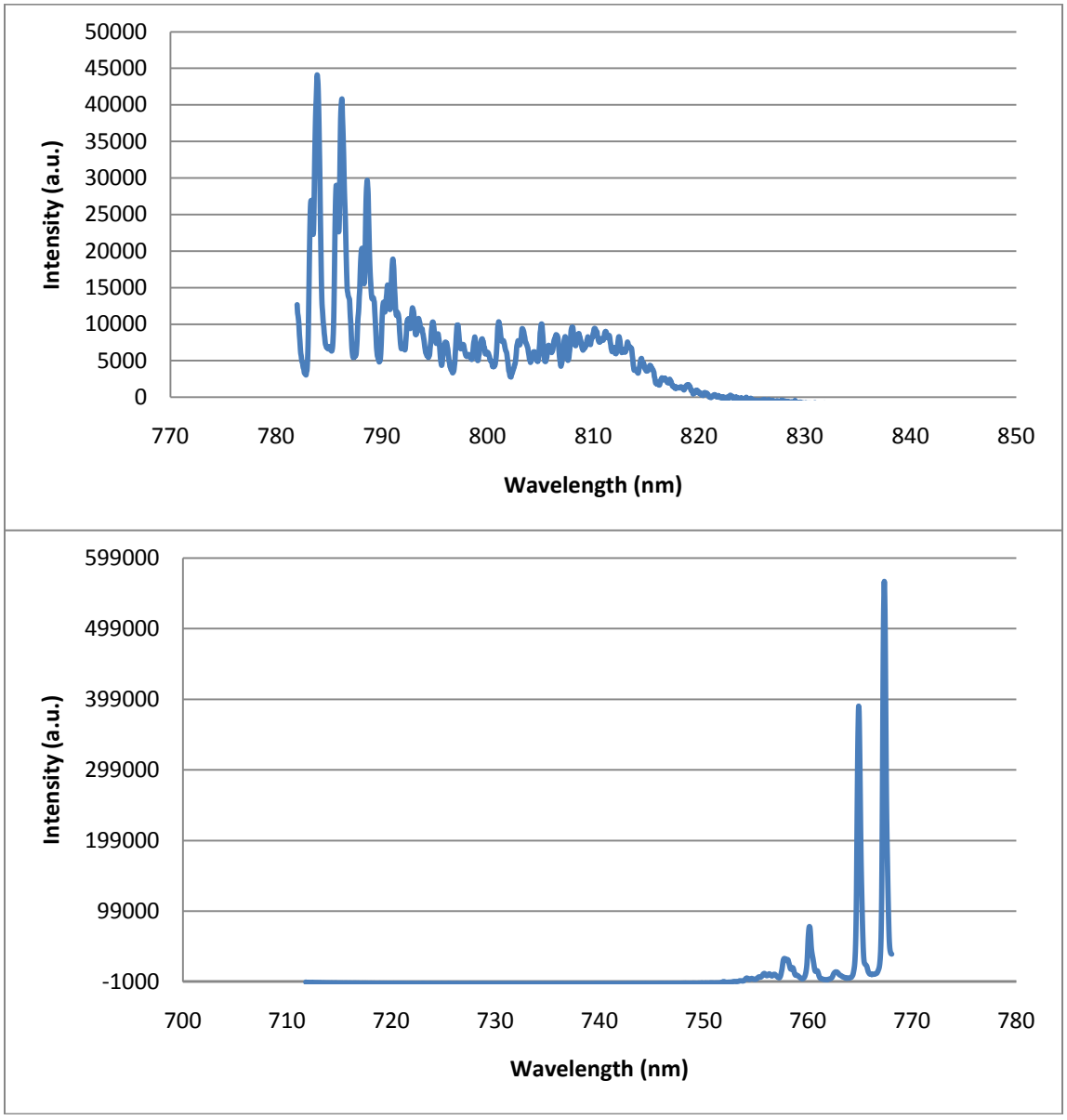
50000
45000
40000
35000
30000
25000
20000
15000
10000
5000
0
Intensity (a.u.)
770
780
790
800
810
820
830
840
850
Wavelength (nm)
599000
499000
399000
299000
199000
99000
-1000
Intensity (a.u.)
700
710
720
730
740
750
760
770
780
Wavelength (nm)

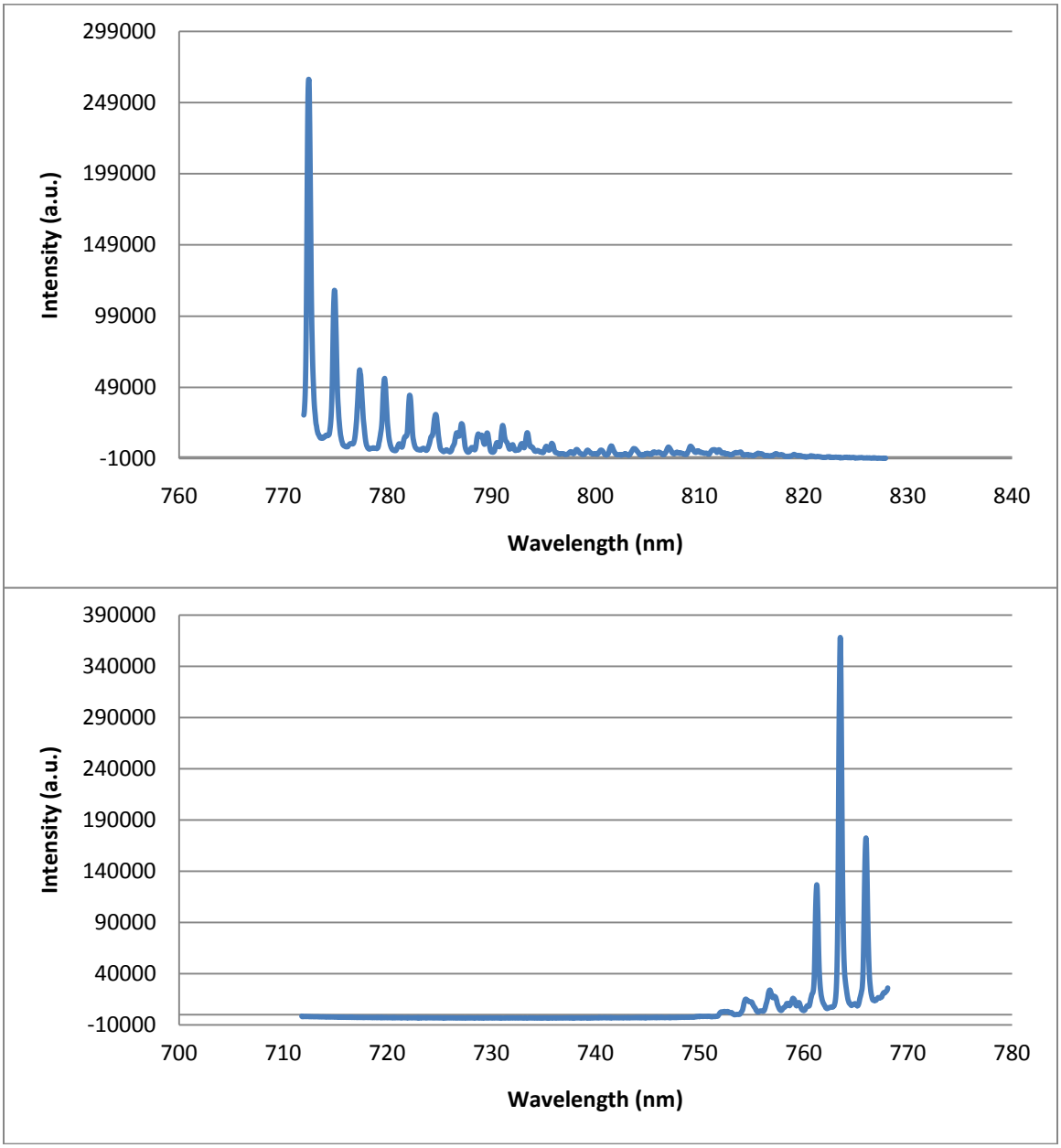
299000
249000
199000
149000
99000
49000
-1000
Intensity (a.u.)
760
770
780
790
800
810
820
830
840
Wavelength (nm)
390000
340000
290000
240000
190000
140000
90000
40000
-10000
Intensity (a.u.)
700
710
720
730
740
750
760
770
780
Wavelength (nm)

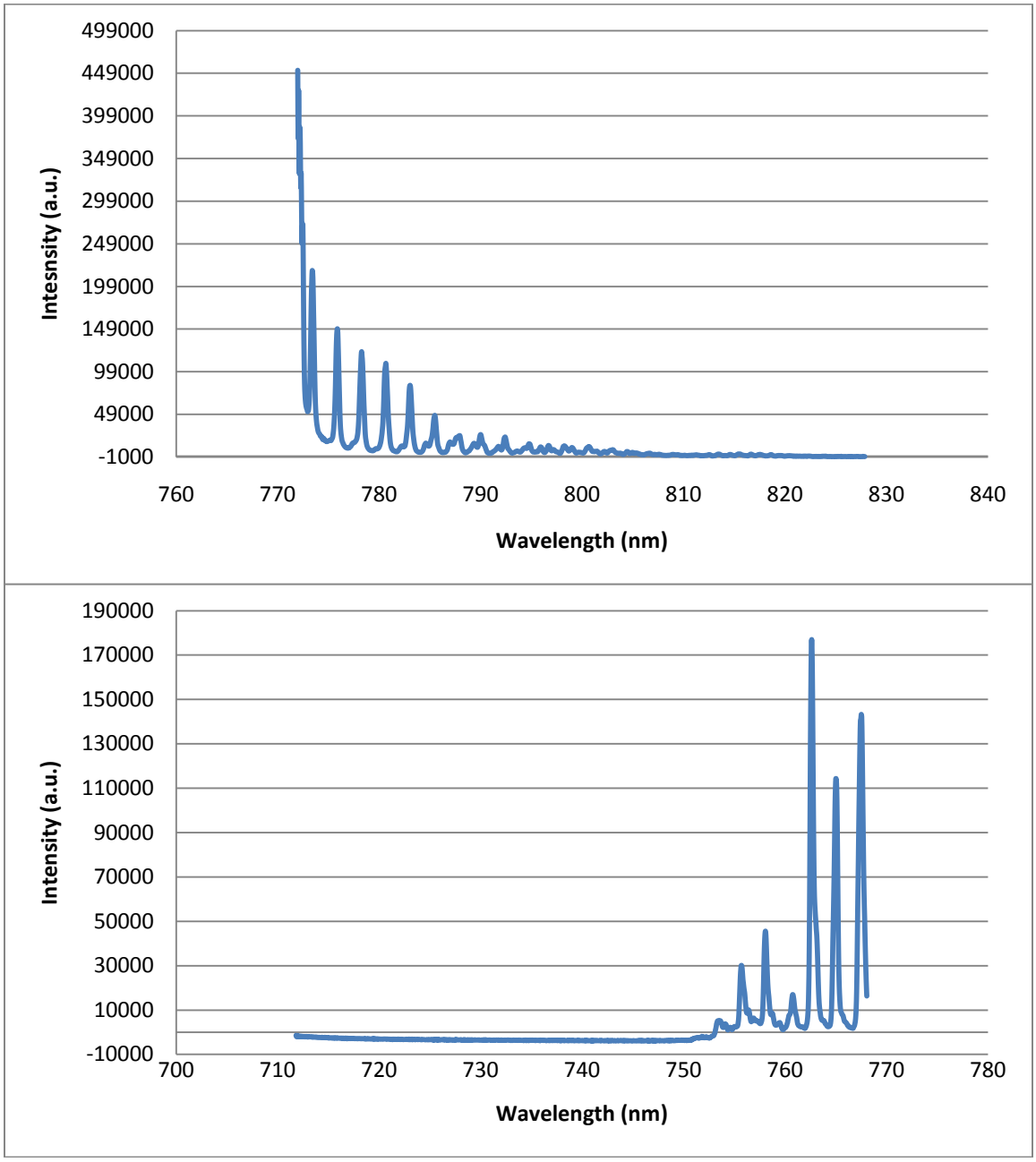
499000
449000
399000
349000
299000
249000
199000
149000
99000
49000
-1000
Intesnsity (a.u.)
760
770
780
790
800
810
820
830
840
Wavelength (nm)
190000
170000
150000
130000
110000
90000
70000
50000
30000
10000
-10000
Intensity (a.u.)
700
710
720
730
740
750
760
770
780
Wavelength (nm)

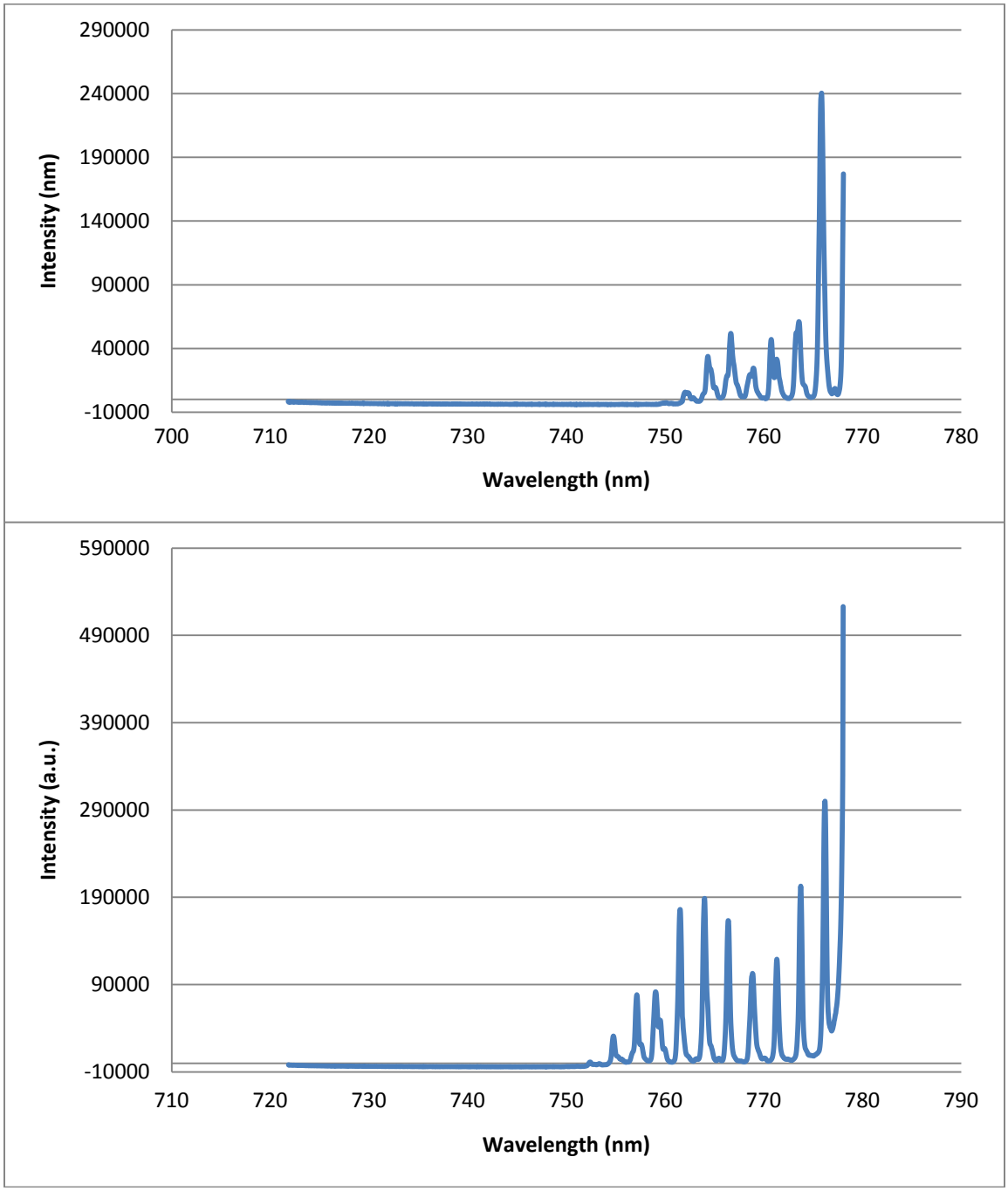
290000
240000
190000
140000
90000
40000
-10000
Intensity (nm)
700
710
720
730
740
750
760
770
780
Wavelength (nm)
590000
490000
390000
290000
190000
90000
-10000
Intensity (a.u.)
710
720
730
740
750
760
770
780
790
Wavelength (nm)

Appendix 2

This appendix holds all the experiments completed to investigate the temperature dependence of cesium dimer concentration. Although the experiment points to the optimum temperature as below 260 C, the test was redone every few months and the optimum temperature would change between each test. If the test was redone on the same day, the optimal temperature would be the same. This test led to investigating the temperature gradient inside the heat pipe.

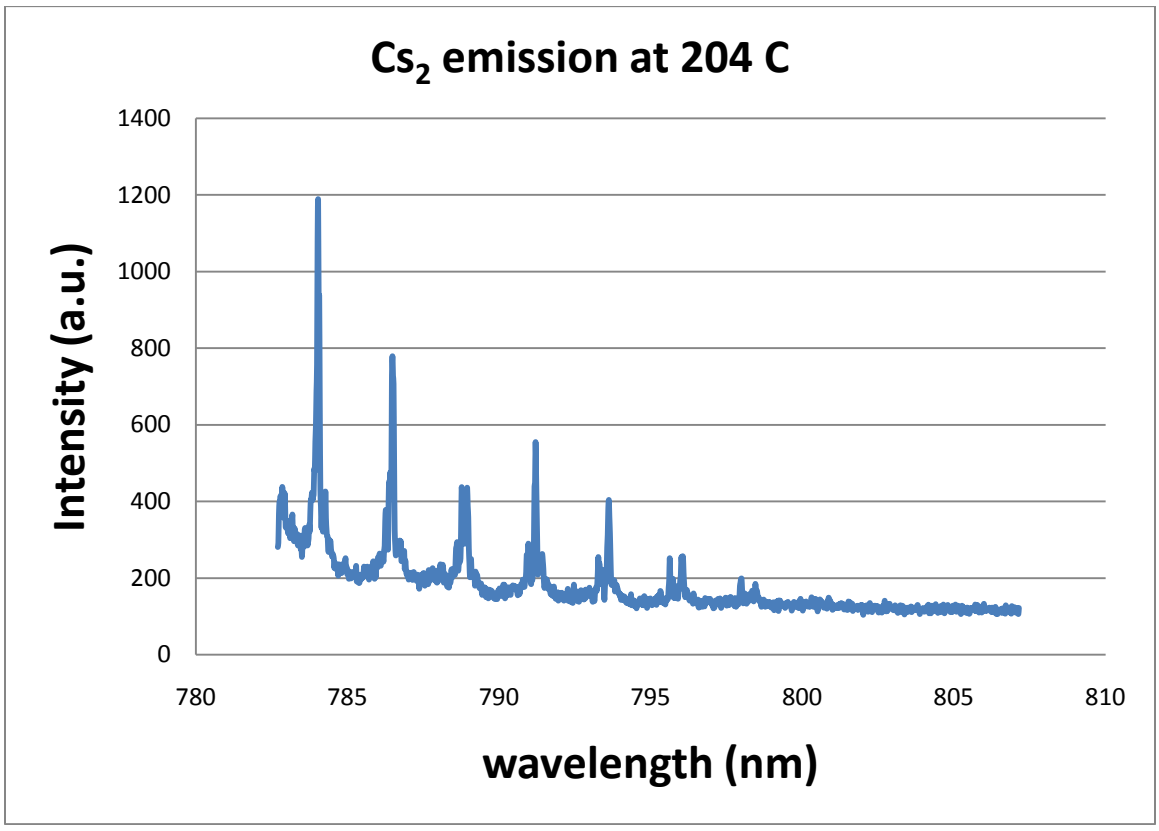

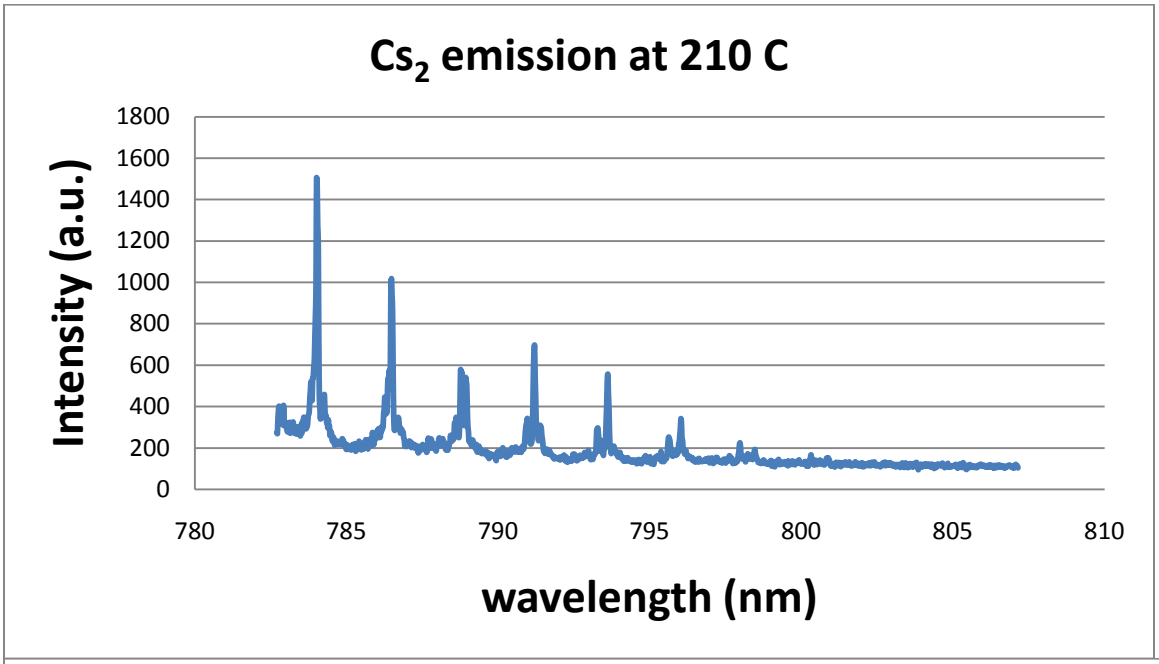
Cs2 emission at 210 C
Intensity (a.u.)
1800
1600
1400
1200
1000
800
600
400
200
0
780
785
790
795
800
805
810
wavelength (nm)

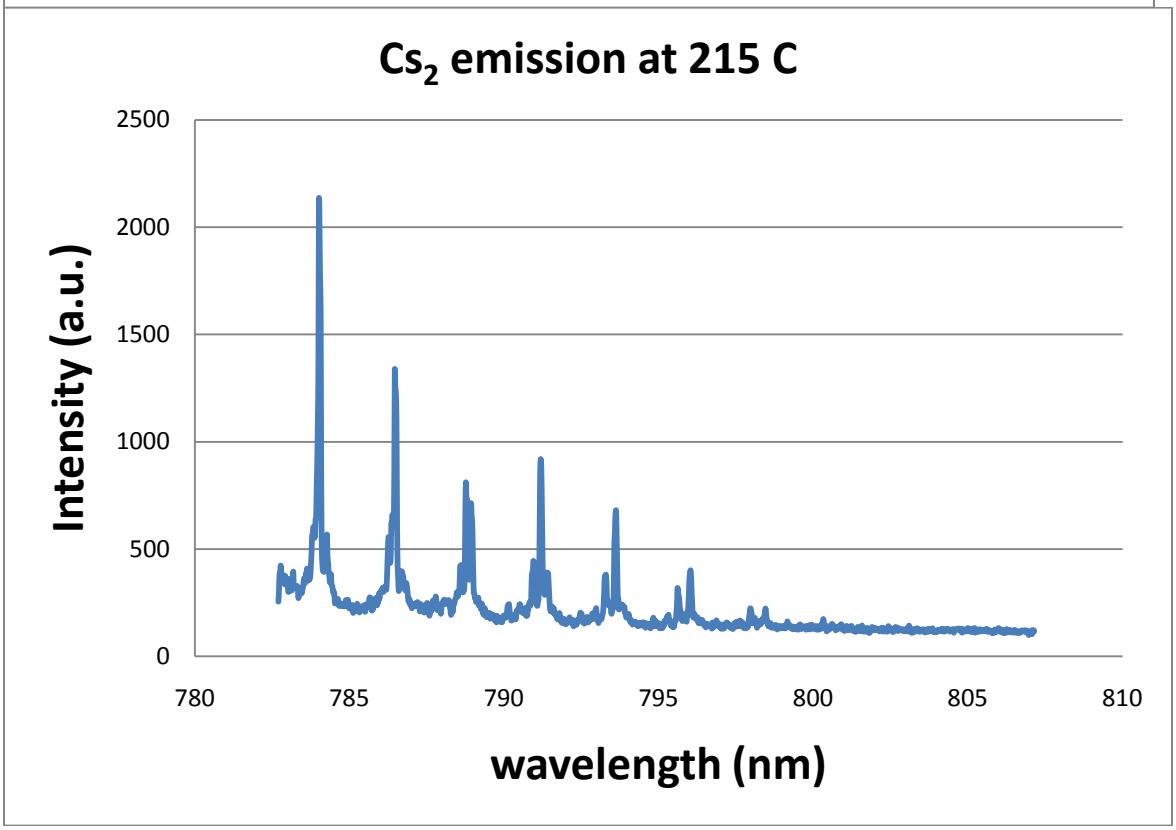
Cs2 emission at 215 C
Intensity (a.u.)
2500
2000
1500
1000
500
0
780
785
790
795
800
805
810
wavelength (nm)

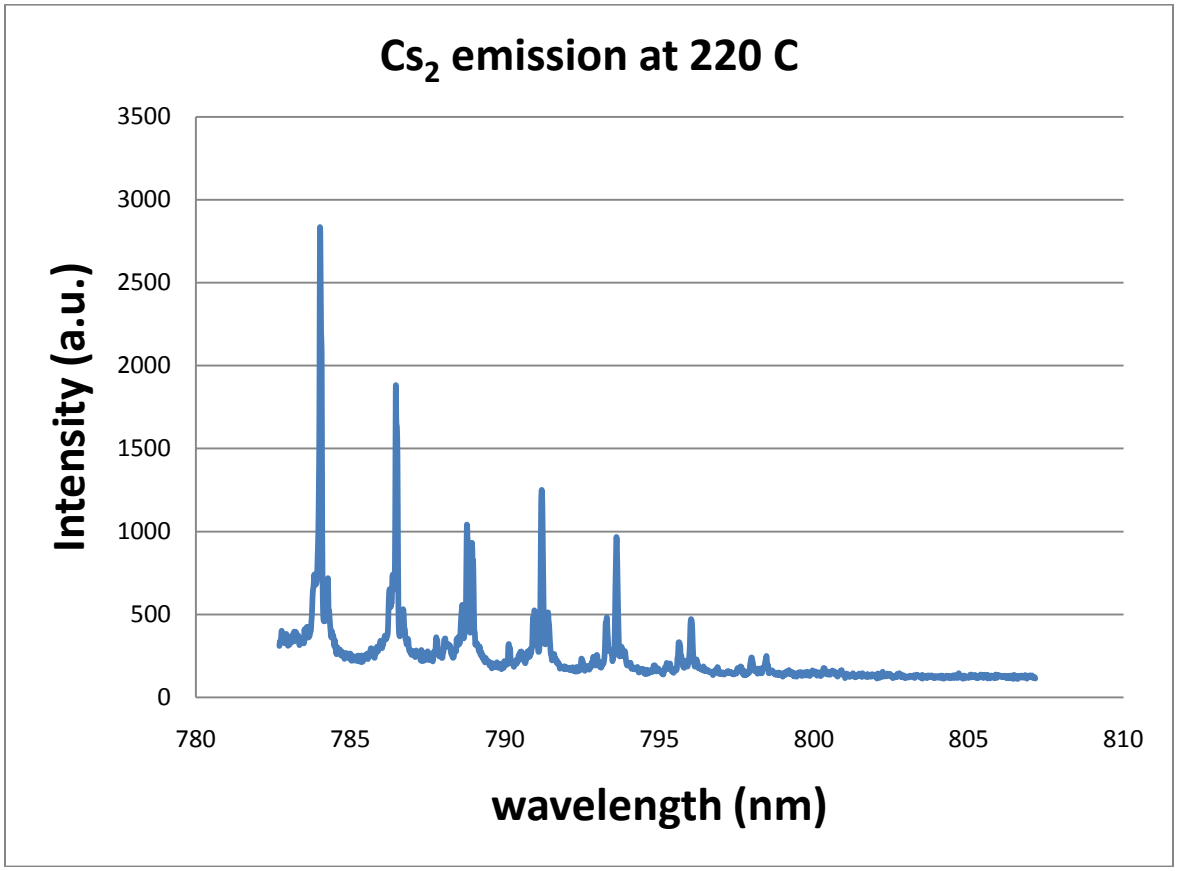
Cs2 emission at 220 C
Intensity (a.u.)
3500
3000
2500
2000
1500
1000
500
0
780
785
790
795
800
805
810
wavelength (nm)

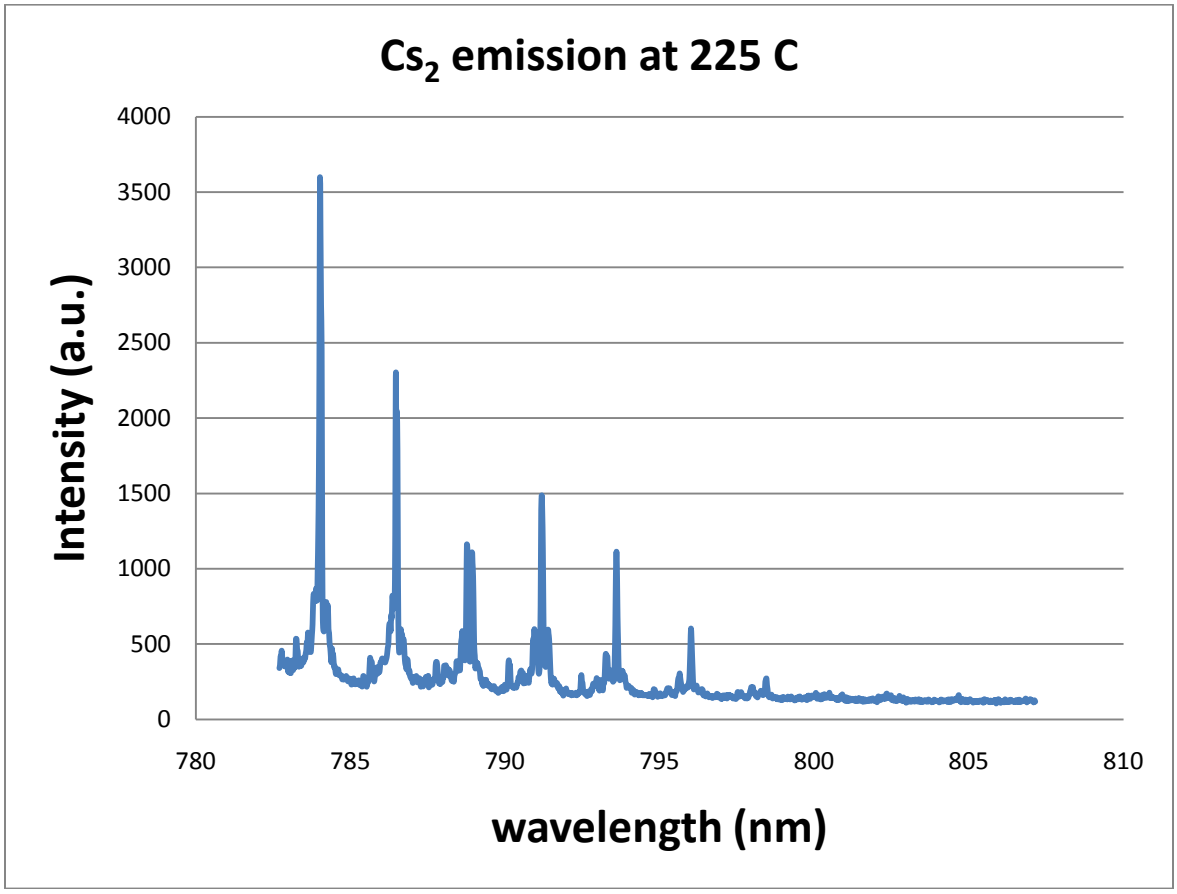
Cs2 emission at 225 C
Intensity (a.u.)
4000
3500
3000
2500
2000
1500
1000
500
0
780
785
790
795
800
805
810
wavelength (nm)

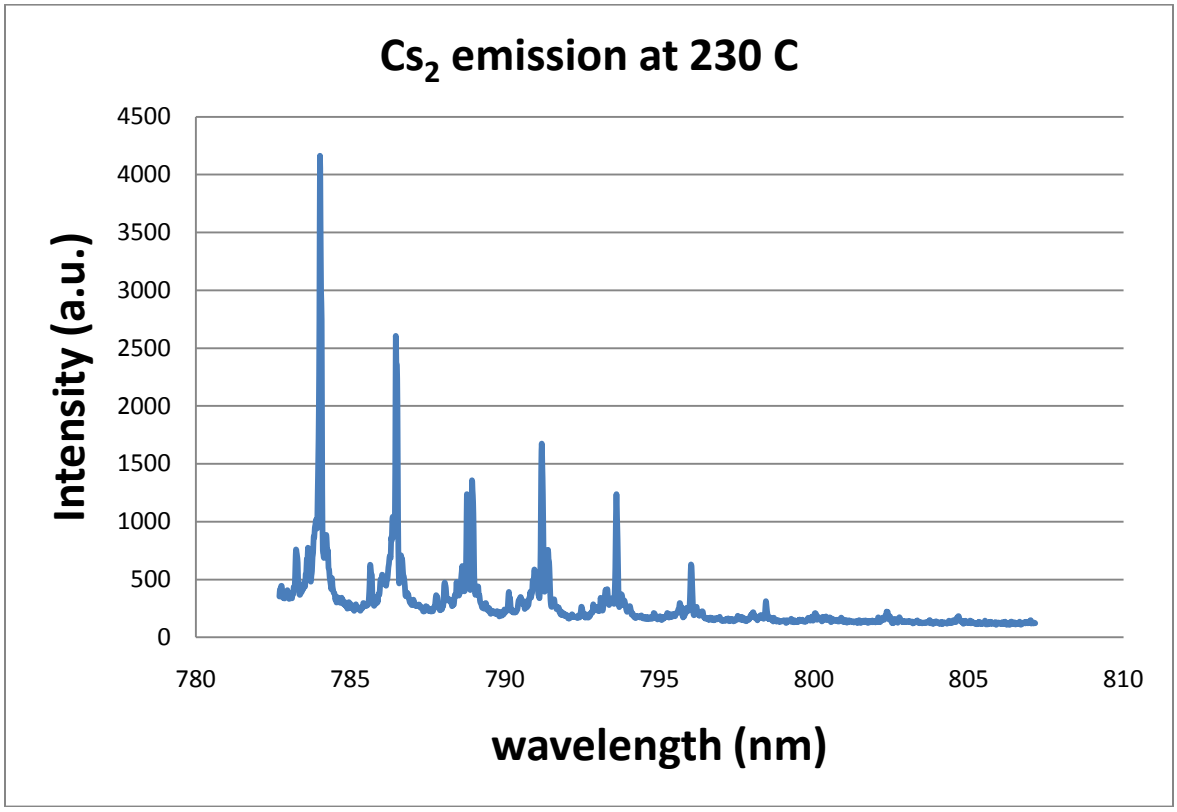
Cs2 emission at 230 C
Intensity (a.u.)
4500
4000
3500
3000
2500
2000
1500
1000
500
0
780
785
790
795
800
805
810
wavelength (nm)

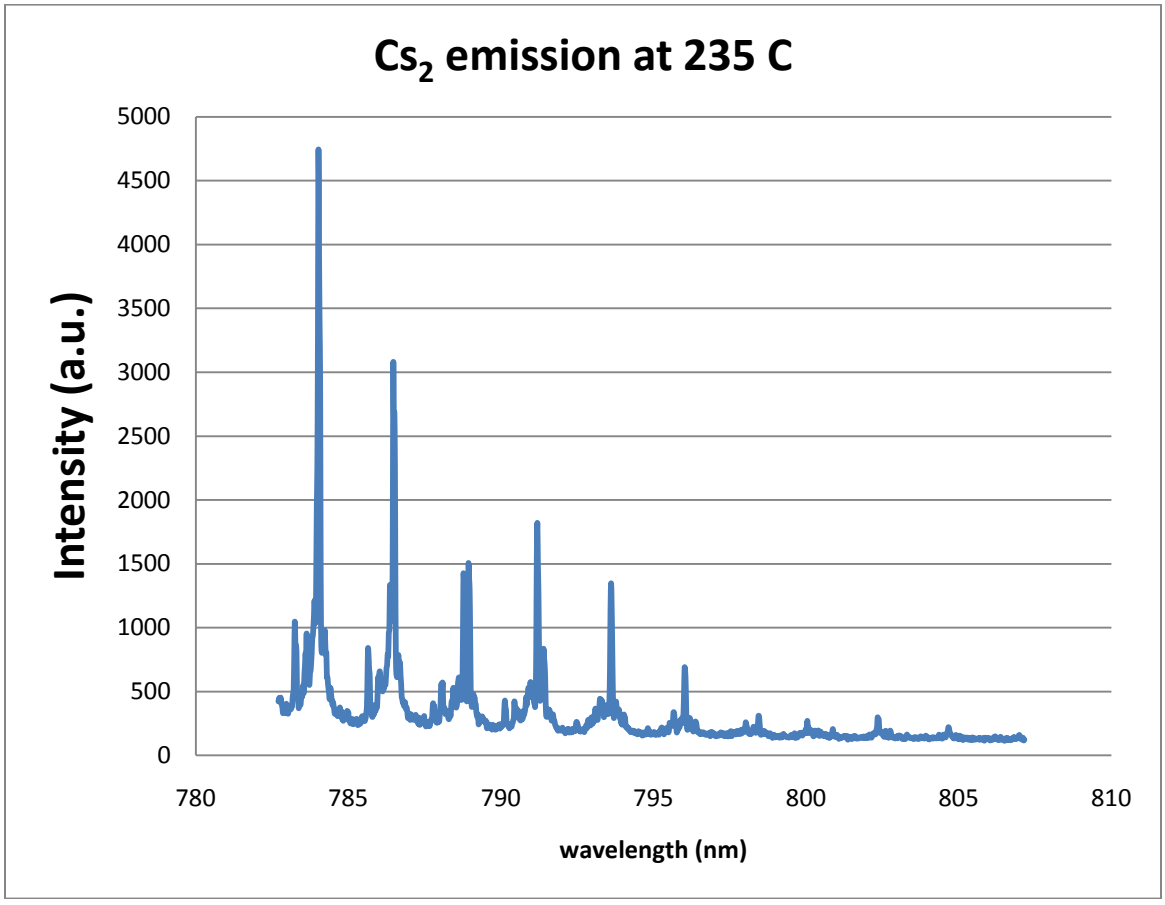
Cs2 emission at 235 C
Intensity (a.u.)
5000
4500
4000
3500
3000
2500
2000
1500
1000
500
0
780
785
790
795
800
805
810
wavelength (nm)

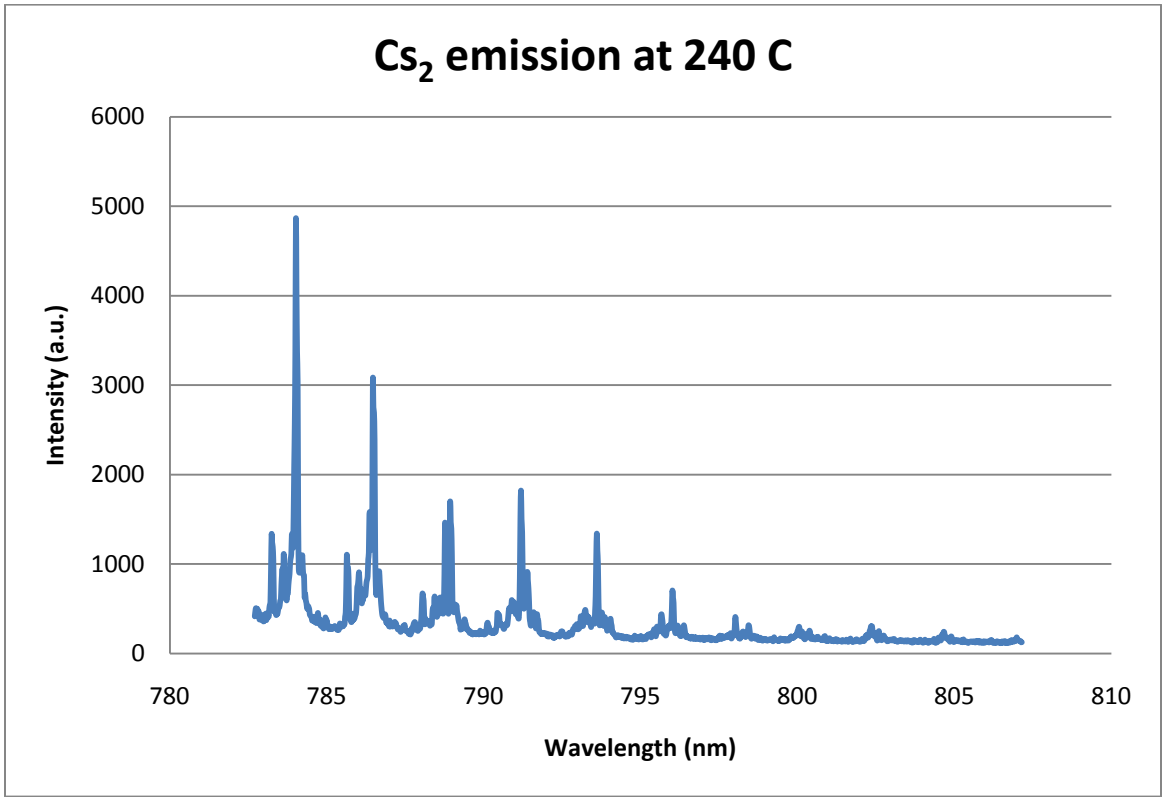
Cs2 emission at 240 C
6000
5000
4000
3000
2000
1000
0
Intensity (a.u.)
780
785
790
795
800
805
810
Wavelength (nm)

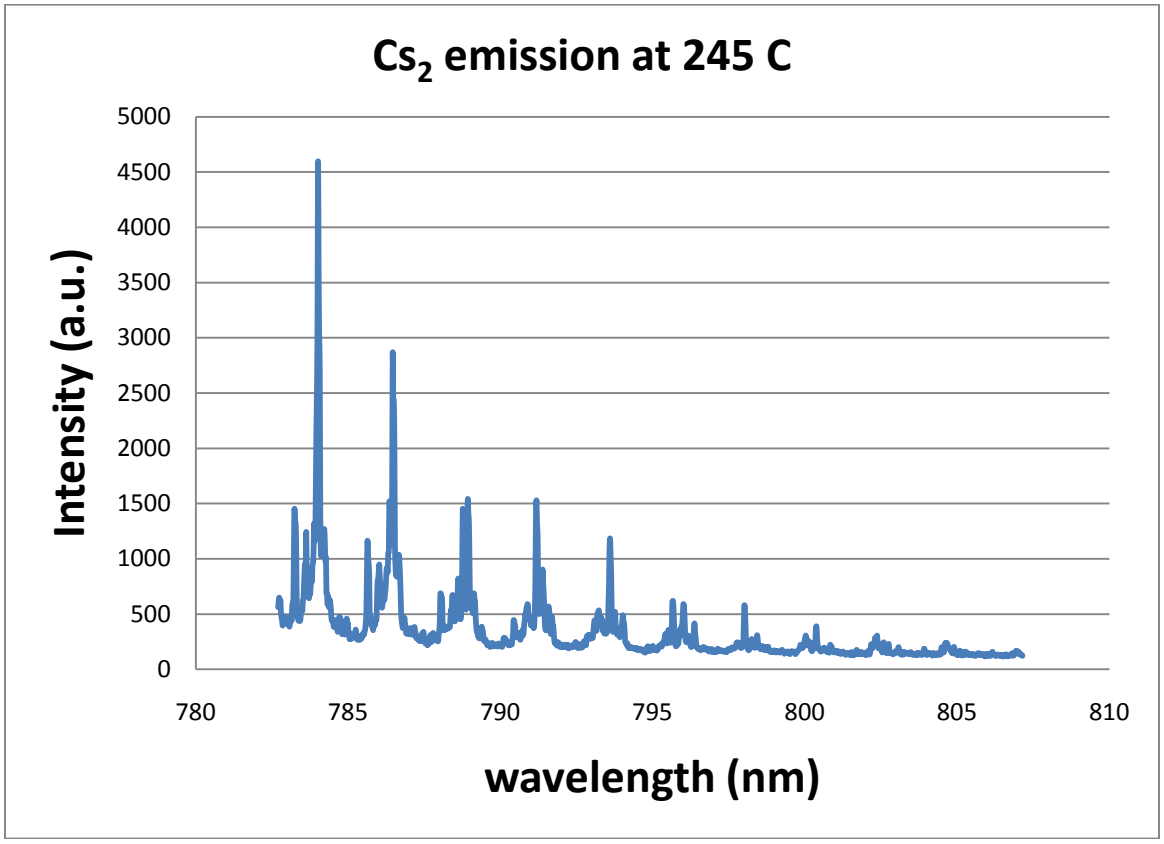
Cs2 emission at 245 C
Intensity (a.u.)
5000
4500
4000
3500
3000
2500
2000
1500
1000
500
0
780
785
790
795
800
805
810
wavelength (nm)

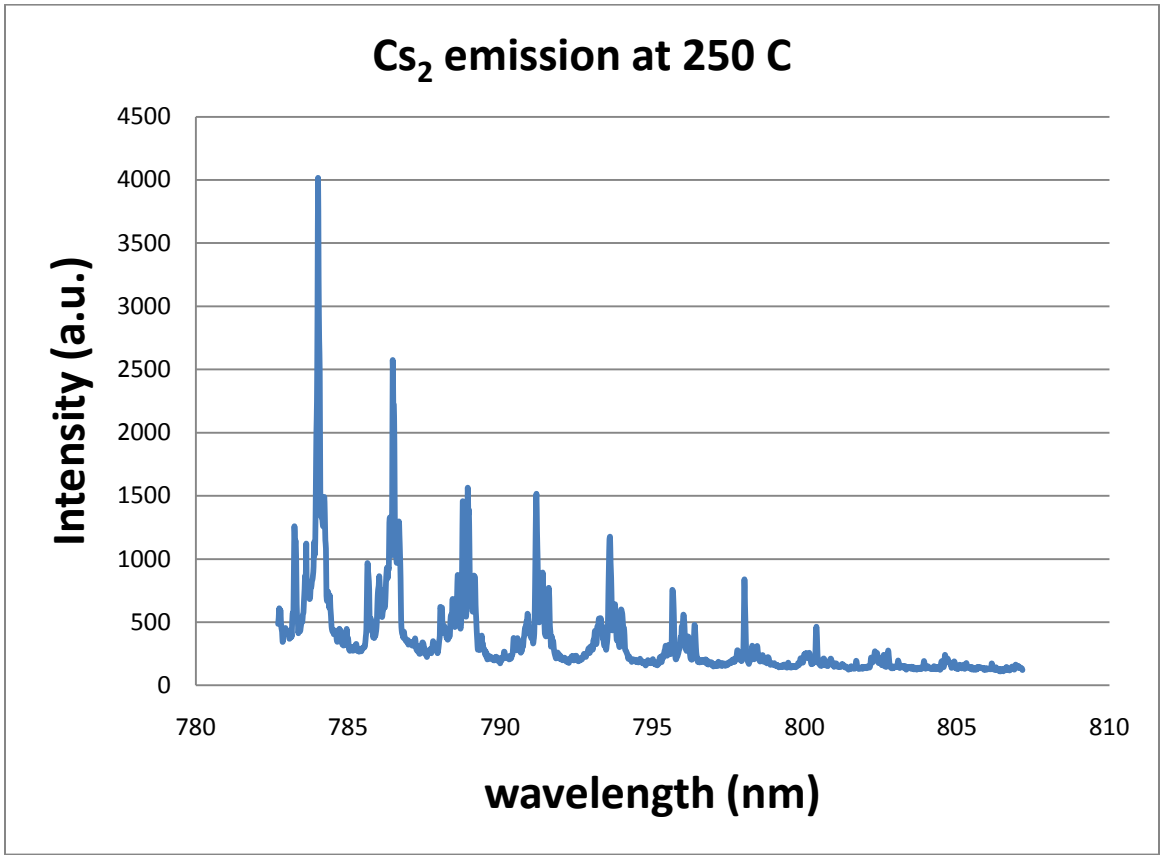
Cs2 emission at 250 C
Intensity (a.u.)
4500
4000
3500
3000
2500
2000
1500
1000
500
0
780
785
790
795
800
805
810
wavelength (nm)

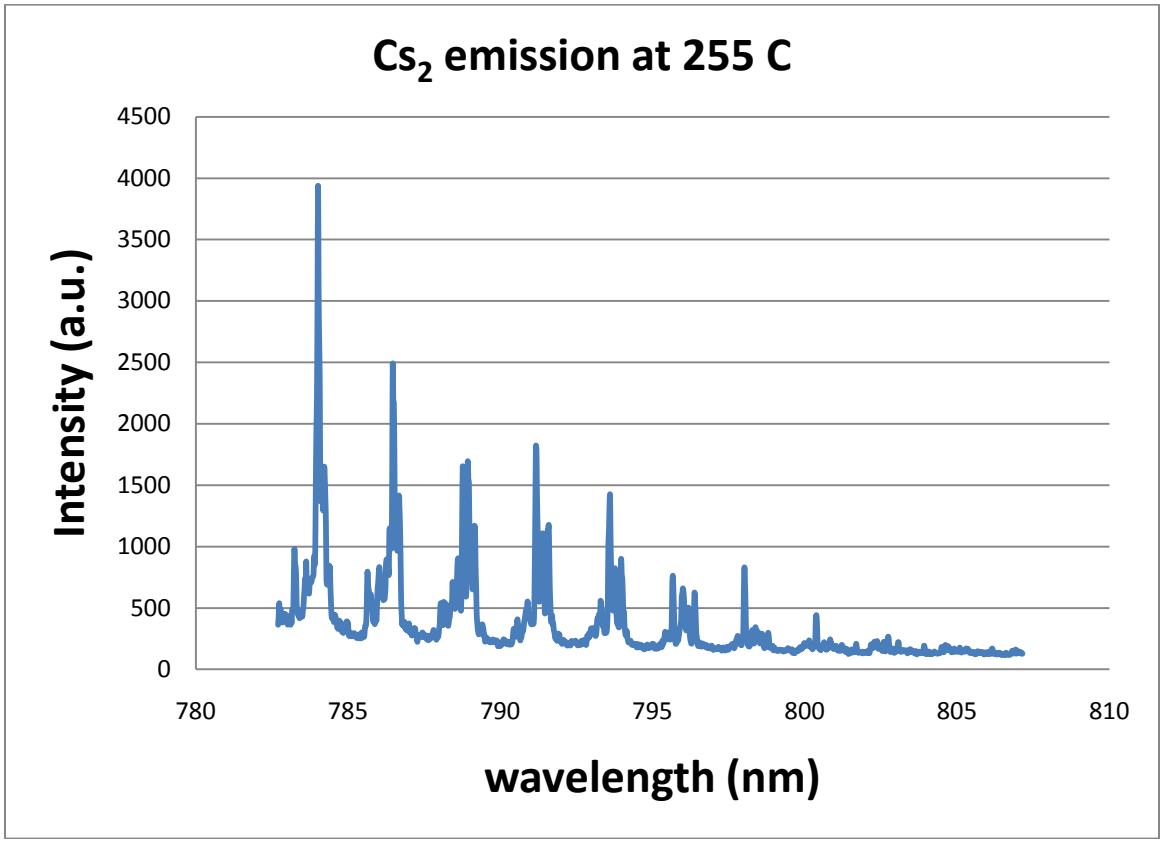
Cs2 emission at 255 C
Intensity (a.u.)
4500
4000
3500
3000
2500
2000
1500
1000
500
0
780
785
790
795
800
805
810
wavelength (nm)

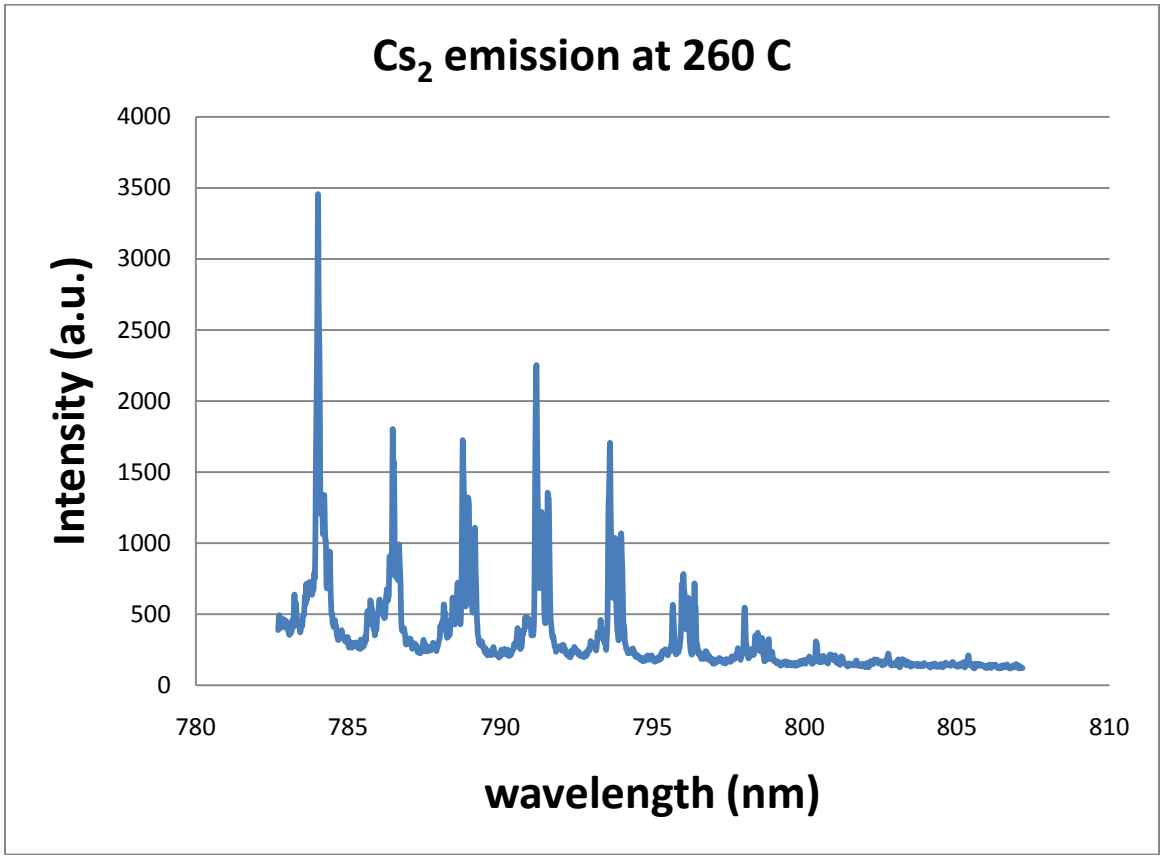

Appendix 3

This appendix holds all emission results from the experiment exploring the emission of the cesium molecule. Although there were only a few transistions that were of interest, all of the emission was recorded and used to determine it was cesium atoms and not cesium dimer emission. The cesium atom was pumped with the pulsed YAG pumped dye laser at 742 nm. Energy was sufficient to excite many different transitions with emission of the blue, 455 and 457 nm being of most interest.

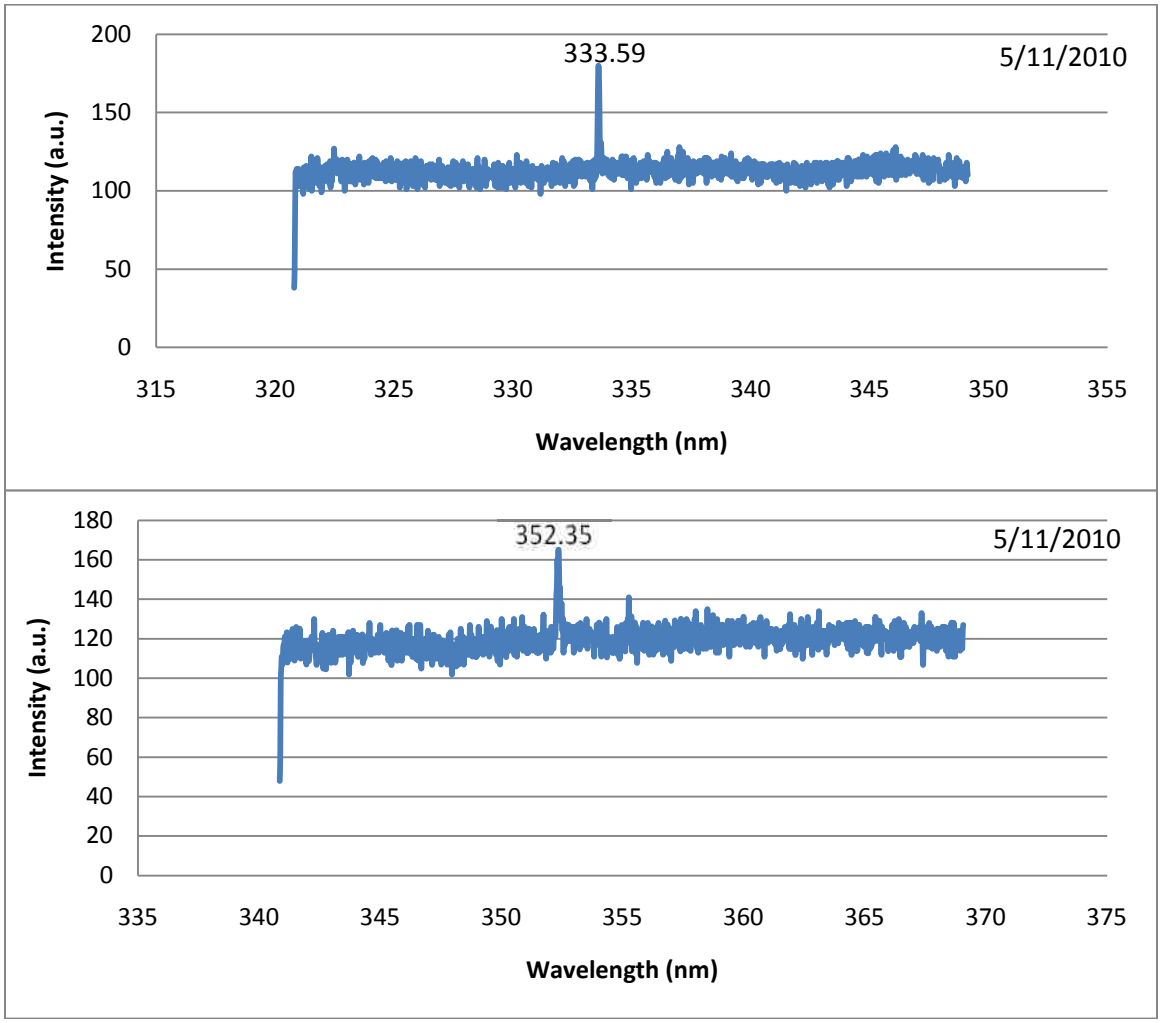
333.59
5/11/2010
Intensity (a.u.)
200
150
100
50
0
315
320
325
330
335
340
345
350
355
Wavelength (nm)
352.35
5/11/2010
Intensity (a.u.)
180
160
140
120
100
80
60
40
20
0
335
340
345
350
355
360
365
370
375
Wavelength (nm)

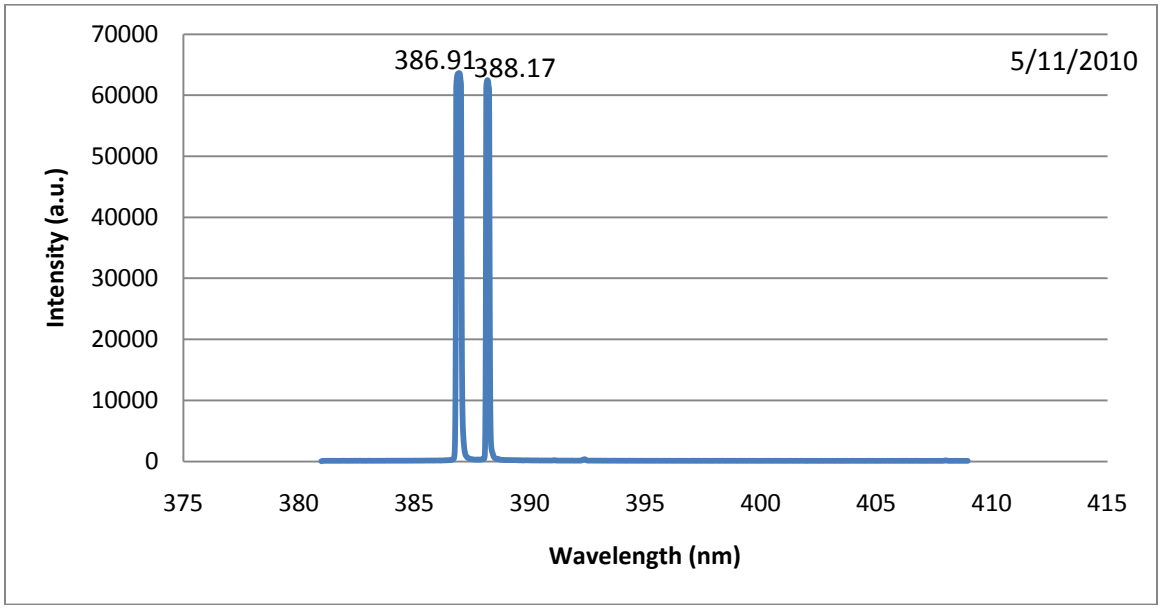
70000
60000
50000
40000
30000
20000
10000
0
Intensity (a.u.)
386.91
388.17
5/11/2010
375
380
385
390
395
400
405
410
415
Wavelength (nm)

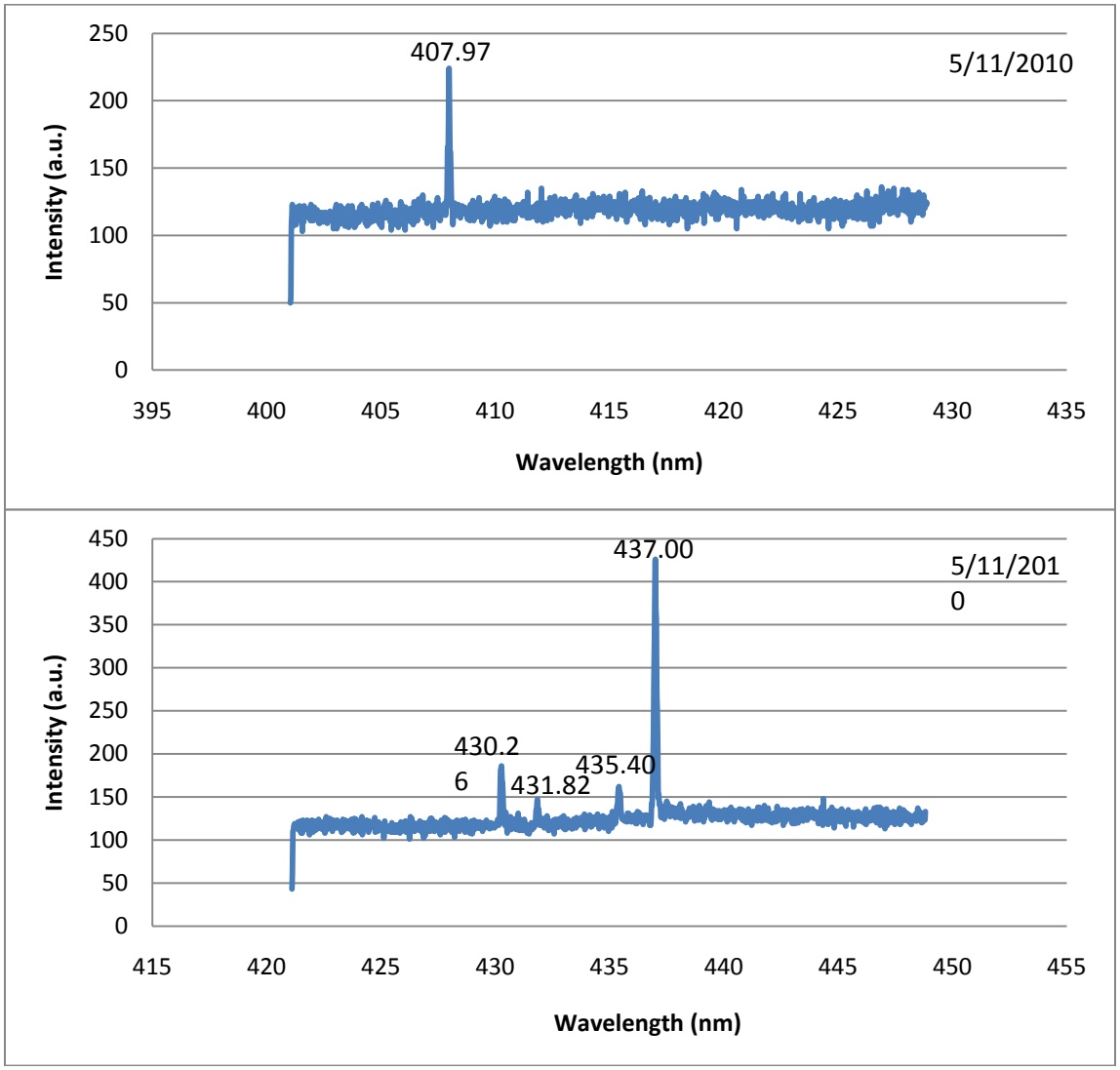
250
200
150
100
50
0
Intensity (a.u.)
407.97
5/11/2010
395
400
405
410
415
420
425
430
435
Wavelength (nm)
450
400
350
300
250
200
150
100
50
0
Intensity (a.u.)
437.00
5/11/201
0
430.2
6
431.82
435.40
415
420
425
430
435
440
445
450
455
Wavelength (nm)

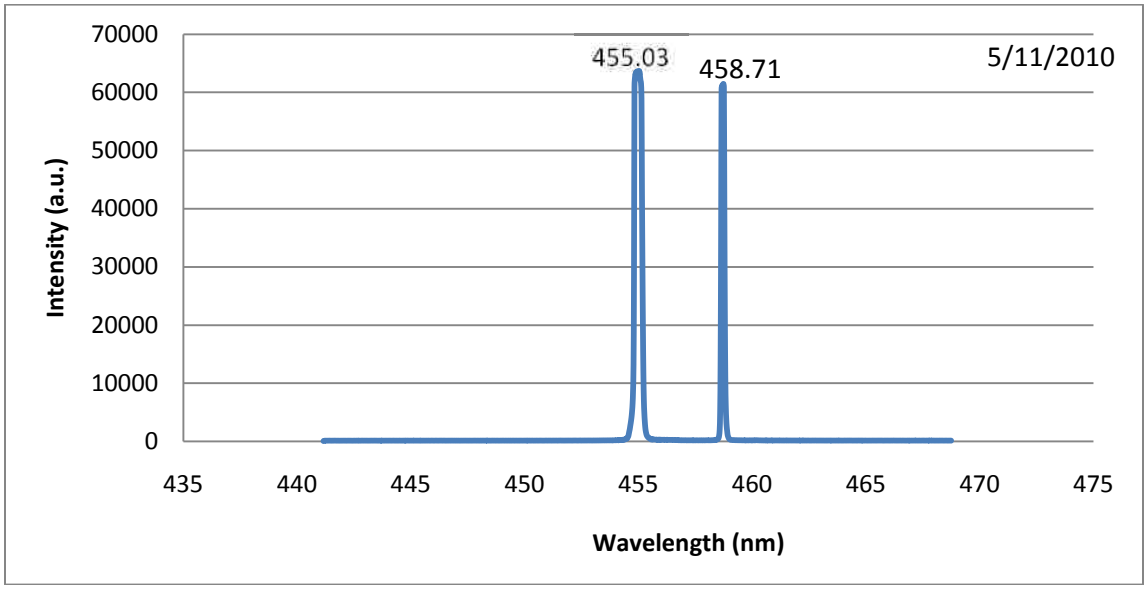
70000
60000
50000
40000
30000
20000
10000
0
Intensity (a.u.)
455.03
458.71
5/11/2010
435
440
445
450
455
460
465
470
475
Wavelength (nm)

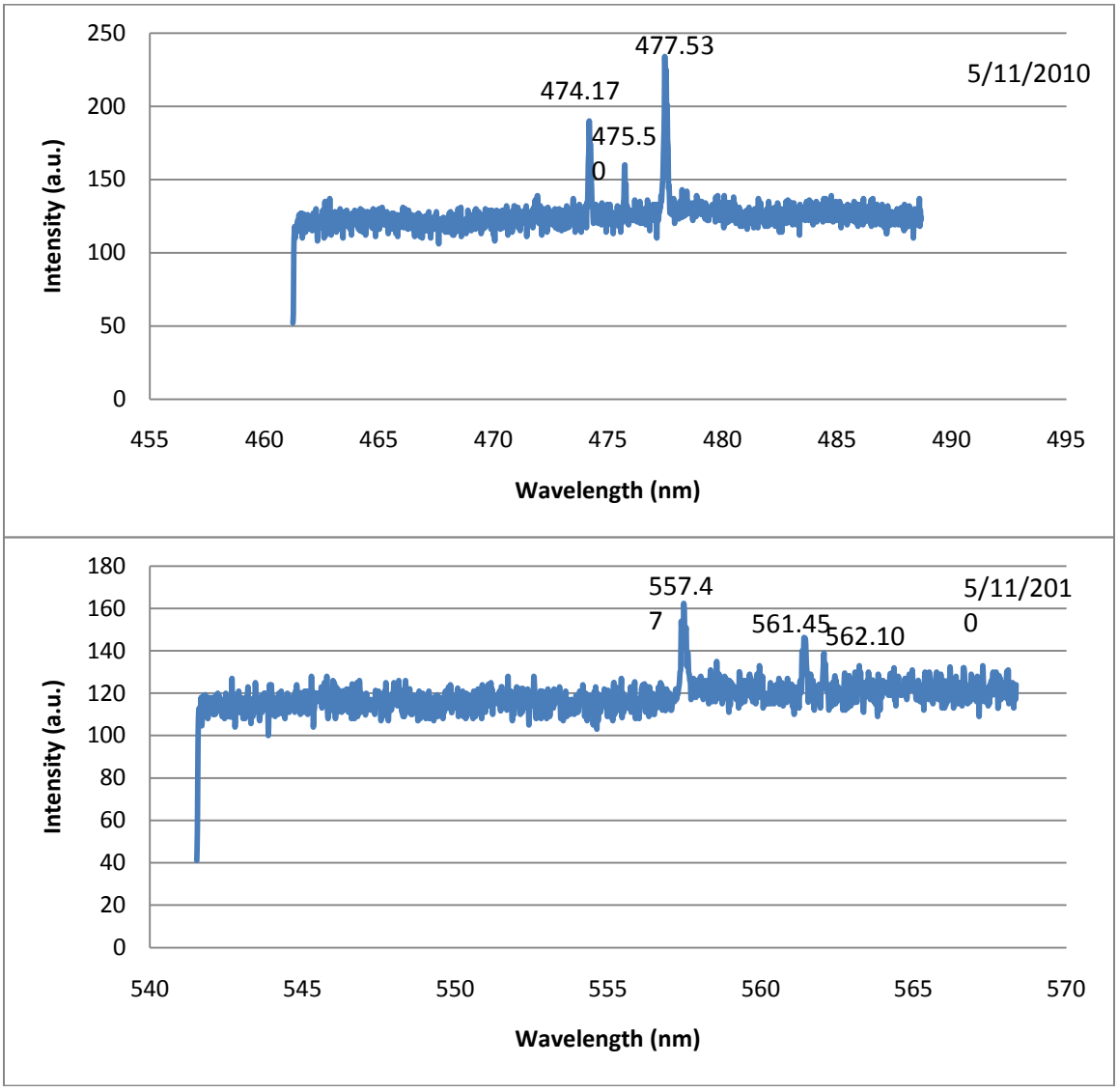
250
200
150
100
50
0
Intensity (a.u.)
477.53
474.17
475.50
5/11/2010
455
460
465
470
475
480
485
490
495
Wavelength (nm)
180
160
140
120
100
80
60
40
20
0
Intensity (a.u.)
557.47
561.45
562.10
5/11/2010
540
545
550
555
560
565
570
Wavelength (nm)

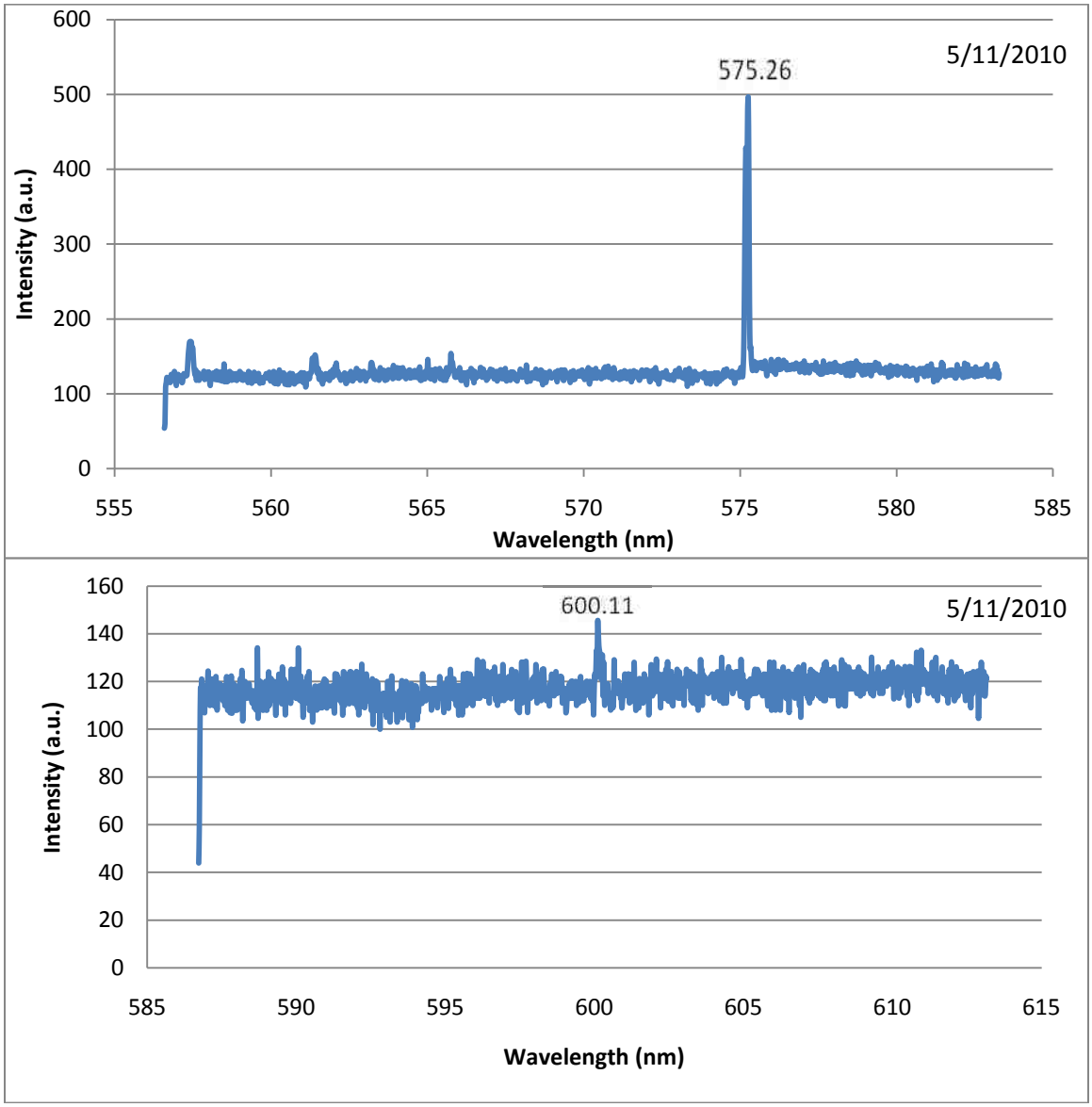
600
500
400
300
200
100
0
Intensity (a.u.)
575.26
5/11/2010
555
560
565
570
575
580
585
Wavelength (nm)
160
140
120
100
80
60
40
20
0
Intensity (a.u.)
600.11
5/11/2010
585
590
595
600
605
610
615
Wavelength (nm)

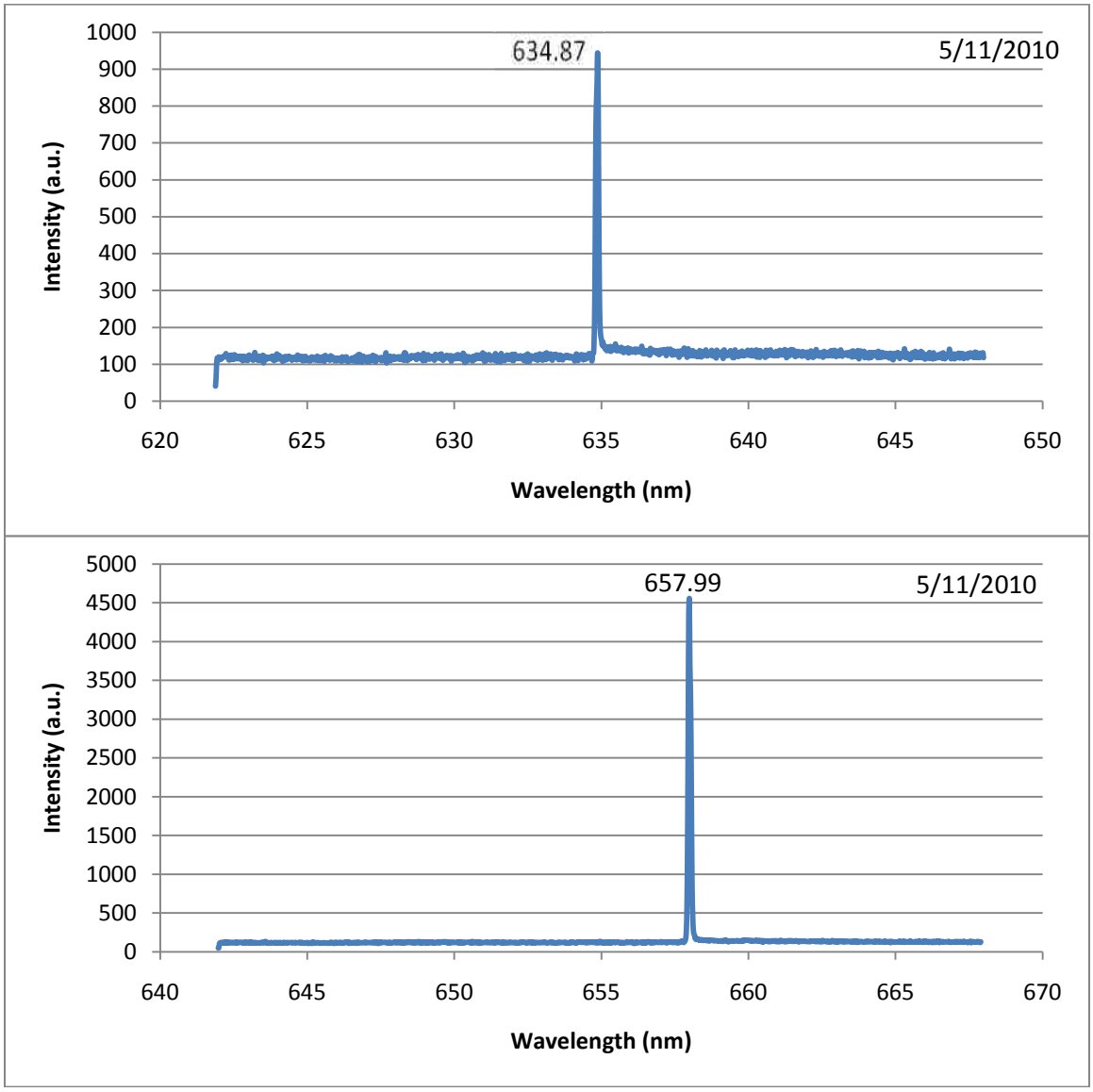
634.87
5/11/2010
Intensity (a.u.)
1000
900
800
700
600
500
400
300
200
100
0
620
625
630
635
640
645
650
Wavelength (nm)
657.99
5/11/2010
Intensity (a.u.)
5000
4500
4000
3500
3000
2500
2000
1500
1000
500
0
640
645
650
655
660
665
670
Wavelength (nm)

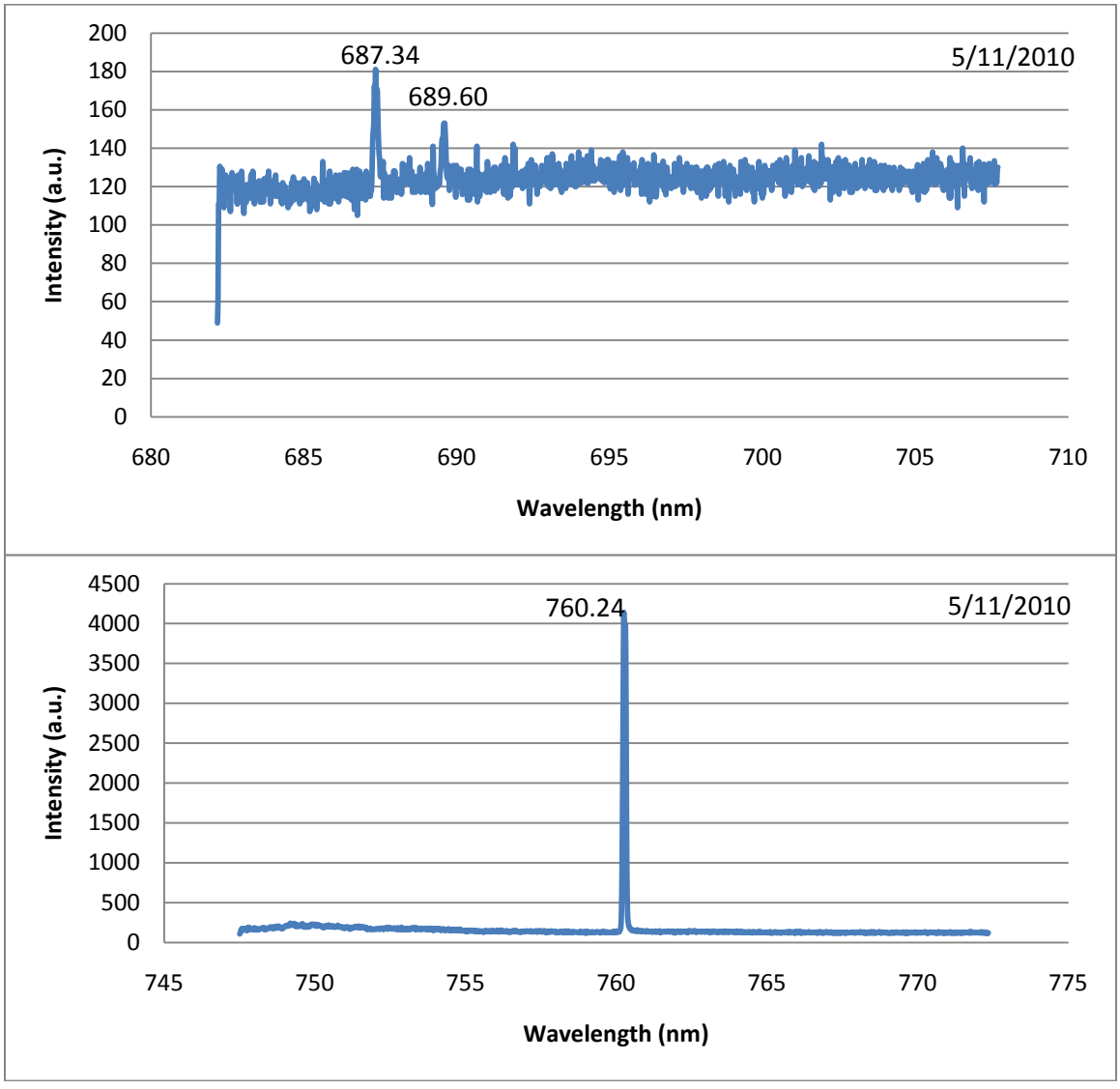
687.34
689.60
5/11/2010
Intensity (a.u.)
Wavelength (nm)
760.24
5/11/2010
Intensity (a.u.)
Wavelength (nm)

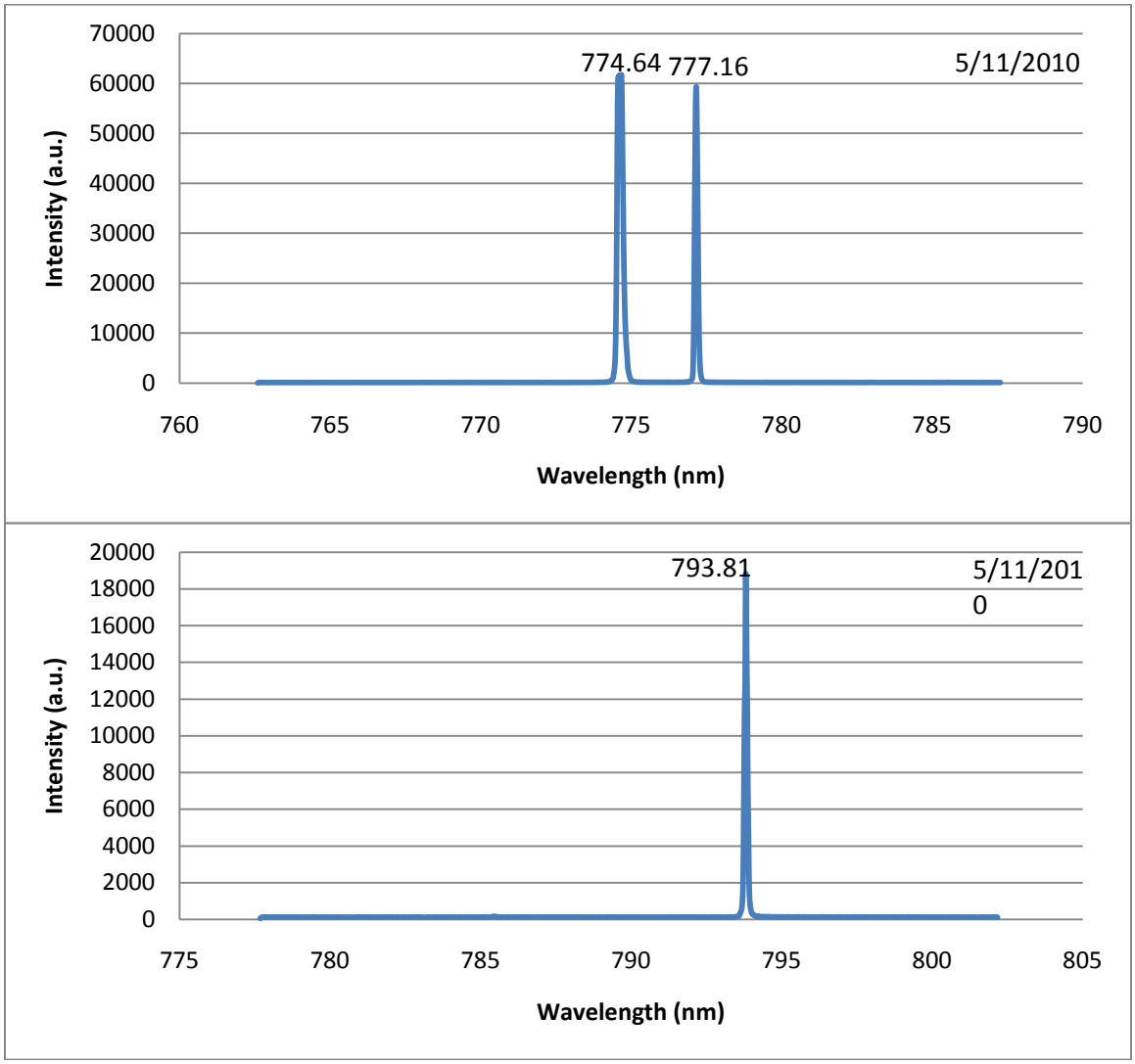
70000
60000
50000
40000
30000
20000
10000
0
Intensity (a.u.)
774.64
777.16
5/11/2010
760
765
770
775
780
785
790
Wavelength (nm)
20000
18000
16000
14000
12000
10000
8000
6000
4000
2000
0
Intensity (a.u.)
793.81
5/11/201
0
775
780
785
790
795
800
805
Wavelength (nm)

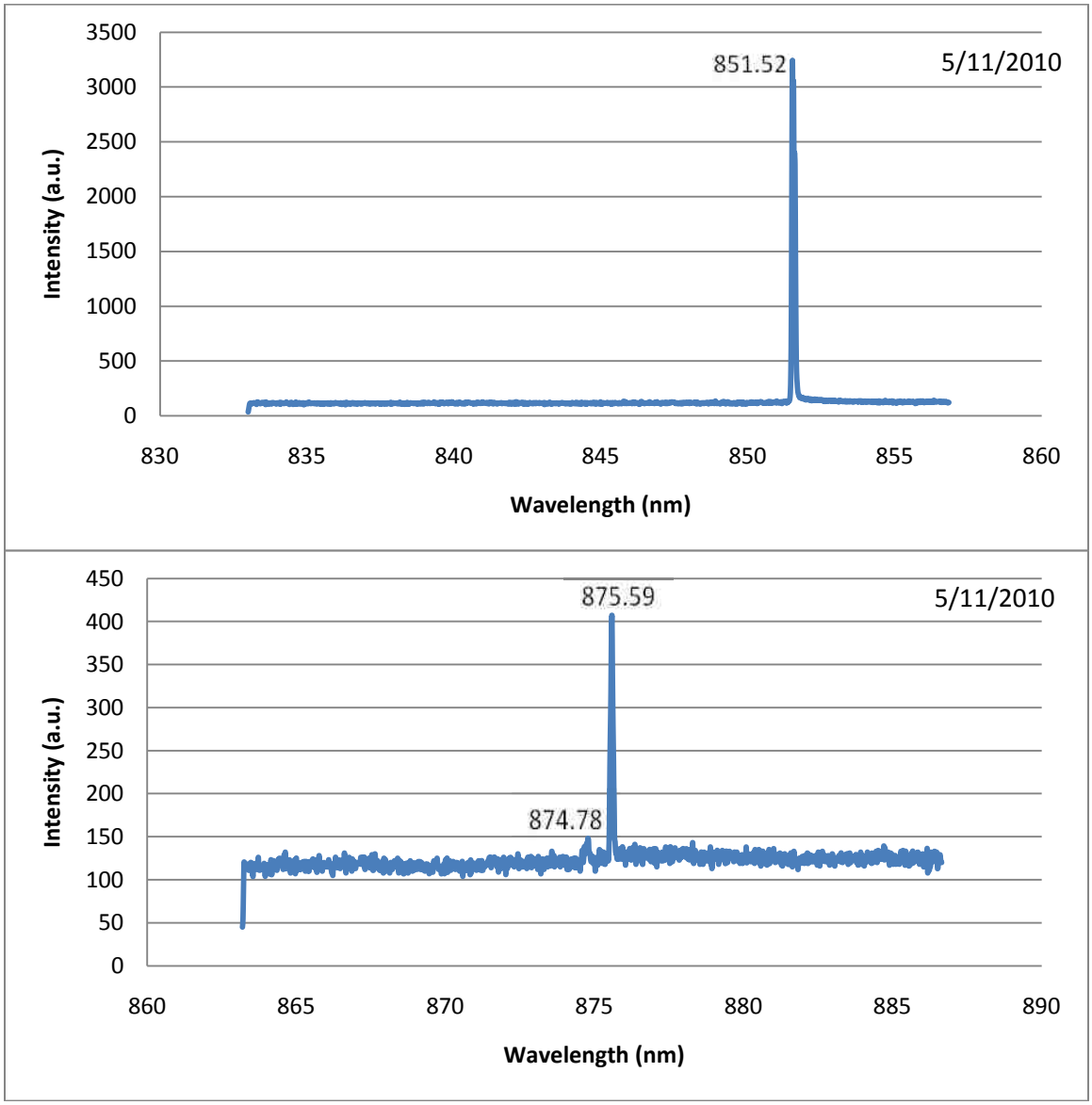
3500
3000
2500
2000
1500
1000
500
0
Intensity (a.u.)
851.52
5/11/2010
830
835
840
845
850
855
860
Wavelength (nm)
450
400
350
300
250
200
150
100
50
0
Intensity (a.u.)
875.59
874.78
5/11/2010
860
865
870
875
880
885
890
Wavelength (nm)

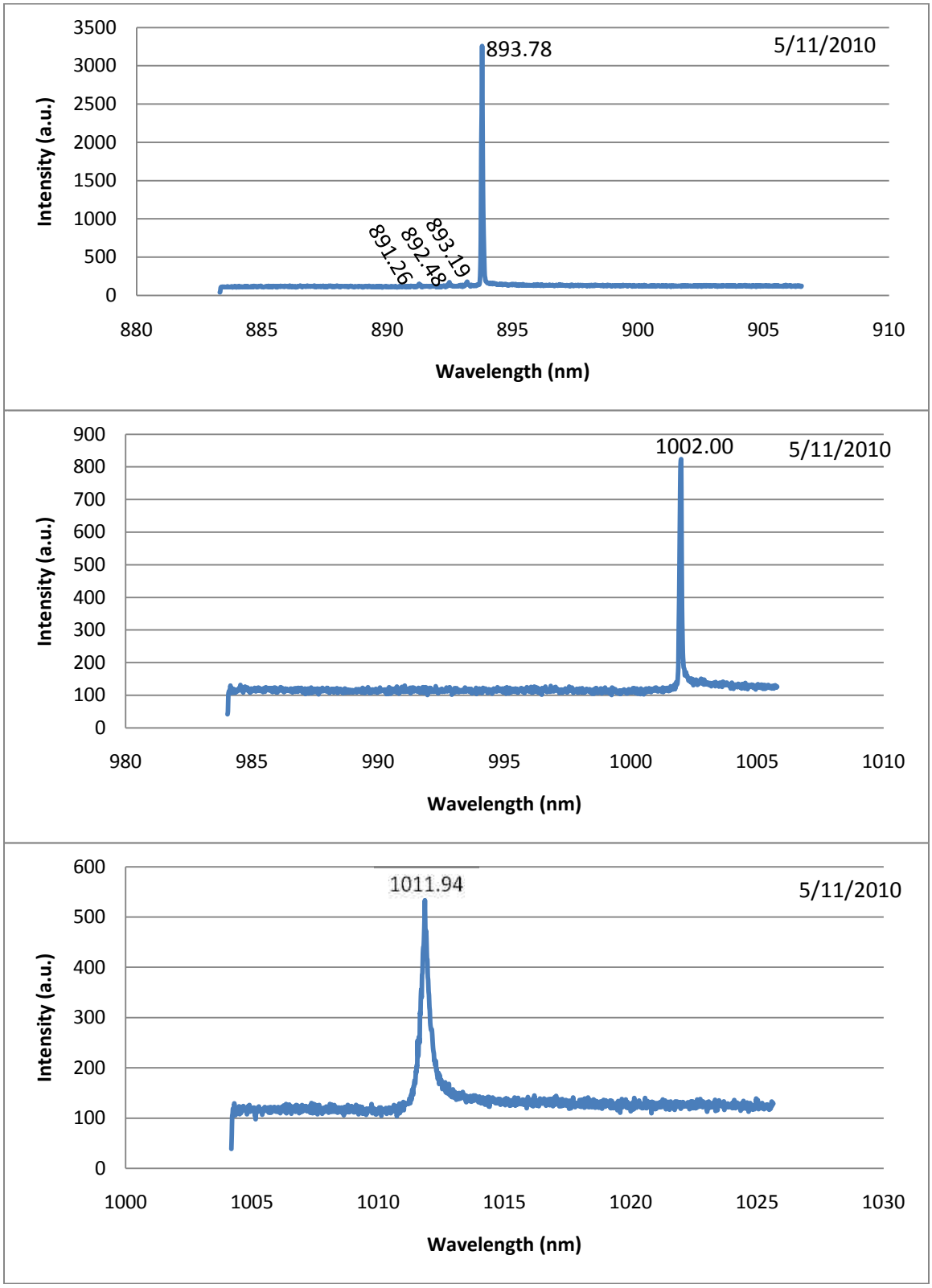
3500
3000
2500
2000
1500
1000
500
0
Intensity (a.u.)
893.78
5/11/2010
891.26
892.48
893.19
880
885
890
895
900
905
910
Wavelength (nm)
900
800
700
600
500
400
300
200
100
0
Intensity (a.u.)
1002.00
5/11/2010
980
985
990
995
1000
1005
1010
Wavelength (nm)
600
500
400
300
200
100
0
Intensity (a.u.)
1011.94
5/11/2010
1000
1005
1010
1015
1020
1025
1030
Wavelength (nm)

Appendix 4

This appendix holds the experimental results from testing the multiphoton absorption transition that creates the blue 457 nm emission from pumping at 742 nm. The tests were completed at different temperatures to make sure there is a resonance.

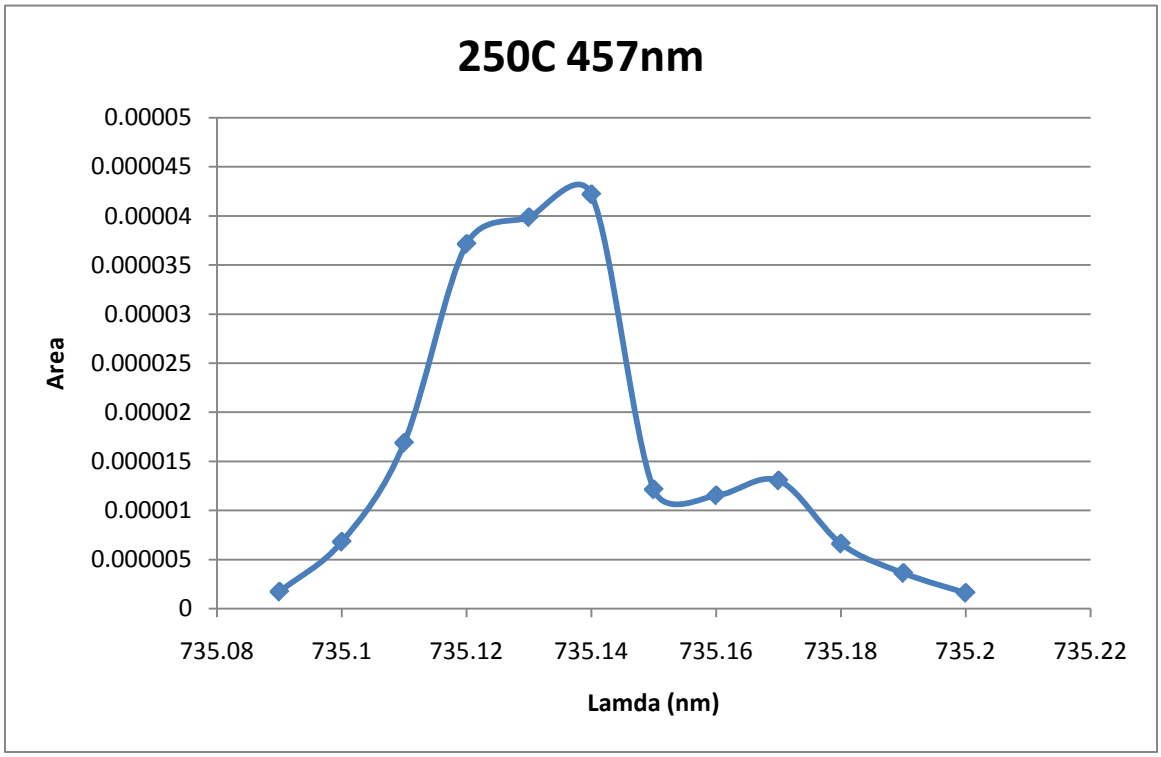

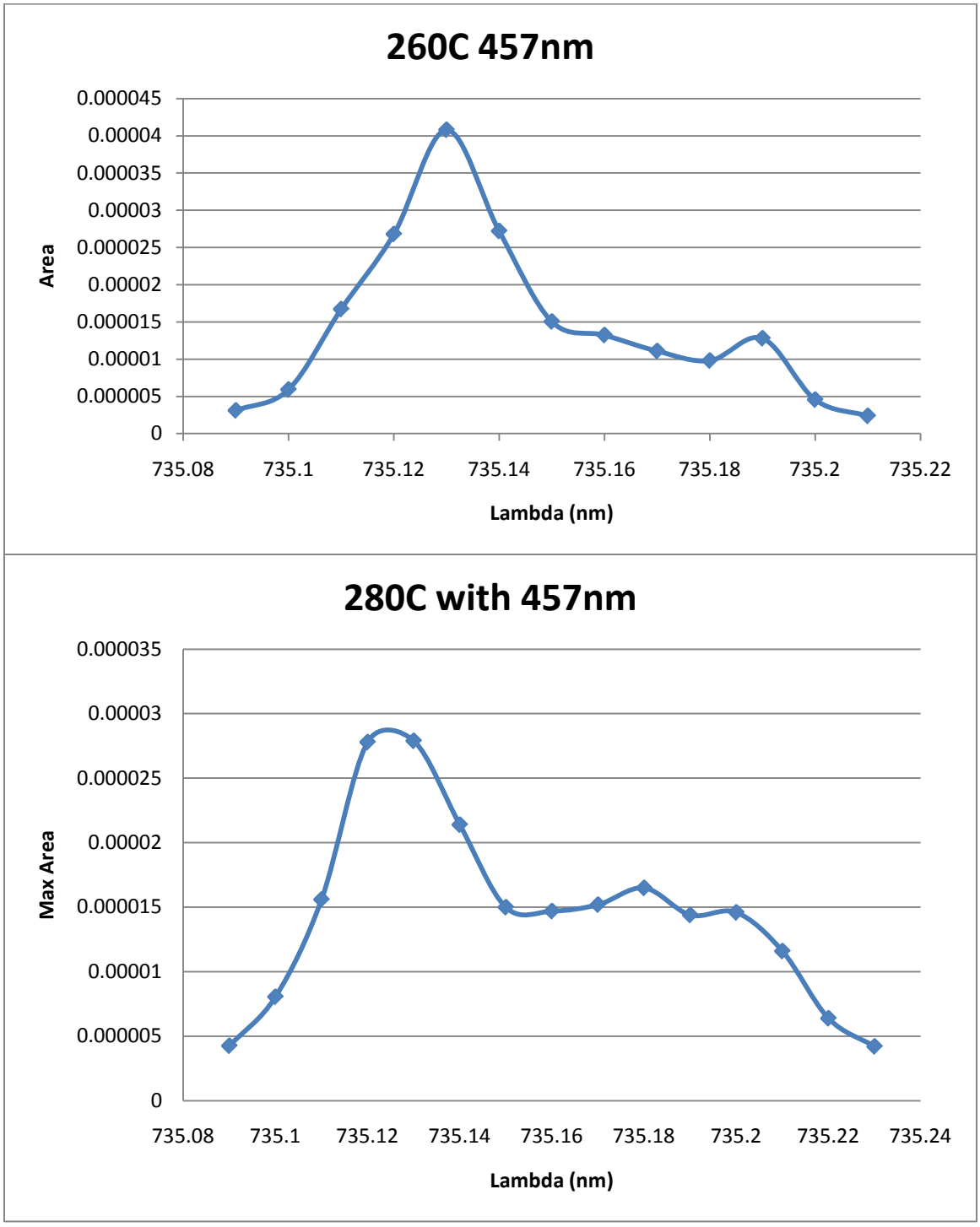
260C 457nm
Area
0.000045
0.00004
0.000035
0.00003
0.000025
0.00002
0.000015
0.00001
0.000005
0
735.08
735.1
735.12
735.14
735.16
735.18
735.2
735.22
Lambda (nm)
280C with 457nm
Max Area
0.000035
0.00003
0.000025
0.00002
0.000015
0.00001
0.000005
0
735.08
735.1
735.12
735.14
735.16
735.18
735.2
735.22
735.24
Lambda (nm)

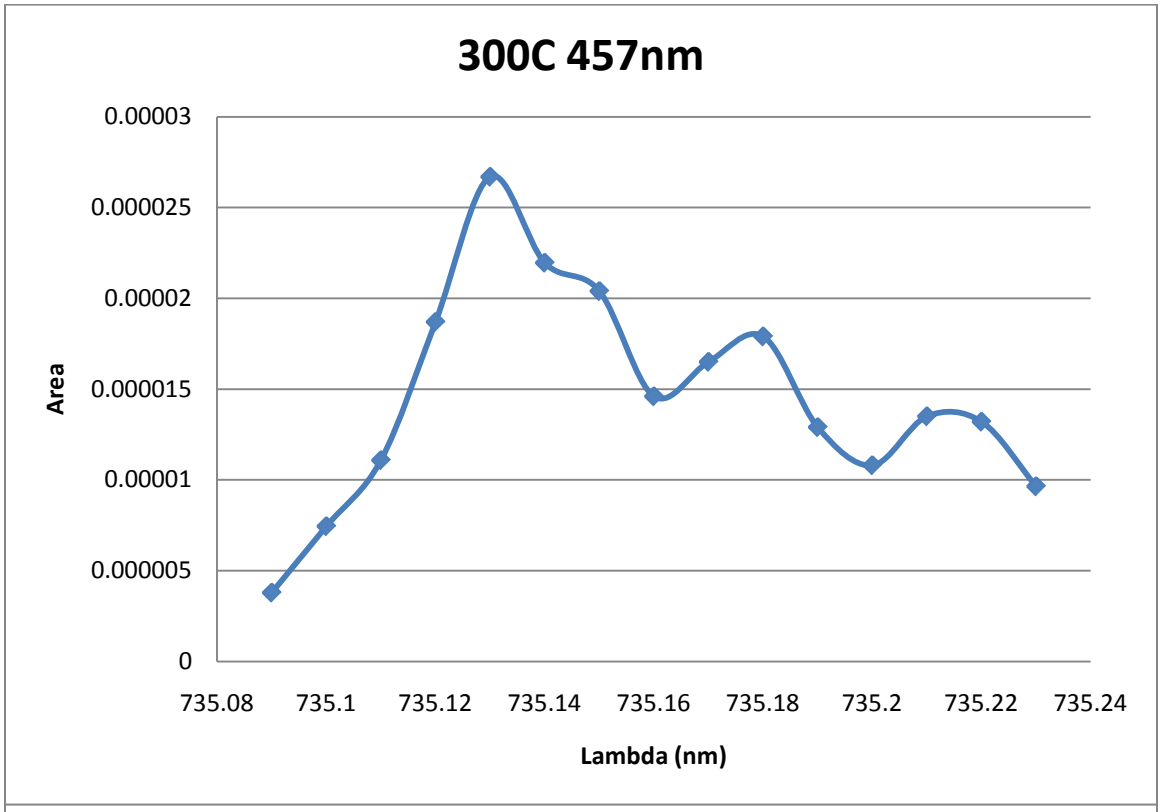
300C 457nm
0.00003
0.000025
0.00002
0.000015
0.00001
0.000005
0
Area
735.08
735.1
735.12
735.14
735.16
735.18
735.2
735.22
735.24
Lambda (nm)

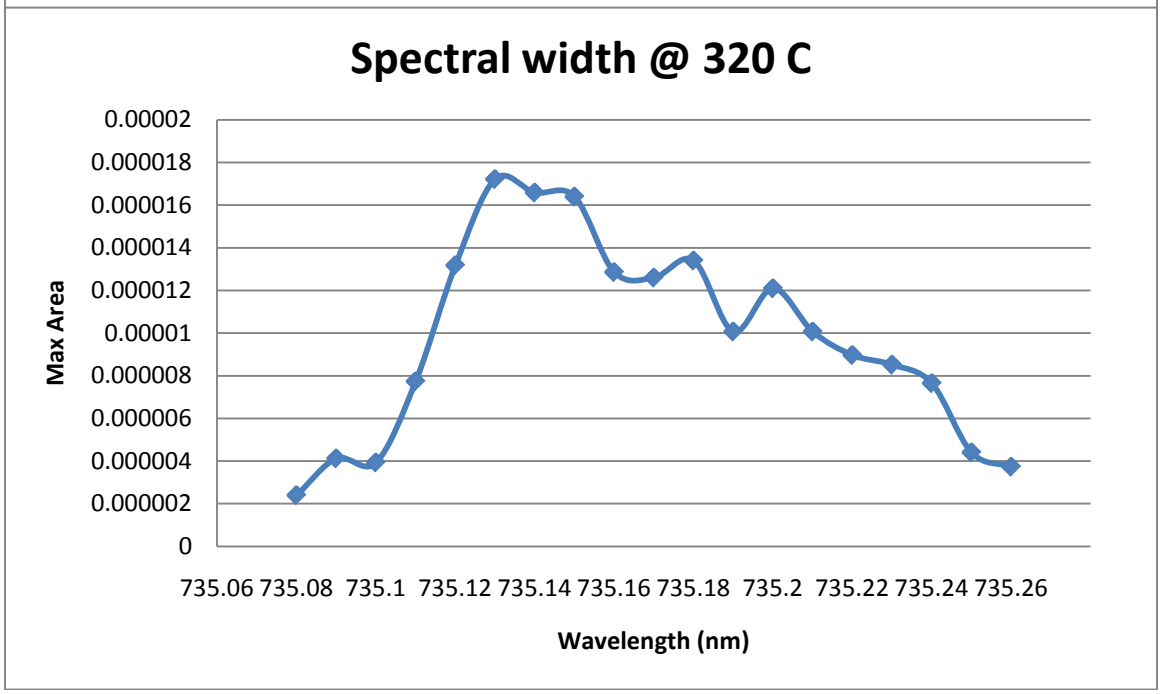
Spectral width @ 320 C
0.00002
0.000018
0.000016
0.000014
0.000012
0.00001
0.000008
0.000006
0.000004
0.000002
0
Max Area
735.06
735.08
735.1
735.12
735.14
735.16
735.18
735.2
735.22
735.24
735.26
Wavelength (nm)

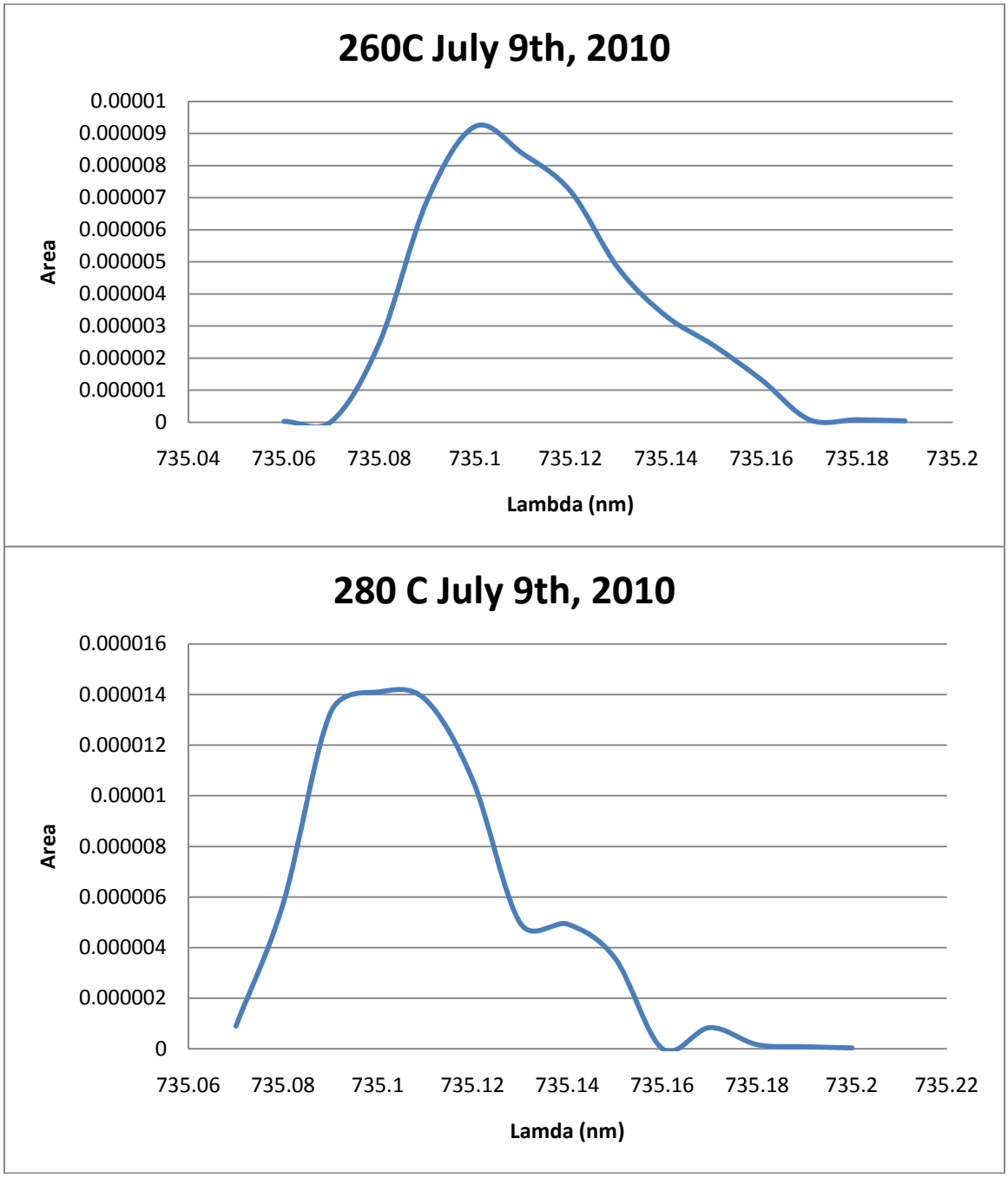
260C July 9th, 2010
Area
0.00001
0.000009
0.000008
0.000007
0.000006
0.000005
0.000004
0.000003
0.000002
0.000001
0
735.04
735.06
735.08
735.1
735.12
735.14
735.16
735.18
735.2
Lambda (nm)
280 C July 9th, 2010
Area
0.000016
0.000014
0.000012
0.00001
0.000008
0.000006
0.000004
0.000002
0
735.06
735.08
735.1
735.12
735.14
735.16
735.18
735.2
735.22
Lamda (nm)

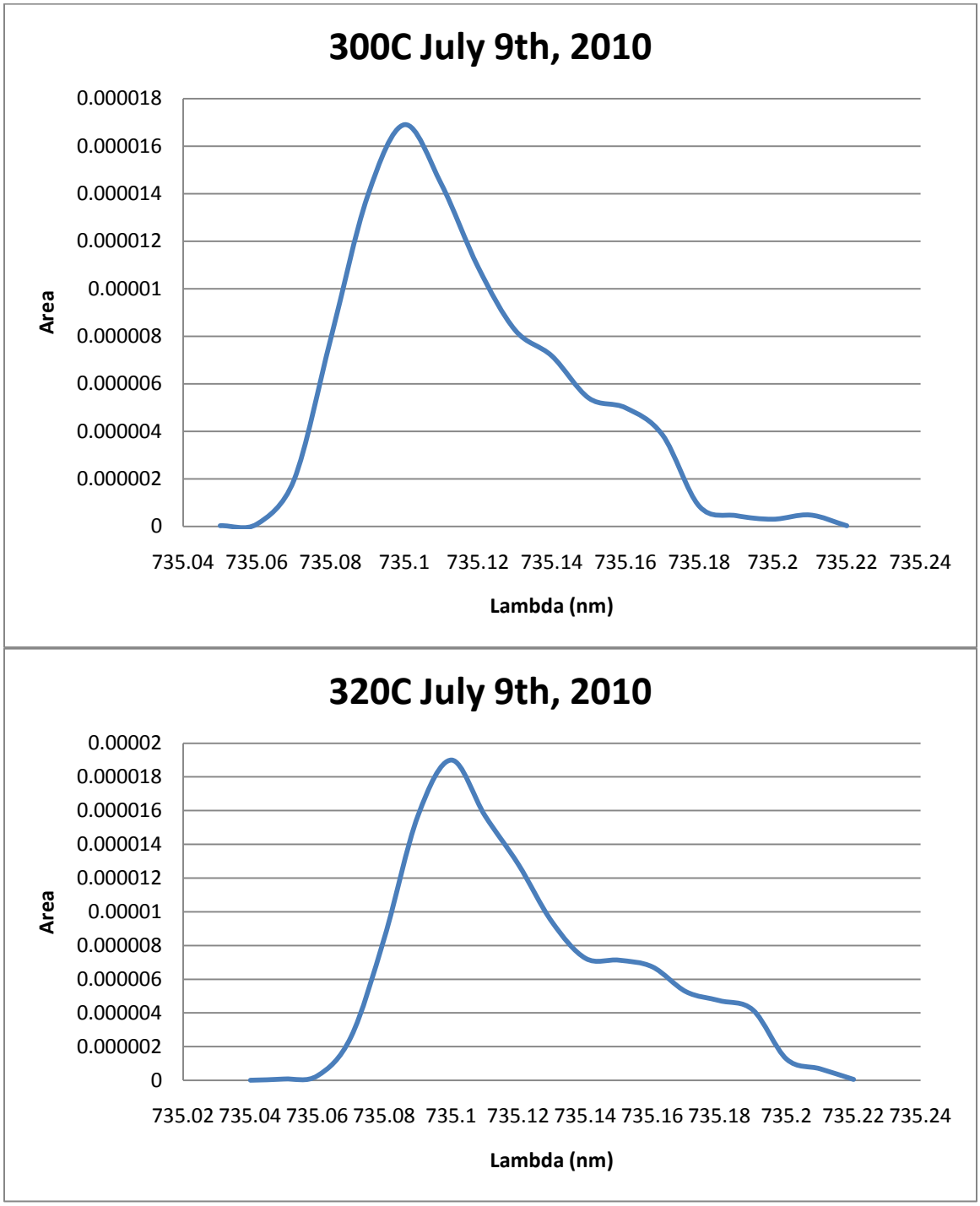
300C July 9th, 2010
0.000018
0.000016
0.000014
0.000012
0.00001
0.000008
0.000006
0.000004
0.000002
0
Area
735.04 735.06 735.08 735.1 735.12 735.14 735.16 735.18 735.2 735.22 735.24
Lambda (nm)
320C July 9th, 2010
0.00002
0.000018
0.000016
0.000014
0.000012
0.00001
0.000008
0.000006
0.000004
0.000002
0
Area
735.02 735.04 735.06 735.08 735.1 735.12 735.14 735.16 735.18 735.2 735.22 735.24
Lambda (nm)